Recovery of rare earth elements from acid mine drainage by co-precipitation with Al and Fe oxyhydroxides

Mateus Lanna Borges de Moraes

2020

COMISSÃO NACIONAL DE ENERGIA NUCLEAR - CNEN
CENTRO DE DESENVOLVIMENTO DA TECNOLOGIA NUCLEAR - CDTN
Programa de Pós-Graduação em Ciência e Tecnologia das Radiações, Minerais e Materiais

UNIVERSIDAD DE SALAMANCA – USAL
ESCUELA DE DOCTORADO "STUDII SALAMANTINI"
Programa de Doctorado en Geología

Recovery of rare earth elements from acid mine drainage by co-precipitation with Al and Fe oxyhydroxides

Mateus Lanna Borges de Moraes

Thesis presented to the *Curso de Pós-Graduação em Ciência e Tecnologia das Radiações, Minerais e Materiais* (CDTN-Brazil) in partial fulfilment of the requirements for the degree of Doctor and to the School of Doctorate of the *Universidad de Salamanca* (USAL-Spain) in partial fulfilment of the requirements for the degree of *Doctor en Geología*.

Tese apresentada ao Curso de Pós-Graduação em Ciência e Tecnologia das Radiações, Minerais e Materiais (CDTN-Brasil), como requisito parcial à obtenção do título de Doutor, e à Escola de doutorado da *Universidad de Salamanca* (USAL-Espanha) como requisito parcial à obtenção do título de *Doctor em Geología*.

Área de concentração no CDTN: Ciência e Tecnologia dos Minerais e Meio Ambiente
Línea de investigación en la USAL: Propiedades físicas y químicas de rocas y minerales de aplicación industrial

Advisors:
Profª. Drª. Ana Claudia Queiroz Ladeira (CDTN-BR)
Profª. Drª. Ascensión Murciego (USAL-ES)
Drª. Esther Álvarez-Ayuso (IRNASA-ES)
Co-advisor:
Prof. Dr. Jaime Wilson Vargas de Mello (UFV-BR)

Belo Horizonte, Maio de 2020

"One never notices what has been done; one can only see what remains to be done."

Marie Curie, Letter to her brother (1894)

"Humanity stands... before a great problem of finding new raw materials and new sources of energy that shall never become exhausted. In the meantime, we must not waste what we have, but must leave as much as possible for coming generations."

Svante Arrhenius, Chemistry in Modern Life (1925)

ACKNOWLEDGMENTS

First, I would like to thank all my family for the support and for believing in my potential. Thanks Angelina Maria Lanna de Moraes and Fernando Machado Borges de Morais for bringing me to this existence and for educating me. Thanks, Rafael Lanna, for your unconditional brother support. Thanks to all my uncles Aurea, Zé Carlos, Iris, Rosana, Agrício (in memoriam), Léo and Daniel for all financial and emotional support.

Special thanks to my life-partner Roberta Ferreira Monteiro for always being at my side, for believing in my mission and for your daily support. Thanks to my mother-in-law Rosália Ferreira Monteiro and my father-in-law Maj. Idemar Monteiro (in memoriam) for everything. Thanks also to my brother-in-law Maj. Roberto Monteiro and all his family.

I would like to acknowledge Prof[a]. Ana Claudia Queiroz Ladeira for the opportunity of studying at the CDTN under your supervision, for the trust in my work and for your important collaboration to the research.

Thank you very much Prof[a]. Ascensión Murciego and Prof[a]. Esther Álvarez-Ayuso for the opportunity of studying at Salamanca under your supervision, for our partnership, for the unconditional help and for the unforgettable life experience. ¡Muchísimas gracias, Vale!

Thanks to all my professors that shared their knowledge with me, contributing directly and indirectly to this thesis. Special thanks to Prof. Francisco Javier Rios (CDTN) and Clemente Recio (USAL) for creating the opportunity of double doctorate between the two institutions.

Special thanks to Mr. Julius Martins for your high-quality proofreading.

I would like to thank *Indústrias Nucleares do Brasil (INB)* for the partnership, the *Comissão Nacional de Energia Nuclear (CNEN)* for the scholarship, and *CNPq, FINEP, Fapemig* and *Inct-Acqua* for funding the research. I am also thankful to the *Centro Nacional de Microscopía Electrónica -CNME* (Madrid-Spain) for the TEM analysis, the Faculty of Chemistry of the *Universidad Complutense de Madrid* for the RMN analysis. I would like to thank the CDTN-Applied Physics Laboratory for the XPS analysis, especially to Prof. Pedro Lanna Gastelois and the CDTN Microscopy Laboratory for the and SEM analysis, especially to Dr. Tércio Assunção Pedrosa. Special thanks to Prof. José Domingos Ardisson (CDTN) for the ^{57}Fe Mössbauer spectroscopy analysis.

Special thanks to the technicians and undergraduate internship students of all institutions, whose hard work and dedication were essential. Thanks to the undergraduate students Mariana Fadul, Ana Flávia Marinho Saraiva, Thales Augusto Carneiro and Augusto Alves Camargos for your unmeasurable contribution at the laboratory. Thanks to all my colleagues, especially Dr[a]. Elaine Felipe, Dr[a] Janúbia Amaral, Thiago Sales, Rodrigo Santiago and Kelvin Batista for the partnership. Special thanks to my Mozambique fellows Dr. Edson Fernandes Raso, Dr. Luciano Bernardo José and Dr. Egídio Francisco for the friendship. Thanks to the CDTN technicians Dr. Rodrigo Albuquerque, Dr. Carlos Antônio de Morais, Luiz Carlos da Silva, Marcos Antônio Evangelista (Professor), Ariovaldo Neves, João Batista Santos Barbosa, Antônio Furquim, Mônica Elizetti de Freitas, José Carlos Ferreira, among many others, for your help and exchanged ideas. Thanks to all friends, colleagues and all people that I may forget to mention here.

ABSTRACT

Rare earth elements (REE) are used for different applications worldwide in new technologies that are fundamental for the world's society. REE are considered critical and strategic materials in the current globalized scenario and the concern about this resource is constantly gaining attention. The search for new sources of REE is a current issue and researchers are seeking for recycling and recovering REE from secondary sources. Acid mine drainage (AMD) is an important secondary source of REE because this effluent can contain a considerable amount of these precious elements. Furthermore, as AMD is a serious environmental issue and demands treatment before discharge, the union of metal recovery and pollution control is something desirable when sustainability is the goal. There is a closed uranium mine in the state of Minas Gerais-Brazil, with the occurrence of an REE-rich AMD. This peculiar site was selected due to its *sui generis* geochemical characteristics. In this scenario, this investigation aimed to evaluate the co-precipitation of REE from AMD effluents using oxyhydroxides of Al and Fe as the major co-precipitants. A 'PHREEQC' geochemical model of the AMD system indicates that Ln^{3+}, $LnSO_4^+$ and LnF^{2+} are the dominant REE species at pH 3.5. The neutralization of the AMD with KOH produced an amorphous precipitate containing 14% of REE oxides. The precipitate contains Al_{13}-polymers and accounts for the REE removal when the pH is raised to 8, thus promoting adsorption and entrapment simultaneously. Sequential extraction revealed that 60% of the REE could be leached with the use of acetic acid. In sequence, the role of iron in the co-precipitation of REE and uranium by Fe-Al-precipitates in AMD was studied. It was concluded that the presence and the amount of Fe in the initial solution can positively influence the REE removal efficiency, especially at acidic environments. The influence caused by the addition of Fe was irrelevant when the pH of the AMD was raised to values equal to 7-8. The removal of U was not influenced by the addition of Fe to the AMD before pH neutralization. Sequential extraction results showed that precipitates containing higher amounts of Fe, the REE tend to be less labile. ^{57}Fe Mössbauer spectroscopy studies revealed that the REE can occupy iron sites in the structure of the amorphous precipitates. Subsequently, the influence of soluble Ca and Zn over the co-precipitation of REE by amorphous aluminium precipitates was studied. It was concluded that Ca exerts a negative influence over the co-precipitation as well as over the adsorption of Pr and Eu on amorphous aluminium precipitates. On the other hand, the co-precipitation and adsorption of the elements Nd and Sm did not suffer any influence of the presence of Ca in the solution. Finally, a study concerning the recovery of REE by co-

precipitation with Al_{13}-polymers from AMD using $Ca(OH)_2$ for pH control showed that about 90% of the REE present in the AMD sample could be recovered by co-precipitation with amorphous Al-precipitates. The precipitate contains about 7% of REE oxides. The results of the acid-leaching experiment show that about 60%, 65% and 85% of the REE can be extracted from the precipitates using 2 mol L^{-1} HCl, 1.7 mol L^{-1} H_2SO_4 and 2 mol L^{-1} CH_3COOH, respectively. The economic potential of the REE-recovery considering an AMD sample from the studied site was also estimated, revealing the great potential of AMD treatment combined with REE production, in compliance with the United Nations sustainable development goals.

KEYWORDS: rare earth elements, acid mine drainage, metal recovery, amorphous aluminium oxyhydroxides, Al_{13}-polymers, amorphous iron oxyhydroxides, pH control.

RESUMEN

Las tierras raras (TR) son utilizadas para diferentes aplicaciones en todo el mundo en nuevas tecnologías que son fundamentales para la sociedad. Las TR se consideran materias primas críticas y estratégicas en el escenario globalizado actual y la preocupación por ellas cada vez se acrecienta más. La búsqueda de nuevas fuentes de TR es un problema actual y los investigadores están tratando de desarrollar métodos para reciclarlas y recuperarlas a partir de fuentes secundarias. El drenaje ácido de minas (DAM) es potencialmente una fuente secundaria importante de TR, dado que este efluente puede contener una cantidad considerable de estos elementos de gran valor. Además, como el DAM es un problema ambiental grave y exige tratamiento antes de ser descargado en el medioambiente, conseguir la recuperación de metales a la par que el control de la contaminación es algo crucial para lograr la sostenibilidad. En el estado de Minas Gerais-Brasil se encuentra una mina de uranio cerrada que produce un DAM rico en TR. Este sitio peculiar fue seleccionado para realizar el estudio debido a sus características geoquímicas *sui generis*. En este escenario, esta investigación tuvo como objetivo evaluar la coprecipitación de TR de los efluentes de DAM utilizando oxihidróxidos de Al y Fe como principales agentes coprecipitantes. La aplicación del modelo geoquímico 'PHREEQC' al sistema de DAM indicó que Ln^{3+}, $LnSO_4^+$ y LnF^{2+} son las especies de TR dominantes a un pH 3.5. La neutralización del DAM con KOH produjo un precipitado amorfo que contenía 14% de óxidos de TR. El precipitado contiene polímeros de Al_{13} que son los responsables de la eliminación de las TR cuando el pH se eleva a 8, promoviendo así la adsorción y el atrapamiento de las TR simultáneamente. La extracción secuencial reveló que el 60% de las TR pueden ser lixiviadas del precipitado utilizando ácido acético. A continuación, se estudió el papel del hierro en la coprecipitación de TR y uranio en los precipitados de Fe-Al en el DAM. Se concluyó que la presencia y la cantidad de Fe en la solución inicial pueden influir positivamente en la eficiencia de eliminación de TR, especialmente en ambientes ácidos. La influencia causada por la adición de Fe fue irrelevante cuando el pH del DAM se elevó a valores iguales a 7-8. La eliminación de uranio no resultó influenciada por la adición de Fe en el DAM antes de la neutralización del pH. Los resultados de la extracción secuencial mostraron que, cuanto mayor es la cantidad de Fe en los precipitados, menos lábiles tienden a ser las TR. Los estudios de espectroscopía Mössbauer del ^{57}Fe revelaron que las TR pueden ocupar posiciones del hierro en la estructura de los precipitados amorfos. Posteriormente, se estudió la influencia de Ca y Zn solubles en la coprecipitación de TR en precipitados de aluminio amorfos. Se concluyó que el Ca ejerce una influencia negativa en la coprecipitación así como en la

adsorción de Pr y Eu en precipitados de aluminio amorfo. Por otro lado, la presencia de Ca en la solución no influyó en la coprecipitación y adsorción de los elementos Nd y Sm. Finalmente, un estudio sobre la recuperación de TR de DAM por coprecipitación con polímeros de Al_{13} usando $Ca(OH)_2$ para el control del pH mostró que aproximadamente el 90% de las TR presentes en la muestra de DAM pueden ser recuperadas por coprecipitación en precipitados de aluminio amorfos. El precipitado contiene aproximadamente el 7% de óxidos de TR. Los resultados del experimento de lixiviación ácida muestran que alrededor del 60%, 65% y 85% de las TR pueden extraerse de los precipitados usando HCl 2 mol L^{-1}, H_2SO_4 1,7 mol L^{-1} y CH_3COOH 2 mol L^{-1}, respectivamente. También se estimó el potencial económico de la recuperación de TR considerando una muestra de DAM del sitio estudiado, revelando el gran potencial del tratamiento de DAM combinado con la producción de TR, en consonancia con los Objetivos de Desarrollo Sostenible de las Naciones Unidas.

PALABRAS CLAVE: tierras raras, drenaje ácido de minas, recuperación de metales, oxihidróxidos de aluminio amorfos, polímeros de Al_{13}, oxihidróxidos de hierro amorfos, control de pH.

RESUMO

Os elementos terras raras (ETR) são usados para diferentes aplicações em todo o mundo em novas tecnologias que são fundamentais para a sociedade mundial. Os ETR são considerados materiais críticos e estratégicos no atual cenário globalizado e a preocupação com esse recurso está constantemente ganhando atenção. A pesquisa sobre novas fontes de ETR é um problema atual e os pesquisadores procuram desenvolver métodos para reciclar e recuperar ETR de fontes secundárias. A drenagem ácida de mina (DAM) é uma importante fonte secundária de ETR porque esse efluente pode conter uma quantidade considerável desses elementos preciosos. Além disso, como a DAM é um sério problema ambiental e requer tratamento antes de ser despejada no meio ambiente, é desejável a união da recuperação de metais ao controle da poluição quando a meta é a sustentabilidade. Existe uma mina de urânio fechada no estado de Minas Gerais-Brasil, onde ocorre uma DAM rica em ETR. Este local peculiar foi selecionado para realização deste estudo devido às suas características geoquímicas *sui generis*. Nesse cenário, esta pesquisa teve como objetivo avaliar a co-precipitação de ETR a partir de efluentes de DAM usando os hidróxidos de Al e Fe como os principais agentes co-precipitantes. Um modelo geoquímico 'PHREEQC' do sistema de DAM indicou que Ln^{3+}, $LnSO_4^+$ y LnF^{2+} são as espécies dominantes de ETR a pH 3,5. A neutralização de DAM com KOH produziu um precipitado amorfo contendo 14% de óxidos de ETR. O precipitado contém polímeros Al_{13} que são responsáveis pela remoção dos ETR quando o pH é elevado para 8, promovendo assim a adsorção e o aprisionamento dos ETR simultaneamente. A extração sequencial revelou que 60% dos ETR podem ser lixiviados com o uso de ácido acético. Em sequência, estudou-se o papel do Fe na co-precipitação de ETR e urânio em DAM por precipitados de Fe-Al. Concluiu-se que a presença e a quantidade de Fe na solução inicial podem influenciar positivamente a eficiência de remoção dos ETR, principalmente em ambientes ácidos. A influência causada pela adição de Fe foi irrelevante quando o pH da DAM foi elevado para valores iguais a 7-8. A remoção de urânio não foi influenciada pela adição de Fe na DAM antes da neutralização do pH. Os resultados da extração sequencial mostraram que os precipitados que contêm maiores quantidades de Fe, os ETR tendem a ser menos lábeis. Os estudos de espectroscopia Mössbauer do ^{57}Fe revelaram que os ETR podem ocupar sítios do ferro na estrutura dos precipitados amorfos. Posteriormente, estudou-se a influência de Ca e Zn solúvel na co-precipitação de ETR por precipitados de alumínio amorfos. Concluiu-se que o Ca exerce influência negativa na co-precipitação, bem como na adsorção de Pr e Eu em precipitados de alumínio amorfo. Por outro lado, a co-precipitação e adsorção dos elementos Nd e Sm não sofreram influência da presença

de Ca na solução. Finalmente, um estudo sobre a recuperação de ETR de DAM por co-precipitação com polímeros de Al_{13} utilizando $Ca(OH)_2$ para o controle de pH mostrou que aproximadamente 90% dos ETR presentes na amostra de DAM podem ser recuperados por co-precipitação com precipitados de alumínio amorfo. O precipitado contém aproximadamente 7% de óxidos de ETR. Os resultados do experimento de lixiviação ácida mostram que cerca de 60%, 65% e 85% dos ETR podem ser extraídos dos precipitados utilizando HCl 2 mol L^{-1}, H_2SO_4 1,7 mol L^{-1} e CH_3COOH2 mol L^{-1}, respectivamente. O potencial econômico da recuperação dos ETR também foi estimado considerando uma amostra de DAM do local estudado, revelando o grande potencial do tratamento da DAM combinado com a produção de ETR, em consonância com os Objetivos de Desenvolvimento Sustentável das Nações Unidas.

PALAVRAS-CHAVE: elementos terras raras, drenagem ácida de mina, recuperação de metais, hidróxidos de alumínio amorfos, polímeros de Al_{13}, oxihidróxidos de ferro amorfos, controle de pH.

CONTENTS

INTRODUCTION

Rare earth elements (REE) are a group of seventeen chemical elements displayed together in the periodic table, consisting of scandium (Sc), yttrium (Y) and the 15 lanthanide elements (La, Ce, Pr, Nd, Pm, Sm, Eu, Gd, Tb, Dy, Ho, Er, Tm, Yb and Lu). These elements have many similar properties and are used for different applications worldwide, especially in medicine, transport, communication, defence, among many others that are fundamental for the world's society. As REE are considered critical and strategic materials for many nations in the current globalized scenario, the concern about REE is gaining attention every day.

The search for new sources of REE is a current issue and researchers are constantly developing on novel techniques of recycling and recovering REE from secondary sources. Mine effluents generated during the base metal processing may present high concentration of trace elements, becoming a potential secondary source of REE. An important secondary source of REE being currently investigated is acid mine drainage (AMD), an effluent that can contain a considerable amount of these precious elements. AMD is a ubiquitous problem in base metal mineralization because the generation of acid water can lead to mineral solubilisation and, consequently, increase the mobilization of elements undesirable to the environment. Furthermore, as AMD is a serious environmental issue and demands treatment before discharge, the union of metal recovery and pollution control is something desirable when the goal is sustainability. Some techniques for REE recovery from AMD have been reported in recent literature, approaching nanofiltration, adsorption and co-precipitation.

The exposure of sulphide minerals to atmospheric conditions followed by AMD generation is observed in some gold (Au) and uranium (U) mines in Minas Gerais-Brazil. There is a closed uranium mine in the state of Minas Gerais-Brazil, under decommissioning, with the occurrence of AMD with extremely high concentrations of REE. This peculiar site became the object of study of the current research project due to its *sui generis* geochemical characteristics.

In this scenario, this investigation aimed at recovering REE from AMD effluents by co-precipitation techniques, approaching oxyhydroxides of aluminium and iron as the major co-precipitants.

The current thesis was divided in four chapters:

Chapter 1 approaches the role of amorphous aluminium precipitates in the recovery of REE from AMD by co-precipitation and reports a 'PHREEQC' geochemical model of the AMD system.

Chapter 2 approaches the role of iron in the co-precipitation of REE and uranium by Fe-Al-precipitates in AMD.

Chapter 3 approaches the influence of soluble calcium and zinc over the co-precipitation of REE by amorphous aluminium precipitates.

Chapter 4 addresses the recovery of REE by co-precipitation with Al_{13}-polymers from AMD using $Ca(OH)_2$ for pH control and brings a preliminary economic assessment of the purposed REE recovery activity.

Chapter 1

The role of Al_{13}-polymers in the recovery of rare earth elements from acid mine drainage through pH neutralization

MORAES, M. L. B.[1, 2], MURCIEGO, A.[2], ÁLVAREZ-AYUSO, E.[3], LADEIRA, A. C. Q. [1].

[1] CDTN, Centro de Desenvolvimento da Tecnologia Nuclear, Belo Horizonte, Brasil.
[2] Departamento de Geología, Facultad de Ciencias, Universidad de Salamanca, Salamanca, Spain.
[3]Instituto de Recursos Naturales y Agrobiología de Salamanca, Salamanca, Spain.

Paper published in Applied Geochemistry 113 (2020) 104466
https://doi.org/10.1016/j.apgeochem.2019.104466

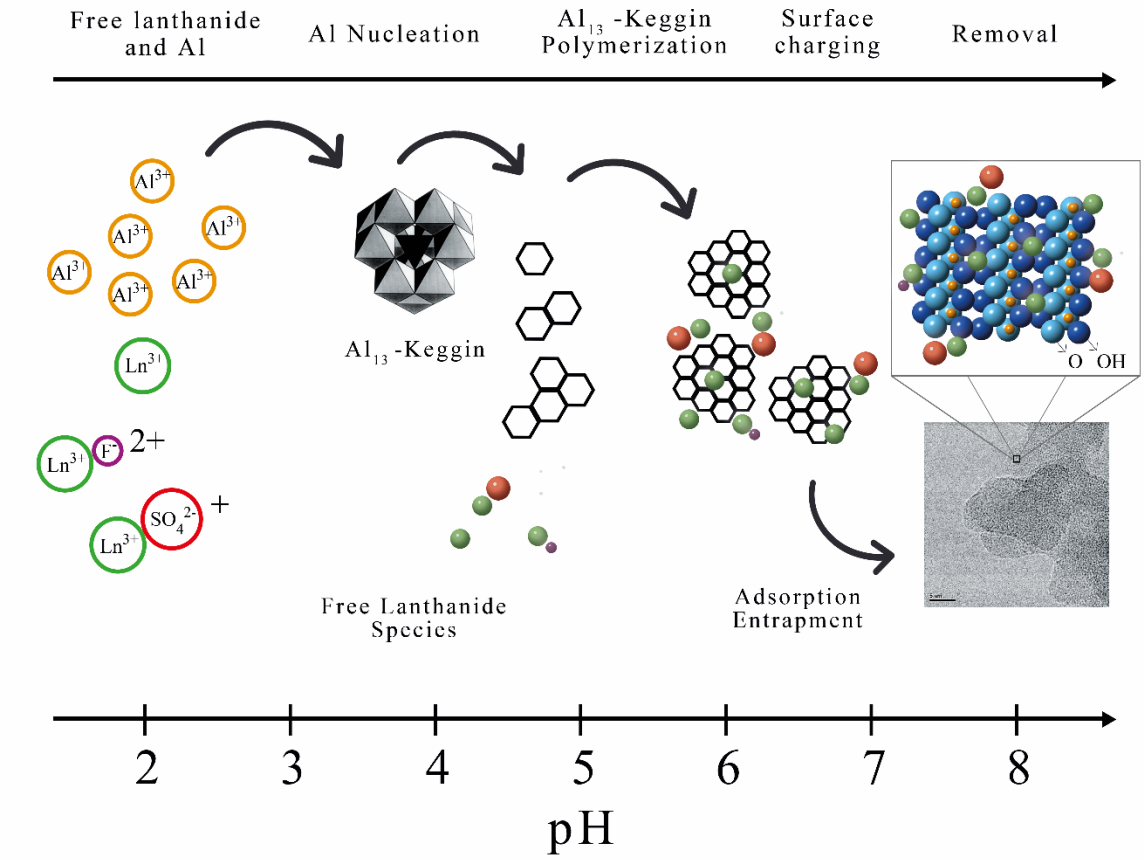

Abstract: Rare Earth Elements (REE) are crucial to the development of new technologies, given their strategic importance, a wide range of actions has been implemented to ensure sustainable and affordable supplies. Acid Mine Drainage (AMD) besides being one of the major environmental issues faced by the mining industry is a naturally occurring process involving a considerable amount of REE. The recovery of REE from AMD, which is considered a secondary source, has been investigated worldwide over the past few years aiming at sustainability. The current work seeks to provide an understanding of the geochemistry of the

REE in an AMD system and also of its respective treatment through pH neutralization, as a contribution to the development of novel REE recovery technologies. The approach proposed herein employed acid mine water and sediment sampling, ICP-OES, XRD, SEM-EDS, TEM, ^{27}Al MAS-NMR and XPS analysis, BCR sequential extraction and geochemical modelling by PHREEQC. The results showed that the REE content in the AMD investigated is very high being Ln^{3+}, $LnSO_4^+$ and LnF^{2+} the dominant species in the impoundments at pH ± 3.5. The neutralization of the AMD with an alkali agent promoted a high REE recovery and produced an amorphous precipitate containing 14% of REE oxides. This precipitate contains Al_{13}-polymers and accounts for the REE removal when the pH is raised to 8, thus promoting adsorption and entrapment simultaneously. Sequential extraction revealed that the REE could be efficiently leached with the use of acetic acid, thus supporting novel and promising recovery technologies through co-precipitation processes.

Keywords: rare earth elements, metal recovery, acid mine drainage, Al_{13}, pH neutralization, co-precipitation.

1. INTRODUCTION

Acid mine drainage (AMD) is an important environmental issue resulting from chemical and bacterial oxidation of sulphide minerals, such as pyrite (FeS_2) when exposed to atmospheric conditions during the mining of metal ores and coal (Akcil and Koldas, 2006; Blowes et al., 2013). Acidic waters contain a wide array of metals and sulphur species, mainly sulphate. The dissolved metals can eventually reach rivers, groundwater and lakes causing adverse effects to both flora and fauna. Depending on the mineralization, REE can occur in significant concentrations.

REE are currently an important strategic resource many developing and developed countries depend on, and the increasing concern about the global reserves and supply has encouraged the search for alternative sources. High technology products depend heavily on REE- and some of them, mainly Y, Nd, Eu, Dy and Tb (BAUER et al., 2010; PAULICK; MACHACEK, 2017) are considered critical by the United States of America, however all of them are currently considered equally critical raw materials by the E.U. (EUROPEAN UNION, 2017). Nevertheless, world mineable REE reserves are not evenly distributed. Given this scenario,

Brazil is quite a strategic country, as it is endowed with one of the world's largest reserves, together with China and Vietnam, however, production is still incipient (U.S. GEOLOGICAL SURVEY, 2019).

Studies about the recovery of metals and by-products from liquid effluents have been a constant issue among researchers. Some techniques used in the recovery of REE from liquid effluents, including ion exchange, solvent extraction and co-precipitation have been investigated thoroughly (JHA et al., 2016; ZHANG; HONAKER, 2018), however, there is still a lot to be done. Currently, there has been a common tendency to consider AMD as a secondary source of REE, and the recovery of these valuable elements could provide a revenue source and therefore reduce the costs of AMD treatments. The concentration of an array of elements present in AMD is high enough to justify recovery, REE are amongst them (AYORA et al., 2016). As a result, methods used in the recovery of such elements must be efficient and cost-effective (NORDSTROM et al., 2017; ZHANG; HONAKER, 2018).

The complexity of the interactions between soluble ions and solid phases in AMD depends on the chemical composition of each system, which is directly related to the local environment (geology, climate, hydrology, ecology, etc.). Amongst the possible chemical interactions, adsorption/co-precipitation of REE (also known as "scavenging"), mainly by Al, Mn and Fe oxyhydroxides, is a natural process being investigated by various researchers worldwide (AYORA et al., 2016; BARCELOS et al., 2018; ERICKSON, 2018; PIETRALONGA et al., 2017; PRUDÊNCIO et al., 2015, 2017; SOYOL-ERDENE et al., 2018; STEWART et al., 2017; ZHANG et al., 2015). Co-precipitation is uppermost in the development of novel, efficient and sustainable technologies addressing the recovery of REE from AMD. Sustainability is humankind`s big issue.

The present study focuses on shedding light on the REE geochemistry in an AMD system present in a uranium mine in Brazil; it contemplates the recovery of REE through co-precipitation processes. The current investigation also evaluates the chemistry and mineralogy of the REE-rich precipitates resulting from the AMD alkali treatment. The approach followed in the research employs acid mine water and sediment sampling, microscopy and spectroscopic techniques, co-precipitation experiments, sequential extraction as well as geochemical modelling. Throughout the investigation, Al_{13}-polymers were found to play an important role in the REE removal when treating AMD by pH neutralization, given the adsorption and

entrapment of REE in the precipitate, which is also discussed in this paper. Furthermore, the leaching of the precipitate with acetic acid proved considerably efficient in the REE recovery.

2. SITE DESCRIPTION

The uranium deposit in the Mesozoic alkaline complex of Poços de Caldas (Minas Gerais, Brazil) is a product of subsequent hydrothermal and supergene processes. The lithology of the mine is composed of a sequence of volcanic and subvolcanic phonolites and nepheline syenite intrusions, similar to those of the regional alkaline complex; there is also the occurrence of volcanic breccia pipes characterized by U-Th-Zr-REE mineralization concentrated in the matrix (WABER; SCHORSCHER; PETERS, 1992). Uraninite (UO_2) and brannerite ($(U,Ca,Ce)(Ti,Fe)_2O_6$) are the main U-carriers and monazite ($(REE, Th)PO_4$) represents the major REE-bearing mineral.

The occurrence of uranium in the aforementioned deposit was detected in 1948, but it was not until 1964 that the first exploration and geological investigation began. The operations initiated in 1982 and were interrupted in 1995 (FLORES, 2006). The site is located in the municipality of Caldas in the southwestern region of the state of Minas Gerais (Brazil) (Fig. 1).

Currently, the mine is under decommissioning and, as the AMD is the main environmental issue, different techniques for its treatment are under investigation (FERNANDES; FRANKLIN; VEIGA, 1998; LADEIRA; GONCALVES; MORAIS, 2011; NÓBREGA; LIMA; LEITE, 2008). The major sulphide mineral accounting for the generation of AMD in the waste rock piles is Pyrite (FeS_2) (FONSECA, 2009; WABER; SCHORSCHER; PETERS, 1992). There are two main waste rock piles in this mine, whose drainage flows into two distinct impoundments and then is pumped to a treatment plant. One of the impoundments is named BIA and the other BNF. They are located to the southwest and northeast of the open-pit mine, respectively (Fig. 1).

Due to the complex mineralogy of the waste rock, a wide range of elements, such as U, Th, Mn, REE are found in the AMD (MIEKELEY et al., 1992), which, in order to meet the concentrations required by government regulators (CONAMA, 2011) are treated with lime before being discharged into the environment (FONSECA, 2009). The flow rate of the AMD treatment plant stands between 150 and 300 $m^3 h^{-1}$ and the neutralization of the acidic waters consumes about 12 t of lime daily, producing a considerable volume of precipitate, which is currently stored in the mine open pit (FONSECA, 2009). This treatment is considerably costly.

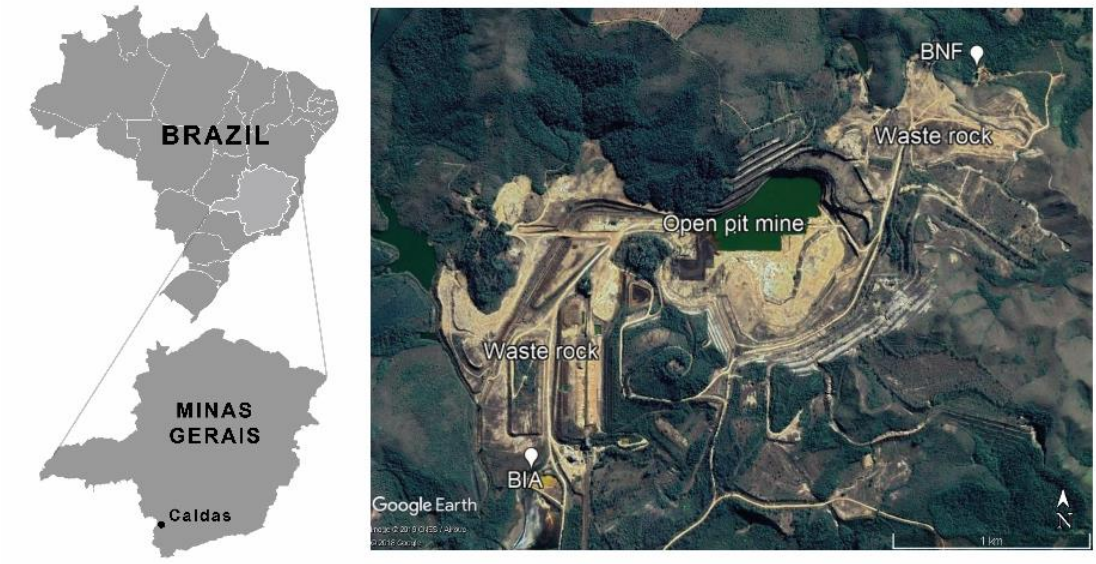

Fig. 1 - Location and satellite image of the uranium open-pit mine, waste rock piles and the BIA and BNF acid mine drainage impoundments.

3. MATERIALS AND METHODS

3.1. Sampling and sample manipulation

The sampling of the water and sediments collected at the BIA and BNF impoundments was carried out on February 17, 2018. The water samples were coined W1 and W2 and the sediment samples coined S1 and S2 for the BIA and BNF impoundments, respectively. The water samples were collected on the water surface of each impoundment with the use of a water-sampling plastic bucket hanging in a nylon rope. A Digimed DM-22 Eh/pH meter with a hydrogen electrode was used to measure the pH and a platinum electrode was employed to determine the redox potential. The water samples for chemical analysis were vacuum filtered through a 0.45 μm nitrocellulose membrane, then stored in acid-cleaned polyethylene bottles, immediately acidified with two drops of concentrated nitric acid and refrigerated at 4°C prior to the analysis. The sediment samples from the bottom of each impoundment were collected with a stainless steel sediment-sampling bucket, also hanging on a nylon rope. The sediments were stored in polyethylene containers filled to the brim to prevent the presence of air, then closed with a lid and sealed with a plastic film and subsequently refrigerated at 4°C prior to preparation. The preparation of the sediment samples consisted in vacuum filtering, drying in an oven at 50°C, disaggregating and sieving through a 150 μm pore size stainless steel sieve.

A third AMD water sample, coined W3 was also investigated. This sample was provided by the mining company and consisted in the W1 water sample whose Mn and Ce were removed by ozonation and the removal of U and Th occurred by ionic exchange. The W3 sample was the one used to produce the precipitate that could be studied in depth, bearing in mind the feasibility of recovering REE from AMD. The, W3 sample was stored in 50 L polyethylene containers at room temperature. For the precipitation experiment, 20 L of the sample was mixed with KOH 2 mol L^{-1} to raise the pH to 8, aiming at simulating the treatment that the AMD is subjected to before being discharged into the environment (FONSECA, 2009). The precipitate obtained was left to decant with the addition of 0.2 μg L^{-1} of gelatinized starch (inert flocculant agent) in glass separation funnels for 1 h, centrifuged at 6000 g, dried at 50°C and stored in polyethylene bottles at room temperature before analysis. This precipitate was coined P3.

Potassium hydroxide was chosen instead of sodium hydroxide to prevent the precipitation of rare earth double sodium sulphate (ABREU; MORAIS, 2010; PORVALI; WILSON; LUNDSTRÖM, 2018), which could lead to a misunderstanding of the REE co-precipitation process. Furthermore, lime was not chosen as the alkali agent, in order to prevent the excess of non-dissolved calcium carbonates, which could lead to experimental and analytical complications and wrong interpretations of the aluminium precipitates removal process.

3.2. Analysis

The chemical composition of the water samples was determined mainly by inductively coupled plasma optic emission spectrometry (ICP-OES) via a SPECTRO ARCOS® apparatus, performed at the CDTN facilities. The sulphate content was determined by turbidimetry and the fluorine content was determined by a selective electrode.

The sediment samples of the two impoundments (S1 and S2) alongside the precipitate (P3) were characterized by powder X-ray diffraction (XRD) with the use of a RIGAKU® X-ray diffractometer under Cu Kα radiation (λ = 0.15418 nm). The equipment was operated at a tube voltage of 40 kV and a tube current of 30 mA with a scanning rate of 4° min^{-1}, from 4 to 80°2θ and a step size of 0.02°. Scanning electron microscopy and energy-dispersive X-ray spectroscopy analysis (SEM-EDS) were also used in the characterization of the samples, with the use of a ΣIGMA-Zeiss® microscope. For these analyses, the dried samples were sieved through 150 and 37 μm pore size stainless steel sieves.

The chemical composition of the P3 precipitate was determined by ICP-OES after digestion with aqua regia. This sample was also submitted to the BCR sequential extraction, as proposed by Rauret et al. (1999). The first step of the sequential extraction was performed by using acetic acid (CH_3COOH 0.11 mol L^{-1}), which extracts the exchangeable fraction and the fraction soluble in weak acid. In the second step, the extraction of the REE was carried out by using hydroxylammonium chloride ($HONH_2 \cdot HCl$ 0.5 mol L^{-1}), which dissolves the reducible fraction of the precipitates. The third step, which extracts the oxidizable fraction, was not carried out in the present study, considering that there were no oxidizable components in the sample. The chemical composition of the extracts was determined by ICP-OES, as aforementioned. The residual phase resulted from the difference between the total content (obtained by aqua regia digestion) and the sum of steps one and two. All extraction experiments were performed in duplicate.

Transmission electron microscopy (TEM) and associated techniques (SAED – selected area electron diffraction, HAADF-STEM - high-angle annular dark-field scanning transmission electron microscopy and EDS mapping), as well as ^{27}Al magic angle spin nuclear magnetic resonance (^{27}Al MAS-NMR) analysis were done to determine the structure of the P3 sample. TEM imaging and related analysis were carried out by a JEM 3000F microscope operating at 300 kV. The ^{27}Al MAS-NMR spectrum was collected at 104.26 MHz by a BRUKER AVANCE 400MHz WIDE BORE and the sample was spun at 12 kHz. The ^{27}Al chemical shifts (δ) are reported in parts per million (ppm), i.e. Hz/MHz, relative to 1 mol L^{-1} $AlCl_3$ solution.

The P3 sample was subjected to X-ray photoelectron spectroscopy (XPS) so that the elements present on the surface of the material could be identified. A VG surface analysis system equipped with a CLAM 2 electron analyser and a monochromatized Mg Kα radiation (1253.6 eV) was used in this analysis. Magnesium radiation was chosen to prevent the superposition of the oxygen KLL signal over the lanthanides 3d binding energies (MOULDER et al., 1995). The C 1s signal (284.6 eV) was employed as a reference in the calibration of the binding energies (BE) of the elements detected. The CasaXPS software was used to process and analyse the data obtained. Survey spectra were acquired considering a step size of 1 eV and a CAE of 200.

3.3. Study of the effect of the pH and particle size of the precipitates on REE removal

An aliquot of 500 mL of each of the W1 and W2 samples was mixed with increasing volumes of KOH 2 mol L^{-1} under stirring to adjust the pH to 4, 5, 6 and 7 two hours after collection. Immediately afterwards, the suspensions were vacuum filtered through nitrocellulose

membranes with pore sizes of 0.45, 0.20 and 0.10 µm, so that the influence of the particle size of the precipitate on the removal of the REE for each defined pH could be assessed. A Digimed DM-22 hydrogen electrode was used for the pH measurement. The chemical composition of the filtrates was determined by ICP-OES as aforementioned, this assessment was based upon the works of Verplanck et al. (2004) and Verplanck (2013).

3.4. Geochemical modelling with PHREEQC software

PHREEQC is a computer program for simulating chemical reactions and transport processes. It is a useful tool employed in various research and industrial activities. This program is based on the equilibrium chemistry of aqueous solutions interacting with minerals, gases, solid solutions, exchangers, and sorption surfaces. It stands for the original acronym - pH-REdox-EQuilibrium (PARKHURST; APPELO, 2013).

The chemical modelling was based on the chemical composition of the W3 sample and was carried out by the PHREEQC V3.4.4 computer program. Some diagrams were plotted by the software PhreePlot (KINNIBURGH; COOPER, 2016). The databases used in the modelling were the *LLNL.dat*, provided by the Lawrence Livermore National Laboratory (USA) and the *Thermoddem_V1.10.dat* (BLANC et al., 2012). The speciation of the REE was modelled by using the *Thermoddem_V1.10.dat* following the method proposed by Lozano et al. (2019), except for Y, whose model was calculated by using the *LLNL* database, which was considered more appropriate for it contains yttrium-sulphate complexes, reactions and equilibrium constants.

The saturation indexes and the Al speciation modelling were calculated by using the *LLNL* database rather than by the *Thermoddem*, taking into account the fact that the former is more complete as far as reactions and equilibrium constants related to aluminium complexes are concerned. This choice was made based on the fact that the *LLNL* database contains the Al_{13}-Keggin ion (i.e. the $Al_{13}O_4(OH)_{24}^{7+}$ complex).

The surface complexation model considering hydrous ferric oxide (Hfo) as the adsorbent was calculated by using the *LLNL* database, fed with the constants concerning REE sorption on Hfo, as proposed by Liu et al. (2017). For this modelling, two assumptions were made: (i) the Al precipitates might have a similar behaviour to the Hfo, in relation to the REE sorption, owing to their analogous structure (FURRER et al., 2002; WEATHERILL et al., 2016); (ii) the specific surface area considered was equal to 600 $m^2\ g^{-1}$ (PARKHURST; APPELO, 2013); the strong

and week sorption sites densities were stabilised as 0.001 and 0.1 mol/mol Fe, respectively (LIU et al., 2017) and the mass of the adsorbent was equal to 0.17 g L^{-1}, assuming that all the Al content of the W3 sample precipitates and consequently all the soluble REE co-precipitate.

4. RESULTS AND DISCUSSION

4.1. Water samples characterization

The chemical compositions of the W1, W2 and W3 samples are compiled in Table 1. The results show high concentrations of Ca, Al and Zn, as well as expressive concentrations of REE, mainly the light ones. The three samples have similar REE concentrations, except for Ce, which was previously removed from the W3 sample through ozonisation pre-treatment, proceeded for Mn precipitation. The heavy REE elements are less abundant in all samples, especially the ones having odd atomic numbers, such as Ho, Tm and Lu, whose concentrations are below detection limits; holmium was an exception in the W3 sample. The sulphate content is also high, as expected for AMD, mainly due to the oxidation of pyrite, assigning 1000 mg L^{-1} for the W1 sample, 900 mg L^{-1} for the W2 sample and 618 mg L^{-1} for the W3 sample. Fluorine was also detected, being 88, 110 and 116 mg L^{-1} for the W1, W2 and W3 samples, respectively.

A comparison between the lanthanide composition according to NASC-normalized (North American Shale Composite) of the W1 sample and other works carried out around the world addressing AMD is depicted in Fig. 2. Due to the similarity in the samples composition W1 was used to represent all samples investigated. The evidence of the high content of REE in the AMD of the uranium mine studied is clear. It is much higher than any other data presented in the literature, being at least one order of magnitude higher than what is found in the Metalliferous Hills in Italy, which is considered high for AMD systems. Looking closely, the concentrations of the light REE investigated in the current study meet the NASC. It is also noticeable that the U concentration of the samples analysed is considerably high, hence justifying the sustainability-focused effort of the company to promote the recovery of this element through an ionic exchange treatment.

Table 1 - Chemical composition of the AMD water samples (mg L^{-1}).

	W1	W2	W3	DL[(a)]
pH	3.4	3.6	2.5	-
Eh (mV)	664	774	791	-
F	88	110	116	0.3
Cl	5.29	4.21	14.1	0.009
SO_4^{2-}	1000	900	618	0.1
Na	3.18	1.62	4.25	0.001
K	12.9	9.7	15.6	0.001
Mg	8.1	7.6	12.8	0.005
Ca	120	103	180	0.005
P	0.174	0.157	0.338	0.009
Al	127	118	172	0.004
Si	17.3	13.0	19.1	0.003
Mn	91.9	85.0	8.2	0.001
Fe	12.5	0.396	1.75	0.002
Co	0.091	0.066	0.009	0.002
Ni	0.083	0.128	0.510	0.002
Mo	0.078	0.068	0.121	0.001
Zn	14.9	13.4	21.3	0.001
Cd	0.044	0.043	0.078	0.001
Sc	< DL	< DL	<DL	0.002
Y	3.49	3.05	4.69	0.002
La	33.1	28.9	48.6	0.001
Ce	27.9	22.7	<DL	0.003
Pr	3.53	2.84	4.92	0.003
Nd	10.1	7.7	14.3	0.002
Sm	1.26	0.872	1.55	0.002
Eu	0.474	0.347	0.683	0.002
Gd	0.889	0.597	1.08	0.001
Tb	0.033	< DL	0.109	0.002
Dy	0.616	0.476	0.818	0.001
Ho	< DL	< DL	0.016	0.001
Er	0.015	< DL	0.198	0.003
Tm	< DL	< DL	<DL	0.001
Yb	0.111	0.090	0.067	0.001
Lu	< DL	< DL	<DL	0.001
U	5.28	5.28	0.935	0.016
Th	0.161	0.148	0.047	0.002

(a) Detection Limit

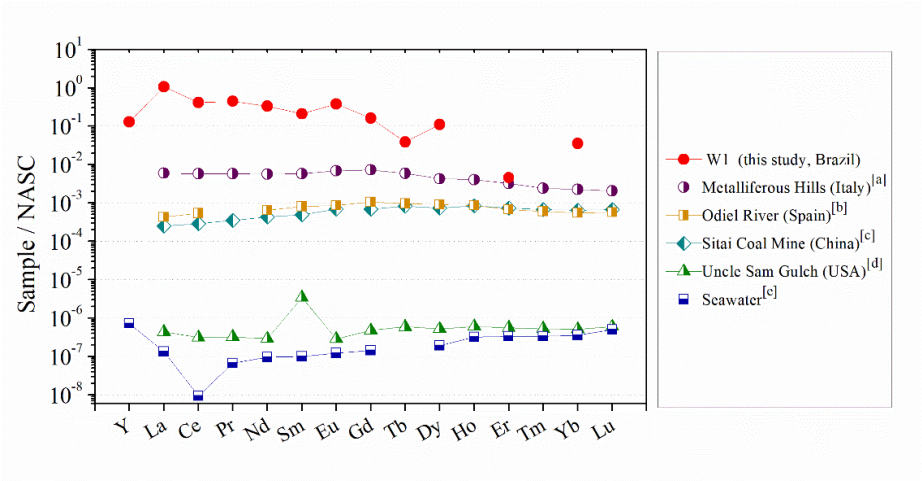

Fig. 2- NASC-normalized REE diagram for the AMD investigated (W1), other AMD water samples and seawater. (References: [a] Protano and Riccobono, 2002; [b] Elbaz-Poulichet and Dupuy, 1999; [c] Zhao et al., 2007; [d] Verplanck et al., 2004; [e] Rollinson, 1993)

4.2. Sediments characterization

The sediments of the two impoundments (S1 and S2) are composed mostly of poorly-crystalline Al, Si and Fe oxyhydroxides, as revealed by SEM-EDS analysis (Fig. 3). In addition, microcline, kaolinite, hematite, goethite, gibbsite and muscovite were identified by XRD analysis (Fig. 4). The intensities of the peaks were considered low, with a maximum of 60 counts per second, indicating low crystallinity and small crystallite size of the minerals present in the sediments. It is pertinent to affirm that most of these minerals, ubiquitous in soils, are carried to the impoundments by flash flood containing eroded soil particles; they probably do not precipitate in situ. On the other hand, the fine particle fraction of the sediments (<37 μm) should be considered "fresh", precipitating in situ. In both impoundments, the coarse fractions of the sediments (<150 μm and >37 μm) are aggregates composed mainly of small spheres (Fig. 3-S1|S2-a-b), detailed in the fine particle fraction.

The fine particle fraction (Fig. 3- S1|S2-c) consists of small spheres (diameter of 0.5 to 2.5 μm in average) and these spheres are formed by small units (flocs) composed mainly of Al, Si and Fe oxyhydroxides, sulphur and potassium, as revealed by SEM-EDS analysis (Fig. 3-S1|S2-d-j). There is a probability that sulphur occurs in the form of adsorbed SO_4^{2-} and potassium might be adsorbed as K^+. Definitely, no REE were detected, revealing that at low pH values, around 3.5, the REE remain in the dissolved phase - in accordance with the findings of Bau (1999) and Verplanck (2013). The spheres observed in the fine fraction of the sediments resemble schwertmannite ($Fe^{3+}_{16}O_{16}(OH)_{12}(SO_4)_2$), as found in a passive AMD treatment system in Spain (CARABALLO et al., 2009). Nevertheless, there are neither peaks related to schwertmannite nor any sulphate-bearing minerals in the XRD powder patterns (Fig. 4).

Assuming that the fine phase (<37 μm) of the sediments represents the solid phase in equilibrium with the AMD in each impoundment (solid-liquid equilibria), it is possible to anticipate the solid phases that could be formed by precipitation by using a computational geochemical model, through the software PHREEQC. This geochemical model is an important tool for the definition of the mineralogy of the sediments and of the precipitate formed by pH neutralization, as will be discussed further on. The mineralogy of the solid samples could not be fully described by XRD analysis alone due to the small crystallite size and low crystallinity of the minerals, as suggested by the low intensity of the peaks (Fig. 4).

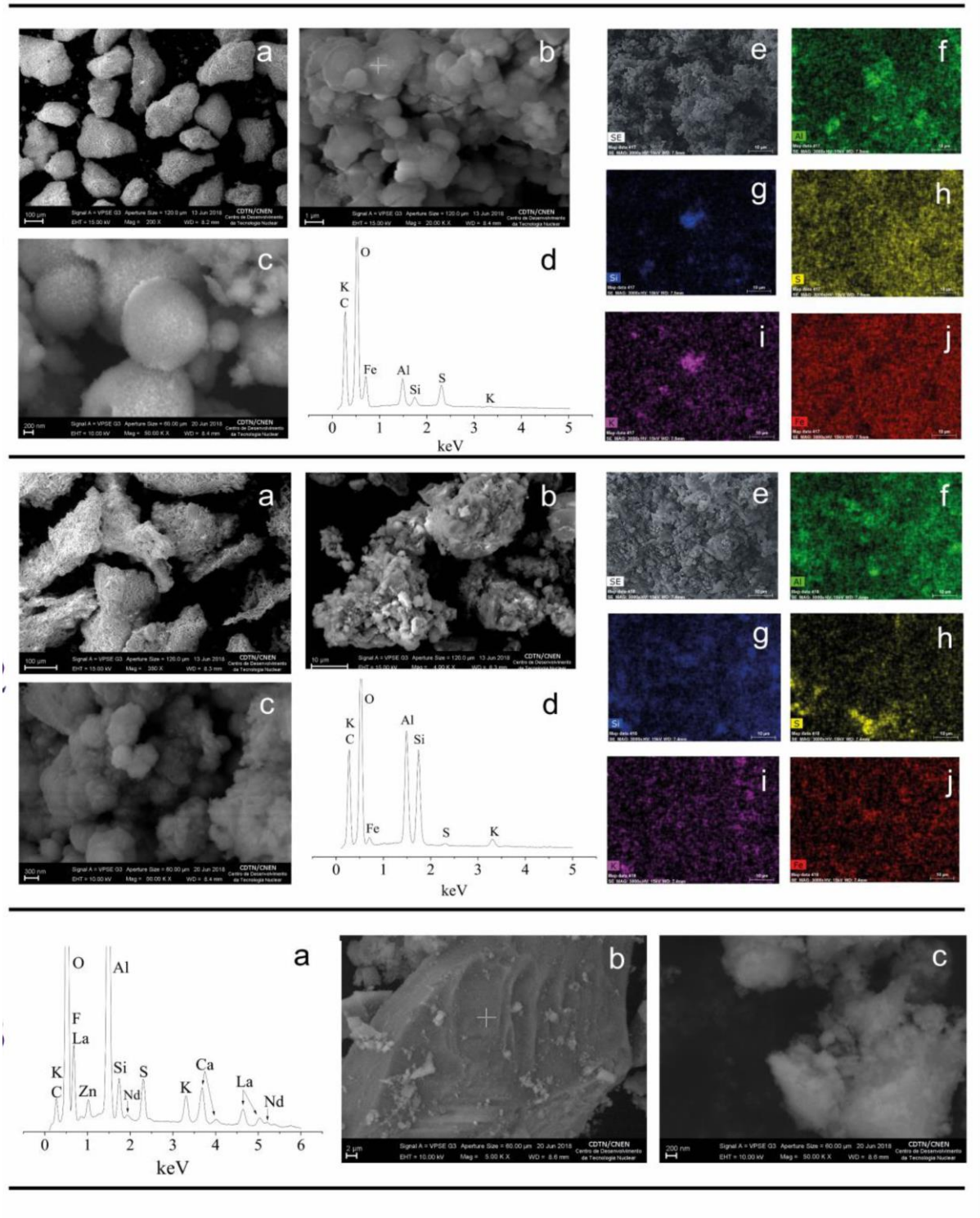

Fig. 3 - Secondary electron images of the S1, S2 and P3 samples. S1: (a) coarse fraction (200x); (b) fine fraction (5,000x); (c) fine fraction (50,000x); (d) EDS spectrum of the spot shown in b; (e) Secondary electrons image used for element mapping; (f-j) Al, Si, S, K and Fe mapping, respectively. S2: (a) coarse fraction (350x); (b) fine fraction (4,000x); (c) fine fraction (50,000x); (d) EDS full area spectrum shown in e; (e) Secondary electrons image used for element mapping; (f-j) Al, Si, S, K and Fe mapping, respectively. P3: (a) EDS spectrum of the spot shown in b; (b) raw precipitate (5,000x); (c) fine fraction, <37 μm (50,000x).

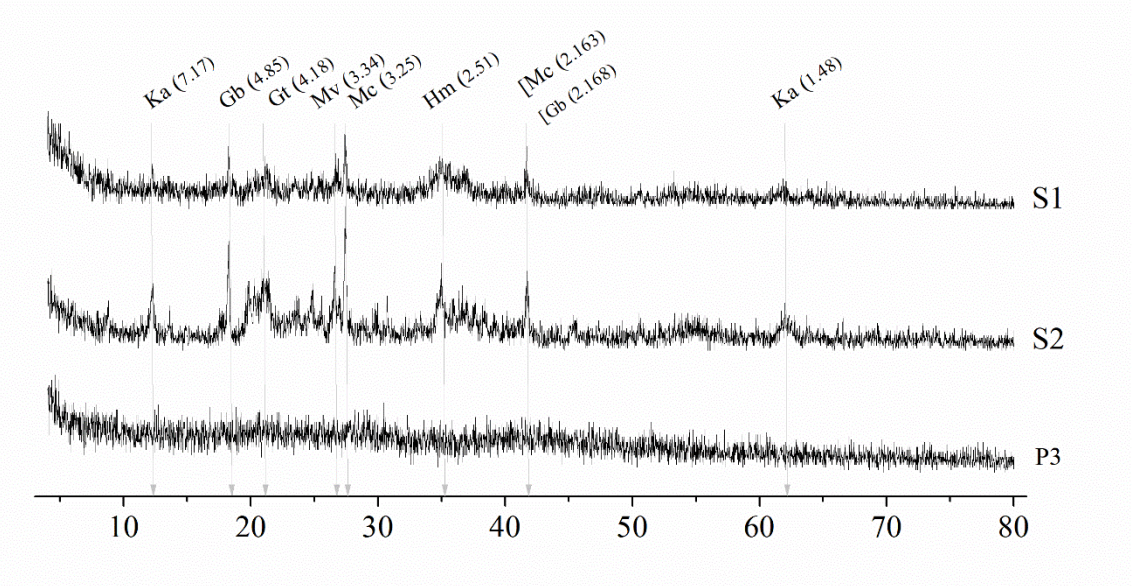

Fig. 4 - XRD powder patterns of the S1, S2 and P3 samples. [Legend: Kln = kaolinite; Gbs = gibbsite; Gt = goethite; Ms = muscovite; Hm = hematite; Mc = microcline. Labels are followed by identified d-spacing in Å in brackets].

4.3. P3 sample characterization

The precipitate obtained from the W3 sample through pH neutralization (P3 sample) did not present any peaks when analysed by XRD, therefore, it was considered amorphous (Fig. 4). SEM analysis revealed that the material did not appear in any sphere-like shape, contrary to those found in the S1 and S2 fine particle fraction. In fact, the precipitate looks like small flocs composed by tiny particles that cannot be individualized at a magnification of fifty thousand times (Fig. 3-P3-c). EDS analysis revealed that the precipitate is composed of Al, Si, K, Ca, Zn, F, S, La and Nd (Fig. 3-P3-a) homogeneous and no segregation was detected.

A closer observation of the P3 sample was possible through the TEM bright-field images (Fig. 5-a-c), revealing the rounded-corner pseudo hexagonal sheet-like shape of the nanomaterial, which has an average size of 20 nm, resembling a plate-like boehmite, as reported by Souza Santos et al. (2009). Iijima et al. (2016) reports atomic organization in the pseudoboehmite nanowires at high magnifications; however, this occurrence was not visualised in the present work. No electron diffraction pattern (Fig. 5-c), as those reported for milled boehmite (γ-AlOOH) by Alex et al. (2016) was observed, suggesting the lack of an identifiable well-defined crystal structure, thus ratifying the amorphous diagnosis. The HAADF-STEM images (Fig. 5-d-f) show that the P3 precipitate is very similar to the $Al(OH)_3$ precipitates reported by Lin et

al. (2009). Moreover, no segregation of any element could be identified, as depicted in Fig. 5-g. The element mapping by EDS analysis revealed that the nanomaterial is uniformly composed of Al, Si, K, Ca, Zn, S, La, Nd and Y, corroborating the results obtained by SEM-EDS analysis (Fig. 3-P3-a). The smaller detection limits of the TEM technique, when compared to SEM, allowed the identification of Y in the precipitates.

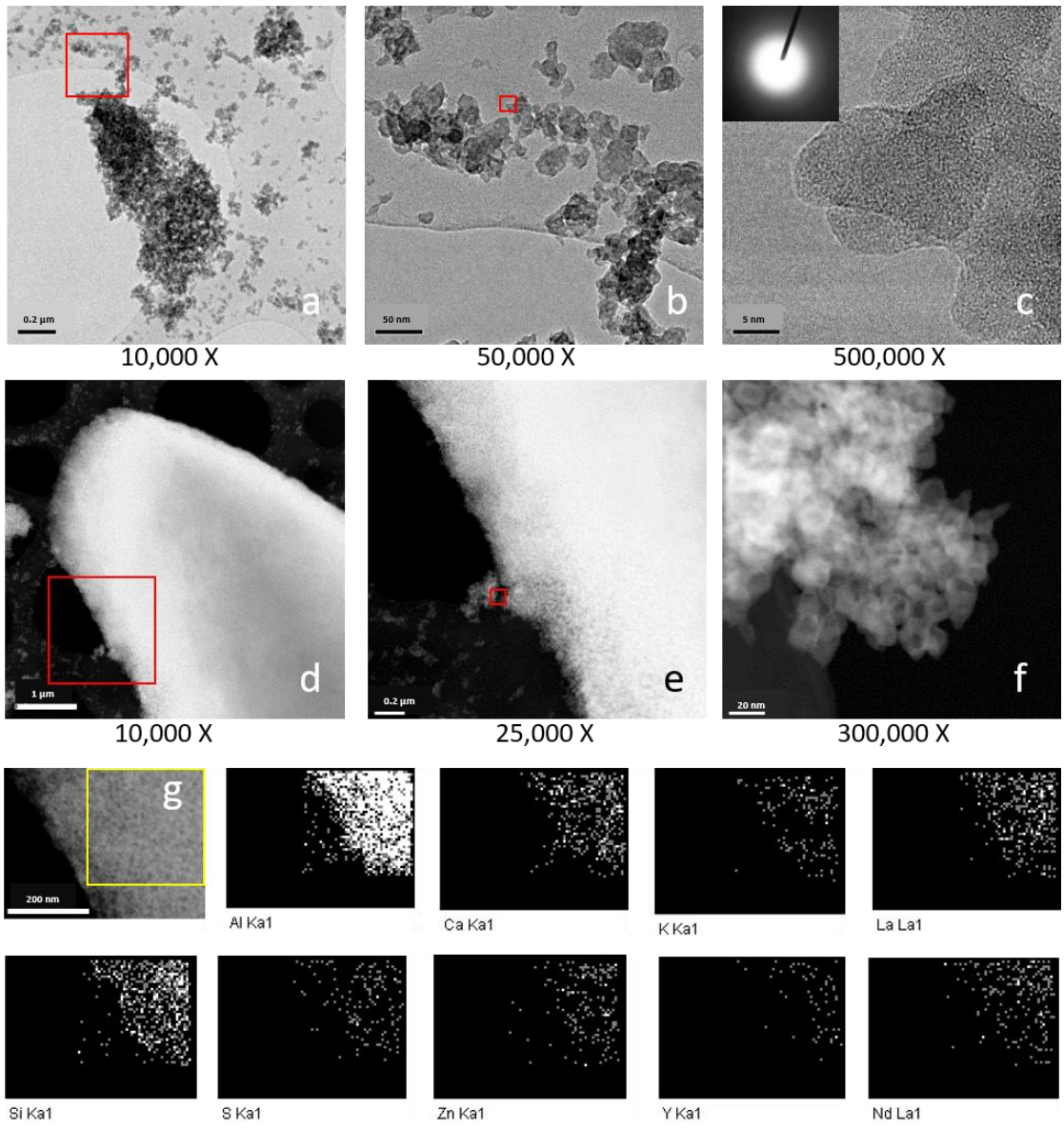

Fig. 5 - TEM images of the P3 sample. (a-c) Bright-field images, the square in c shows the SAED pattern; (d-f) HAADF-STEM images; (g) HAADF-STEM image used in the EDS mapping and element maps; elements are followed by their characteristic X-ray lines analysed.

The formation of hydrolysed aluminium polymers in water systems (Al gels, sol-gel, Al oxyhydroxides, Al_{13}-Keggin polymers, etc.) is a phenomenon which has been thoroughly investigated (BOTTERO et al., 1987; CASEY; PHILLIPS; FURRER, 2010; FURRER; LUDWIG; SCHINDLER, 1992; FURRER; TRUSCH; MÜLLER, 1992; LIU; ZHAO, 2010). The Al amorphous precipitates were previously reported as having a sheet-like morphology - also referred to as "wrinkled tissue paper" or super-amorphous gels (WEFERS; MISRA, 1987), resembling the morphology of the P3 precipitate.

Furrer et al. (2002) showed that the aluminium flocs commonly found in polluted streams originate mainly from the condensation of Al_{13}-Keggin ($Al_{13}O_4(OH)_{24}^{7+}$) molecules composed of one central tetrahedrally coordinated Al atom surrounded by 12 octahedrally coordinated Al atoms (BOTTERO et al., 1987). The ^{27}Al MAS-NMR results revealed the presence of both Al(6) and Al(4) (Fig. 6-a). The chemical shift peak at 4.93 ppm is indicative of the octahedrally coordinated aluminium, whereas the peak at 58 ppm is presented in the literature as corresponding to a tetrahedrally coordinated aluminium (FURRER et al., 2002; KIM, 2015). Therefore, in addition to the XRD and TEM results, the ^{27}Al MAS NMR spectrum suggests that the precipitate is made up of an amorphous phase formed by the condensation/aggregation of Al_{13}-Keggin ions and Al_{13}-polymers - in accordance with the findings of Furrer et al. (2002), Kim (2015) and Leetmaa et al. (2014).

These Al_{13}-Keggin polymers form rapidly and then aggregate when the pH of the effluent reaches the value of 5. Each of the octahedra carries one terminal water ligand, which means that Al_{13}^{7+} is a polyprotic acid bearing 12 identical functional groups. The deprotonation of the terminal water ligands generates hydroxyl groups that exhibit excellent binding characteristics, similar to those observed in aluminium hydroxide surfaces. The deprotonation of the Al_{13}^{7+} species starts around pH 6, depending on the total concentration of the polymer, causing aggregation and subsequent precipitation of the polymers (FURRER; TRUSCH; MÜLLER, 1992; LOTHENBACH; FURRER; SCHULIN, 1997). This phenomenon, alongside the large specific surface area of the precipitate, may result in the removal (co-precipitation/adsorption) of other metals in solution, such as the trivalent REE in the AMD, as observed in the present study.

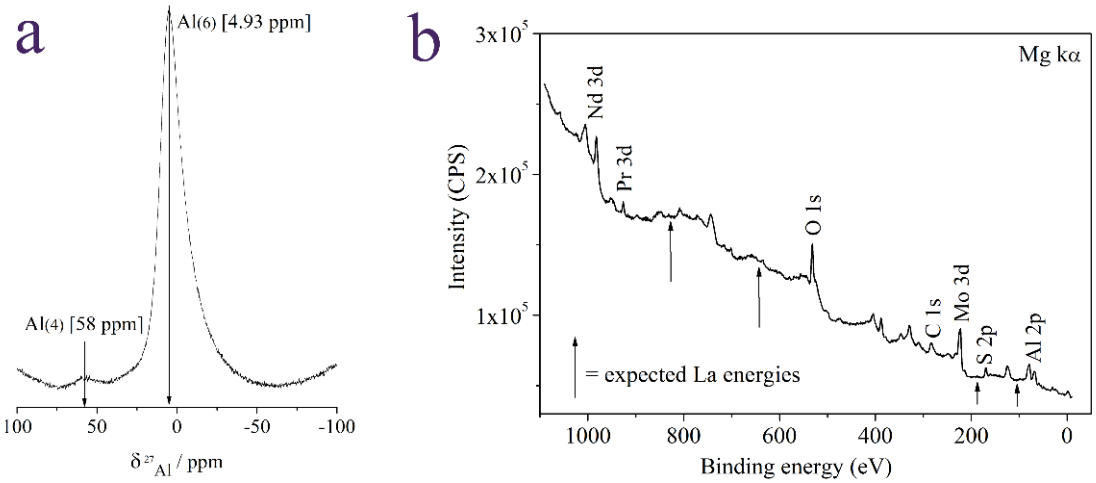

Fig. 6 – (a) ^{27}Al MAS-NMR spectrum of the P3 sample. (b) XPS spectrum of the P3 sample. Note: In the XPS spectra, the C 1s signal refers to the carbon tape used to hold the powder and the Mo 3d signal refers to the sample holder.

The P3 sample was submitted to XPS analysis so that the chemical composition of the surface of the material could be assessed, which contributed to the understanding of the REE removal process. The results showed that only praseodymium and neodymium were detected at the surface of the Al_{13}-polymers (Fig. 6-b) and the peaks detected in the Pr and Nd 3d orbitals agree with those reported for REE hydroxides by Mullica et al. (1995), the observations aforementioned also meet findings reported by Moulder et al. (1995) for REE oxides. Therefore, neither lanthanum (the most abundant REE) nor yttrium were identified in this analysis, however, these elements were detected by STEM-EDS mapping (Fig. 5-g). In conclusion, the amount of Pr and Nd on the surface of the Al_{13}-polymers was high enough to make it detectable by XPS analysis, which means that these elements are most probably adsorbed on the surface of the precipitate.

The BCR sequential extraction of the P3 sample revealed that high dissolution of each REE was attained, i.e. over 80% in the first step, except for La and Y (about to 50% and 60%, respectively), as depicted in Fig. 7. The overall extraction of the total REE was about 60% in this step. In the case of Al, Mn and Fe, the first step of the BCR extraction revealed a relatively high solubility of the precipitate, supporting the general understanding of its amorphous nature, as revealed by XRD, SEM and TEM analysis. The results for Al extraction with acetic acid

revealed that the Al_{13}-polymers could not be fully solubilized in the first step (pH = 2.8), as predicted by the geochemical modelling discussed below.

Considering that Y and La extraction in the first step were lower than figures presented by the other REEs and a high amount of these elements remained in the residue, a fraction of the Y and La is believed to have been trapped in the structure of the precipitate, corroborating the XPS results. The same seems to happen to U, which remains mostly in the residue. Differently, the behaviour of Pr, Nd, Sm and Gd suggests that these elements are in all probability adsorbed on the surface of the precipitate, as they are soluble in acetic acid – the first step of the sequential extraction.

The concentration of the REE in the P3 sample is expressively high, about 14% of REE oxides (Fig. 7), being much higher than the concentration of the REE in some ores found in Brazil - 5% of REE oxides (LAPIDO-LOUREIRO; SANTOS, 2013). The possibility of acetic acid leaching as well as the presence of 2.5% of Nd_2O_3 in the precipitate highlights and reinforces the importance of the findings obtained in the current study concerning a selective recovery of this valuable element.

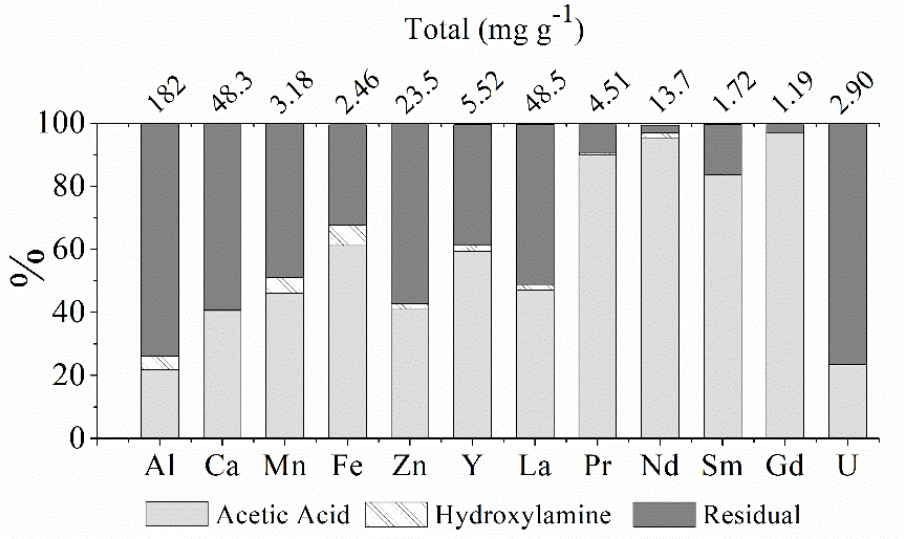

Fig. 7- Al, Ca, Mn, Fe, Zn, REE and U partitioning in the P3 sample (BCR sequential extraction procedure).

4.4. Effect of pH and the precipitate particle size on REE removal

As depicted in Fig. 8, an increase in pH influences the REE removal efficiency through adsorption/co-precipitation with Al_{13}-polymers. On the other hand, the particle size of the precipitates does not affect the removal, suggesting that the REE are retained in the freshly formed flocs, which are composed of nanometric particles (revealed by TEM analysis) retained in the first membrane (0.45 μm). The results align with the findings of Verplanck (2013) and Verplanck et al. (2004), who stated that the REE remain soluble and are not removed by Al, Fe, and Mn precipitates from the solution in acid environments. However, the concentrations of the REE in the AMD system investigated herein are orders of magnitude higher than those found by the aforementioned authors. Apart from that, the present indicates that the precipitate forms due to pH neutralization, rather than forming in natural systems by the mixture of waters having different compositions.

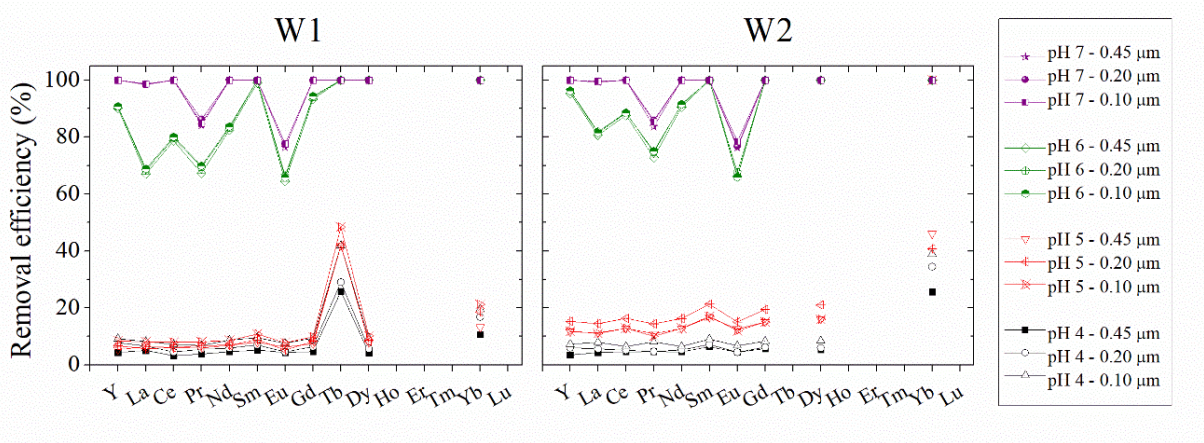

Fig. 8- Removal efficiency depending on the pH and on the particle size of the precipitates formed by neutralizing the pH of the W1 and W2 samples (room temperature, pH raised with KOH 2 mol L^{-1}).

An interesting and noteworthy feature was the lower removal efficiency of Pr and Eu (about 85 and 77%, respectively) in comparison to the other REE (100%) when the pH was raised to 7. The same behaviour was also observed at pH 8 (data not shown). This might have occurred due to the competition of other elements presenting high concentrations (Table 1), such as calcium and zinc (180 and 21.3 mg L^{-1}, respectively) which can be adsorbed onto the Al_{13}-polymers when the pH stands between 4 and 9, as stated by Kinniburgh et al. (2010). The BCR

sequential extraction results (Fig. 7) corroborate this suggestion, showing that about 40% of the Ca and Zn present in the precipitate was leached by acetic acid. Further investigation should be carried out, considering that this phenomenon can lead to novel REE separation technologies.

4.5. Geochemical modelling with PHREEQC

The simple modelling based on the *LLNL* and *Thermoddem_V1.10* databases considering the chemical composition of the AMD samples was able to reveal the most probable speciation of all elements, as well as the phases more likely to precipitate through the calculation of the saturation indexes. The modelling was proceeded considering different pHs in an attempt to provide a clear understanding of the removal mechanism in the AMD system.

The results depicted in Fig. 9 show that the REE are in most cases complexed with sulphate as $LnSO_4^+$, except for Pr. This partially corroborates the results depicted in Fig. 8, where praseodymium exhibits a different behaviour when compared to other REE - as discussed in the previous section. In a smaller proportion, the REE assume the form of Ln^{3+} (Ln = lanthanide). Due to the complexity of the solution in which other anions are present, other complexes coexist but are negligible, given their low concentrations.

Neodymium was selected to illustrate the complexity of the W3 composition as well as the variation of the speciation when the pH varies (Fig. 10-a). Note that $NdSO_4^+$ and Nd^{3+} are the most abundant species up to neutral pH. This information suggests that such species are the ones that react with the surface area of the freshly formed Al_{13}-polymers.

REE-sulphate complexes play an important role in the adsorption of REE on basaluminite ($Al_4(SO_4)(OH)_{10}\cdot 5(H_2O)$) in AMD, as reported by (LOZANO; AYORA; FERNÁNDEZ-MARTÍNEZ, 2019). The author showed that at any given pH value, the sorption increases as the sulphate concentration rises. The absence of Pr sulphate complexes may also contribute to different behaviours of the element, as observed in the current study. This possibility presents an important contribution to the understanding of the co-precipitation of REE by Al_{13}-polymers. Therefore, it encourages further investigation to decipher the enigma of the exact mechanism of interaction between the surface of the precipitate and the REE complexes in AMD systems.

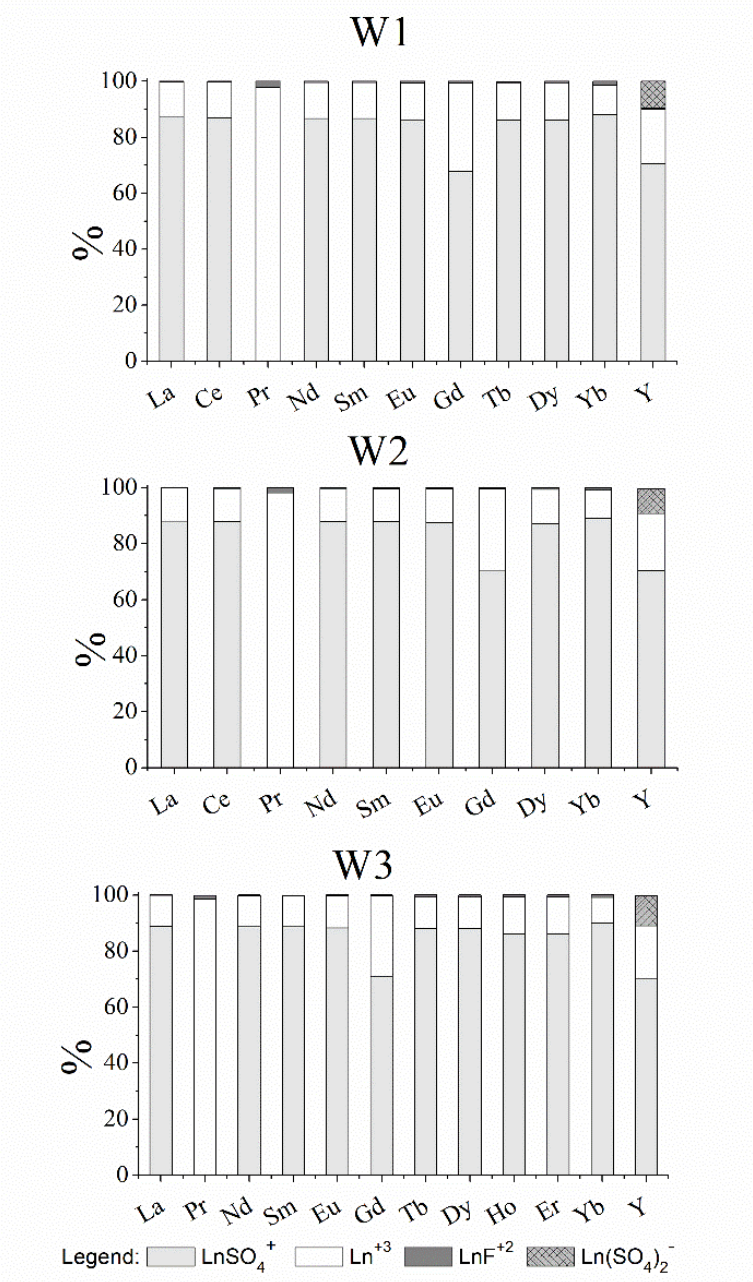

Fig. 9- Chemical speciation of the REE present in the W1, W2 and W3 samples.

Considering the excess of SO_4^{-2} in AMD systems, sulphate was expected to be the main anion to bind to the REE, however, the presence of some fluorine complexes is significant, despite the fact that the F^- content is much lower than the SO_4^{2-} content.

Neodymium was also selected to illustrate the modelling of REE sorption on Hfo (Fig. 10-b). The results of the surface complexation modelling evidenced that Nd should remain in solution in acid environments, up to a pH close to 6. Therefore, the sorption of this element is believed

to be triggered in a smaller proportion at pH 4. All the Nd in solution must be adsorbed at pH 7 and above, highlighting that the solution charge balance becomes neutral at pH 8.

These findings corroborate the results presented and discussed in section 4.4 and shown in Fig. 8, however, the model did not consider aluminium oxyhydroxides as the adsorbent, due to the lack of information fed to the database. In addition, the experimental and modelling results from in the present study corroborates the results from Liu et al. (2017) and Lozano et al. (2019) who discuss the sorption of REE on iron oxyhydroxide and basaluminite, respectively. However, the REE co-precipitation with Al_{13}-polymers is evidenced in the present study as being a complex mechanism that cannot be defined as adsorption alone, as discussed in section 4.6.

The saturation indexes of the minerals calculated by PHREEQC are depicted in Fig. 10-d. Note that at low pH values, generally found in the impoundments (±3), none of the Al, Si and Fe minerals are stable. They are expected to dissolve as they present negative saturation indexes under the conditions considered, except for goethite and hematite. Notwithstanding, besides these two iron oxides, gibbsite was also identified in the S1 and S2 sediment samples. Furthermore, all the soluble REE should only start precipitating individually as REE hydroxides ($Ln(OH)_3$) at a slightly alkaline pH- above 8.5.

Considering the high Al content in the AMD and also the relative lack of Fe and Si, aluminium minerals (pseudoboehmite, boehmite and gibbsite) are more likely to precipitate than aluminosilicates and iron oxyhydroxides. Note that in the W3 sample aluminium speciation diagram (Fig. 10-c) the species $Al_{13}O_4(OH)_{24}^{7+}$, i.e., the Al_{13}-Kegging ions, is the most abundant in a pH 5 to 9 - represented by boehmite in Fig. 10-d. Aluminium polymers should start precipitating at pH above 5, corroborating the findings of Furrer et al. (2002).

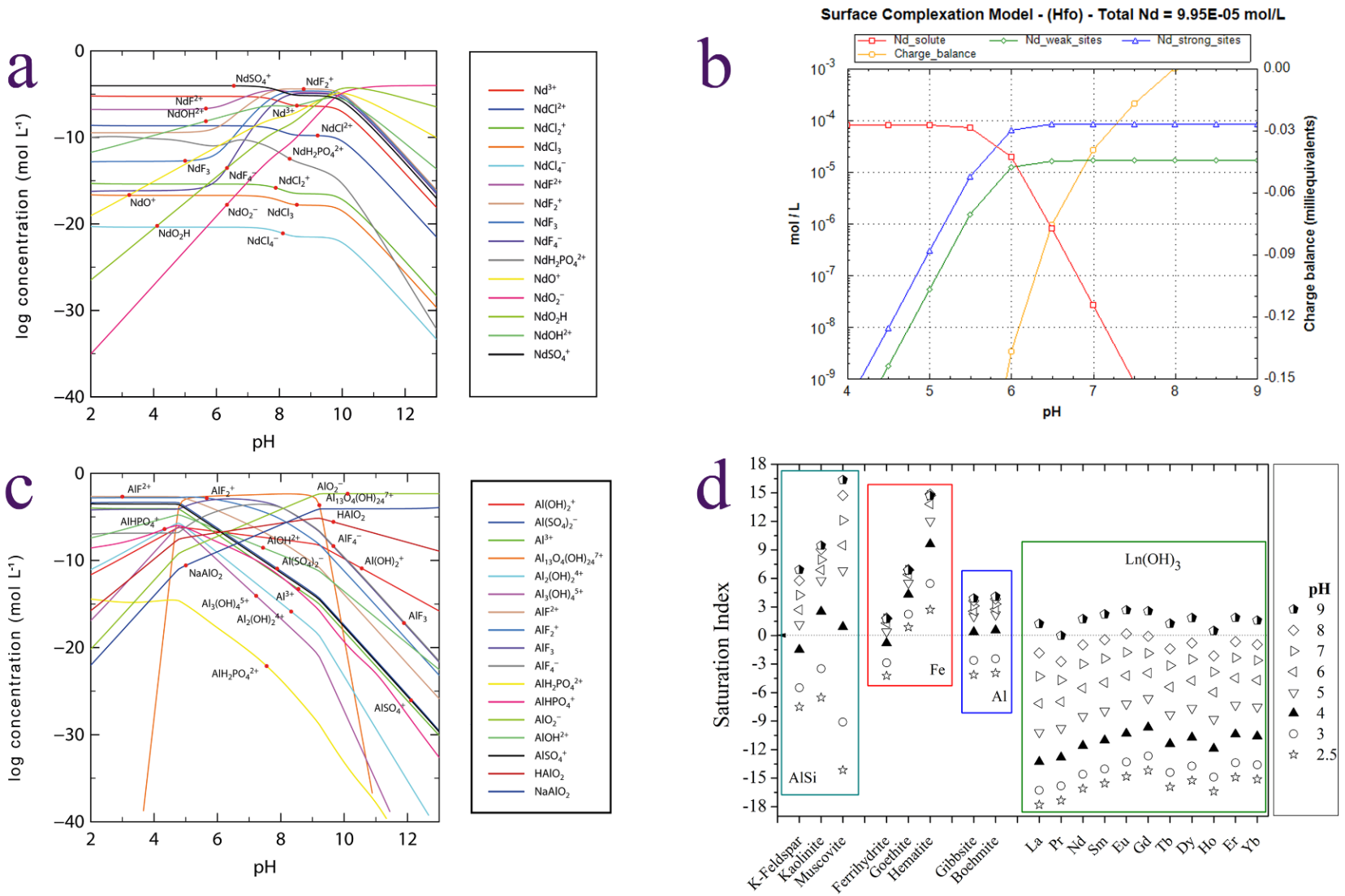

Fig. 10- (a) W3 sample neodymium speciation diagram. (b) W3 sample neodymium surface complexation model. (c) W3 sample aluminium speciation diagram. (d) Saturation indexes of the minerals possibly formed in the AMD system studied at different pH values modelled by PHREEQC (Database: LLNL.dat). (AlSi) = aluminosilicates, (Fe) = iron oxyhydroxides, (Al) = aluminium oxyhydroxides, $Ln(OH)_3$ = Lanthanides hydroxides. Special attention to pH 4, where the Boehmite saturation index has presented a positive value, indicating the start of its precipitation.

4.6. REE removal process

The aluminium precipitate formation mechanism and the consequent removal of soluble metals can be attributed to the polymerization of the Al_{13}-Keggin ions. This phenomenon has been previously discussed by Bi et al. (2004), Bottero et al. (1987) and Wefers and Misra (1987), amongst others. By comparing the findings presented by these authors to the results attained in the present work, an understanding of the removal process is reached. To sum up, as the aluminium polymers are formed by an increase in pH, the surface area of about 250 m^2 g^{-1} (STALIDIS; BAKOYANNAKIS; ZAMBOULIS, 1992) tends to be more negatively charged. The point of zero charge (PZC) for the aluminium polymers (sol-gel) is reported to be between 8.2 and 9.5 (SPOSITO, 1996). The more negatively charged the surface, the more reactive it is and the adsorption/co-precipitation process takes place. In addition, at pH 8 the content of aluminium polymers outstrips the amount of REE. The Al: REE molar ratio in the W3 sample is about 12:1, which explains the high removal efficiencies reached in the present study.

Despite being made so long ago, Kolthoff (1932) proposals concerning the co-precipitation mechanism are still valid and have guided lots of researchers ever since. According to his proposals, three phenomena seem to happen simultaneously in the REE removal by Al_{13}-polymers when the pH of the AMD is neutralized: (i) “Mixed crystals” form when impurities are incorporated into the structure, corresponding to the amorphous precipitate itself, as presented herein. (ii) Entrapment occurs when the impurities are not incorporated into the crystal structure, but they can still be adsorbed during the growth of the “crystals” and give rise to the formation of imperfections in the “crystal”, considering the results obtained by TEM, XPS and BCR sequential extraction for Y and La. These elements are in most cases trapped into the precipitate structure. (iii) The REE surface adsorption occurs after the formation of the precipitate, as observed in the cases of Pr, Nd, Sm and Gd in the current research, also when the TEM, XPS and BCR sequential extraction results are considered as a whole.

Considering all the results altogether, the important role played by the Al_{13}-polymers in the recovery of the REE from AMD is remarkable; it highlights the high REE removal efficiencies attained with pH neutralization as well as their propensity of leaching with acetic acid. Potassium hydroxide is not recommended for use in an industrial scale, due to high cost. However, the findings of the present work can be extrapolated and applied in cases of precipitates of the same AMD treatment system produced with lime as the alkali agent. The

recovery of REE from AMD by using a conventional neutralization treatment appears to be a feasible procedure if the high demand for these elements is to be met. Nevertheless, more efforts and investments are still highly desired as far as pilot projects and investigation is concerned.

5. CONCLUSIONS

Precipitates composed of Al_{13}-polymers are the main players in the removal of the REE when the pH of the AMD is raised with KOH up to 8. They promote adsorption and entrapment processes simultaneously. Under the conditions investigated in the present study, the efficiency of the recovery reached values of about 100% for most of the REE. Sequential extraction revealed that most of the REE could be leached by acetic acid at high-efficiency levels, thus supporting the need for the development of novel technologies for the recovery of metals from AMD through co-precipitation processes.

Considering a total concentration of REE in the W3 sample (77 mg L^{-1}), a current AMD flow rate of 300 m^3h^{-1} and a theoretical recovery of 100%, a daily production of about 554 kg of REE could be expected. If neodymium alone is considered, the daily production could reach about 100 kg. If adopted, the system proposed can potentially reduce the costs of treatment. It will also promote a considerable increase in Brazil's REE production, thus contributing to sustainable economic development.

The same principle could be applied worldwide, considering its feasibility and costs, and the benefits to be yielded represent an increase in global supply, partial mitigation of the current demand for new mining projects and more importantly, the prevention of imminent environmental issues.

6. REFERENCES

ABREU, R. D.; MORAIS, C. A. Purification of rare earth elements from monazite sulphuric acid leach liquor and the production of high-purity ceric oxide. **Minerals Engineering**, v. 23, n. 6, p. 536–540, 2010.

AKCIL, A.; KOLDAS, S. Acid Mine Drainage (AMD): causes, treatment and case studies. **Journal of Cleaner Production**, v. 14, n. 12- 13 SPEC. ISS., p. 1139–1145, 2006.

ALEX, T. C. et al. Mechanical Activation of Al-oxyhydroxide Minerals–A Review. **Mineral Processing and Extractive Metallurgy Review**, v. 37, n. 1, p. 1–26, 2016.

AYORA, C. et al. Recovery of Rare Earth Elements and Yttrium from Passive-Remediation Systems of Acid Mine Drainage. **Environmental Science and Technology**, v. 50, n. 15, p. 8255–8262, 2016.

BARCELOS, G. S. et al. Immobilization of Eu and Ho from synthetic acid mine drainage by precipitation with Fe and Al (hydr)oxides. **Environmental Science and Pollution Research**, v. 25, n. 19, p. 18813–18822, 2018.

BAU, M. Scavenging of dissolved yttrium and rare earths by precipitating iron oxyhydroxide: Experimental evidence for Ce oxidation, Y-Ho fractionation, and lanthanide tetrad effect. **Geochimica et Cosmochimica Acta**, v. 63, n. 1, p. 67–77, 1999.

BAUER, D. et al. US Department of Energy: Critical Materiasl Strategy, December 2010. **Agenda**, n. December, p. 1–166, 2010.

BI, S. et al. Studies on the mechanism of hydrolysis and polymerization of aluminum salts in aqueous solution : correlations between the " Core-links " model and "Cage-like" Keggin-Al13 model. **Coordination Chemistry Reviews**, v. 248, p. 441–455, 2004.

BLANC, P. et al. Thermoddem: A geochemical database focused on low temperature water/rock interactions and waste materials. **Applied Geochemistry**, v. 27, n. 10, p. 2107–2116, out. 2012.

BLOWES, D. W. et al. **The Geochemistry of Acid Mine Drainage**. 11. ed. [s.l.] Elsevier Ltd., 2013. v. 11

BOTTERO, J. Y. et al. Mechanism of formation of aluminum trihydroxide from keggin Al13 polymers. **Journal of Colloid And Interface Science**, v. 117, n. 1, p. 47–57, 1987.

CARABALLO, M. A. et al. Sequential extraction and DXRD applicability to poorly crystalline Fe- and Al-phase characterization from an acid mine water passive remediation system. **American Mineralogist**, v. 94, n. 7, p. 1029–1038, 2009.

CASEY, W. H.; PHILLIPS, B. L.; FURRER, G. Aqueous Aluminum Polynuclear Complexes and Nanoclusters: A Review. **Reviews in Mineralogy and Geochemistry**, v. 44, n. 1, p. 167–190, 2010.

CONAMA. **Resolution N°430, 13/05/2011 - provides conditions and standards for effluent discharge. Conselho Nacional do Meio Ambiente**Brazilian National Envirnonmet Concil, , 2011.

ELBAZ-POULICHET, F. F.; DUPUY, C. Behaviour of rare earth elements at the freshwater-seawater interface of two acid mine rivers: The Tinto and Odiel (Andalucia, Spain). **Applied Geochemistry**, v. 14, n. 8, p. 1063–1072, 1999.

ERICKSON, B. E. **From coal, a new source of rare earths**. Disponível em: <https://cen.acs.org/materials/inorganic-chemistry/coal-new-source-rare-earths/96/i28>.

EUROPEAN UNION, E. U. **Study on the review of the list of critical raw materialsEuropean Comissmion**. Brussels: [s.n.]. Disponível em: <https://publications.europa.eu/en/publication-detail/-/publication/08fdab5f-9766-11e7-b92d-01aa75ed71a1/language-en>.

FERNANDES, H. M.; FRANKLIN, M. R.; VEIGA, L. H. Acid rock drainage and radiological environmental impacts. A study case of the Uranium mining and milling facilities at Pocos de Caldas. **Waste Management**, v. 18, n. 3, p. 169–181, 1998.

FLORES, J. C. D. C. **Fechamento de Mina: Aspectos Técnicos , Jurídicos e Socioambientais**. [s.l.] UNICAMP, Brazil, 2006.

FONSECA, V. Mais energia, menos impacto para o ambiente. **Publicação trimestral da Fundação de Amparo à Pesquisa do Estado de Minas Gerais - FAPEMIG, N°39 - Set-Nov**, p. 62, 2009.

FURRER, G. et al. The origin of aluminum flocs in polluted streams. **Science**, v. 297, n. 5590, p. 2245–2247, 2002.

FURRER, G.; LUDWIG, C.; SCHINDLER, P. W. On the chemistry of the Keggin Al13 polymer I. Acid-base properties. **Journal of Colloid and Interface Science**, v. 149, n. 1, p. 56–67, mar. 1992.

FURRER, G.; TRUSCH, B.; MÜLLER, C. The formation of polynuclear Al 13 under simulated natural conditions. **Geochimica et Cosmochimica Acta**, v. 56, n. 10, p. 3831–3838, 1992.

IIJIMA, S.; YUMURA, T.; LIU, Z. One-dimensional nanowires of pseudoboehmite (aluminum oxyhydroxide γ-AlOOH). **Proceedings of the National Academy of Sciences**, v. 113, n. 42, p. 11759–11764, 2016.

JHA, M. K. et al. Review on hydrometallurgical recovery of rare earth metals. **Hydrometallurgy**, v. 165, p. 2–26, 2016.

KIM, Y. Mineral phases and mobility of trace metals in white aluminum precipitates found in acid mine drainage.

Chemosphere, v. 119, p. 803–811, 2015.

KINNIBURGH, D. G.; COOPER, D. M. **PhreePlot - Creating graphical output with PHREEQC**Gwynedd, UK., 2016. Disponível em: <http://www.phreeplot.org>

KINNIBURGH, D. G.; JACKSON, M. L.; SYERS, J. K. Adsorption of Alkaline Earth, Transition, and Heavy Metal Cations by Hydrous Oxide Gels of Iron and Aluminum. **Soil Science Society of America Journal**, v. 40, n. 5, p. 796–799, set. 1976.

KOLTHOFF, I. M. Theory of Coprecipitation. The Formation and Properties of Crystalline Precipitates. **The Journal of Physical Chemistry**, v. 36, n. 3, p. 860–881, mar. 1932.

LADEIRA, A. C. Q.; GONCALVES, J. S.; MORAIS, C. A. Treatment of effluents from uranium oxide production. **Environmental Technology**, v. 32, n. 2, p. 127–131, 2011.

LAPIDO-LOUREIRO, F. E.; SANTOS, R. L. C. **O Brasil e a reglobalização da indústria das terras raras.** [s.l: s.n.]. v. 1

LEETMAA, K. et al. Comparative molecular characterization of aluminum hydroxy-gels derived from chloride and sulphate salts. **Journal of Chemical Technology and Biotechnology**, v. 89, n. 2, p. 206–213, 2014.

LIN, J. L. et al. The origin of Al(OH)3-rich and Al13-aggregate flocs composition in PACl coagulation. **Water Research**, v. 43, n. 17, p. 4285–4295, 2009.

LIU, H. et al. Rare earth elements sorption to iron oxyhydroxide: Model development and application to groundwater. **Applied Geochemistry**, v. 87, n. December, p. 158–166, dez. 2017.

LIU, J.; ZHAO, F. Structural change and mineralogical transformation mechanism of aluminum hydroxide gels from forced hydrolysis Al(III) solutions containing AlO4Al12(OH)24(H2O)127+ polyoxycation during aging. **Chinese Journal of Geochemistry**, v. 29, n. 1, p. 107–112, 2010.

LOTHENBACH, B.; FURRER, G.; SCHULIN, R. Immobilization of heavy metals by polynuclear aluminium and montmorillonite compounds. **Environmental Science and Technology**, v. 31, n. 5, p. 1452–1462, 1997.

LOZANO, A.; AYORA, C.; FERNÁNDEZ-MARTÍNEZ, A. Sorption of rare earth elements onto basaluminite: The role of sulfate and pH. **Geochimica et Cosmochimica Acta**, v. 258, p. 50–62, ago. 2019.

MIEKELEY, N. et al. Rare-earth elements in groundwaters from the Osamu Utsumi mine and Morro do Ferro analogue study sites, Pocos de caldas, Brazil. **Journal of Geochemical Exploration**, v. 45, p. 365–387, 1992.

MOULDER, J. F. et al. **Handbook of X-ray photoelecton spectroscopy**. Eden Prairie, Minessota, USA.: Physical Electronics, Inc., 1995.

MULLICA, D. F. et al. The X-ray photoemission spectra of Nd(OH)3, Sm(OH)3, Eu(OH)3 and Gd(OH)3. **Journal of Electron Spectroscopy and Related Phenomena**, v. 71, p. 1–20, 1995.

NÓBREGA, F. A.; LIMA, H. M. DE; LEITE, A. DO L. Análise de múltiplas variáveis no fechamento de mina: estudo de caso da pilha de estéril BF-4, Mina Osamu Utsumi, INB Caldas, Minas Gerais. **Rem: Revista Escola de Minas**, v. 61, n. 2, p. 197–202, 2008.

NORDSTROM, D. K. et al. **Challenges in Recovering Resources from Acid Mine Drainage**. (C. Wolkersdorfer et al., Eds.)Mine Water & Circular Economy (Vol II). **Anais**...Lappeenranta, Finland (Lappeenranta University of Technology).: 2017Disponível em: <http://imwa.info/docs/imwa_2017/IMWA2017_Nordstrom_1138.pdf>

PARKHURST, D. L.; APPELO, C. A. J. **Description of Input and Examples for PHREEQC Version 3 — A Computer Program for Speciation , Batch-Reaction , One-Dimensional Transport , and Inverse Geochemical Calculations Chapter 43 of**. Denver, Colorado, USA.: [s.n.].

PAULICK, H.; MACHACEK, E. The global rare earth element exploration boom: An analysis of resources outside of China and discussion of development perspectives. **Resources Policy**, v. 52, n. February, p. 134–153, 2017.

PIETRALONGA, A. G. et al. Lanthanum immobilization by iron and aluminum colloids. **Environmental Earth Sciences**, v. 76, n. 7, p. 1–7, 2017.

PORVALI, A.; WILSON, B. P.; LUNDSTRÖM, M. Lanthanide-alkali double sulfate precipitation from strong sulfuric acid NiMH battery waste leachate. **Waste Management**, v. 71, p. 381–389, 2018.

PROTANO, G.; RICCOBONO, F. High contents of rare earth elements (REEs) in stream waters of a Cu-Pb-Zn mining area. **Environmental Pollution**, v. 117, n. 3, p. 499–514, 2002.

PRUDÊNCIO, M. I. et al. Geochemistry of rare earth elements in a passive treatment system built for acid mine drainage remediation. **Chemosphere**, v. 138, p. 691–700, 2015.

PRUDÊNCIO, M. I. et al. Rare Earth Elements, Iron and Manganese in Ochre-precipitates and Wetland Soils of a Passive Treatment System for Acid Mine Drainage. **Procedia Earth and Planetary Science**, v. 17, p. 932–935, 2017.

RAURET, G. et al. Improvement of the BCR three step sequential extraction procedure prior to the certification of new sediment and soil reference materials. **Journal of Environmental Monitoring**, v. 1, n. 1, p. 57–61, 1999.

ROLLINSON, H. R. **Using Geochemical Data: evaluation, presentation, interpretation**. 1° ed. London-UK: Longman Group UK Limited, 1993.

SOUZA SANTOS, P. et al. Hydrothermal synthesis of well-crystallised boehmite crystals of various shapes. **Materials Research**, v. 12, n. 4, p. 437–445, 2009.

SOYOL-ERDENE, T. O. et al. Mineralogical controls on mobility of rare earth elements in acid mine drainage environments. **Chemosphere**, v. 205, p. 317–327, 2018.

SPOSITO, G. **The Environmental Chemistry of Aluminum**. 2nd. ed. [s.l.] CRC Press, 1996.

STALIDIS, G. A.; BAKOYANNAKIS, D. N.; ZAMBOULIS, D. X. Surface properties of aluminium hydroxide gels prepared from pure and mixed aqueous, ethanolic and acetonic media. **Journal of Chemical Technology & Biotechnology**, v. 54, n. 2, p. 123–127, 1992.

STEWART, B. W. et al. Rare earth element resources in coal mine drainage and treatment precipitates in the Appalachian Basin, USA. **International Journal of Coal Geology**, v. 169, p. 28–39, 2017.

U.S. GEOLOGICAL SURVEY. **Mineral Commodity Summaries**. [s.l: s.n.]. Disponível em: <https://doi.org/10.3133/70202434>.

VERPLANCK, P. L. et al. Rare earth element partitioning between hydrous ferric oxides and acid mine water during iron oxidation. **Applied Geochemistry**, v. 19, n. 8, p. 1339–1354, 2004.

VERPLANCK, P. L. Partitioning of Rare Earth Elements between Dissolved and Colloidal Phases. **Procedia Earth and Planetary Science**, v. 7, p. 867–870, 2013.

WABER, N.; SCHORSCHER, H. D.; PETERS, T. Hydrothermal and supergene uranium mineralization at the Osamu Utsumi mine, Poços de Caldas, Minas Gerais, Brazil. **Journal of Geochemical Exploration**, v. 45, n. 1–3, p. 53–112, nov. 1992.

WEATHERILL, J. S. et al. Ferrihydrite formation: The role of Fe13 Keggin clusters. **Environmental Science and Technology**, v. 50, n. 17, p. 9333–9342, 2016.

WEFERS, K.; MISRA, C. Oxides and Hydroxides of Aluminum. **Alcoa Technical Paper**, v. 19, p. 100, 1987.

ZHANG, W. et al. A review of the occurrence and promising recovery methods of rare earth elements from coal and coal by-products. **International Journal of Coal Preparation and Utilization**, v. 35, n. 6, p. 281–294, 2015.

ZHANG, W.; HONAKER, R. Q. Rare earth elements recovery using staged precipitation from a leachate generated from coarse coal refuse. **International Journal of Coal Geology**, v. 195, p. 189–199, 2018.

ZHAO, F. et al. The geochemistry of rare earth elements (REE) in acid mine drainage from the Sitai coal mine, Shanxi Province, North China. **International Journal of Coal Geology**, v. 70, n. 1- 3 SPEC. ISS., p. 184–192, 2007.

Chapter 2

The role of iron in the co-precipitation of rare earth elements and uranium by Fe-Al-precipitates in acid mine drainage

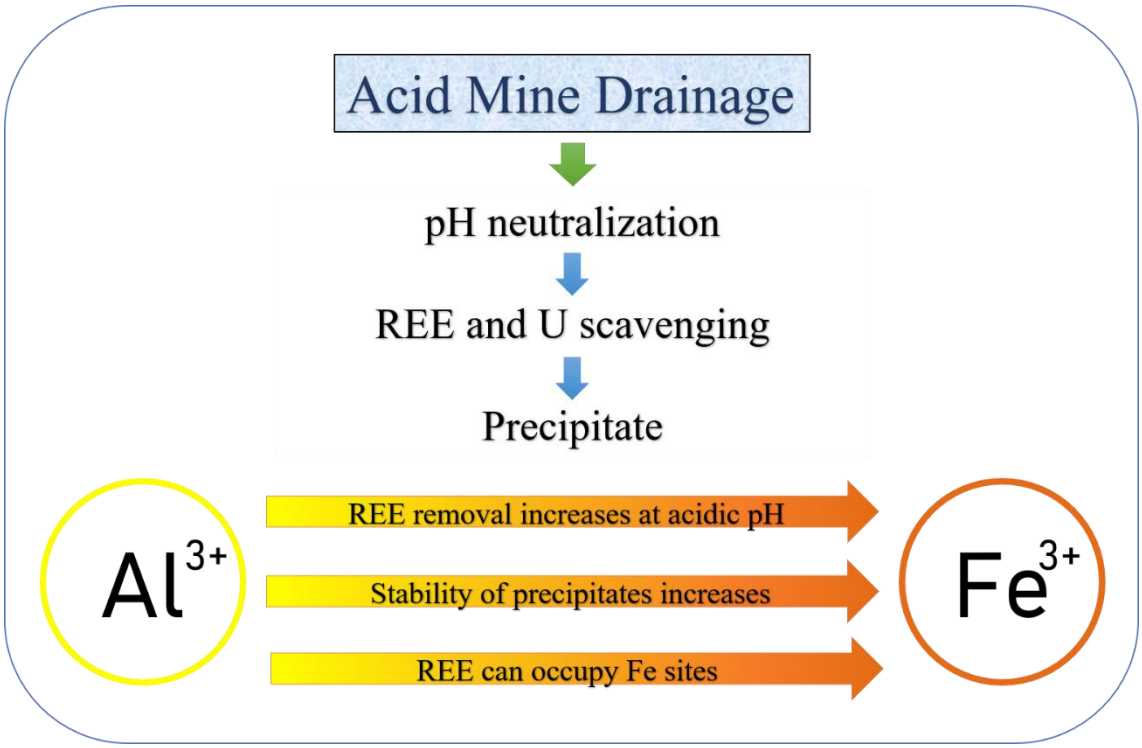

ABSTRACT: The co-precipitation and adsorption - scavenging - of soluble metals by iron and aluminium oxyhydroxides is a natural process that occurs in acid mine drainage (AMD). This phenomenon is relevant for the immobilization, transport and recovery of important resources such as rare earth elements (REE) and uranium (U). Furthermore, a deep understanding about the players and the reactions that govern the scavenging of REE and U by Fe and Al oxyhydroxides in aqueous systems is fundamental for the development of researches in natural and engineering sciences and for the development of management strategies and regulations related to the environment and human health. In this scenario, the current work aimed to investigate the role played by iron in the co-precipitation of REE and U when treating effluents by pH neutralization, in an AMD system located in Brazil. The research employed water sampling, co-precipitation batch experiments, sequential extraction, X-ray diffraction and ^{57}Fe Mössbauer spectroscopy. The results evidenced that the presence and the amount of Fe in the initial solution can positively influence the REE removal efficiency, especially at a slightly acid pH. The effect caused by the addition of Fe was irrelevant when the pH of the AMD was raised

up to values equal to 7-8. The scavenging of U was not influenced by the addition of Fe to the AMD before pH neutralization. The sequential extraction results showed that precipitates containing higher amounts of Fe tend to be less labile. The ^{57}Fe Mössbauer spectra revealed that the REE can occupy iron sites in the structure of the amorphous precipitates. The findings of the current study can be extrapolated for other AMD systems and also contribute to the development of novel REE recovery and hydrometallurgical techniques.

KEYWORDS: rare earth elements; uranium; iron oxyhydroxides; aluminium oxyhydroxides; acid mine drainage; co-precipitation.

1. INTRODUCTION

Rare earth elements (REE) are uppermost in the development and production of manufactured products and the demand for these elements to the global market increases annually (EUROPEAN UNION, 2017; U.S. GEOLOGICAL SURVEY, 2016, 2019). The recovery of REE from secondary sources, such as the recycling of electronic wastes and the recovery from acid mine drainage (AMD) appears to be a feasible way to increase the supply of these highly demanded elements to the industry. The recovery of REE from AMD has been investigated in the past few years seeking for a sustainable route for dealing with environmental issues and with the increasing REE demand (AYORA et al., 2016; BINNEMANS et al., 2013; MORAES et al., 2020; VASS; NOBLE; ZIEMKIEWICZ, 2019a, 2019b; ZIEMKIEWICZ; NOBLE, 2019).

Besides the importance of recycling and recovering of REE, the study of natural processes involving the geochemistry of REE is a matter of interest to many researchers in environmental sciences. It concerns about geology and the formation of some deposits, sedimentology studies, environmental issues such as AMD and its impacts on the environment and human health, waste disposal, among other topics.

Regarding environmental issues, the mobility of the REE in superficial waters, groundwater and seawater is directly correlated to the scavenging - adsorption and co-precipitation - by aluminium and iron oxyhydroxides (BAU, 1999; BAU; KOSCHINSKY, 2009; QUINN; BYRNE; SCHIJF, 2004; VERPLANCK, 2013;

VERPLANCK et al., 2004). The stability of these precipitates in natural systems depends on the water composition, which interferes in the process that can occur, such as adsorption, desorption, dissolution, etc. There are still few studies concerning the stability of REE-bearing Al and Fe precipitates. The available publications report experiments that were conducted only under controlled conditions in the laboratory, disregarding natural conditions, such as the work by Pietralonga et al. (2017) that reports lanthanum immobilization by iron oxyhydroxides and the work by Barcelos et al. (2018) that reports the immobilization of europium and holmium.

The presence of U in AMD is also an important environmental issue and a matter of concern for researchers and regulators, considering the risks to the entire ecosystem (FERNANDES; FRANKLIN; VEIGA, 1998). Furthermore, U can be scavenged from AMD by iron precipitates at neutral pH, forming bidentate surface complexes on ferrihydrite (WAITE et al., 1994). However, information about the stability of the precipitates containing U are still missing.

At this scenario, the present work seeks to evaluate the role of iron (Fe^{3+}) on the scavenging of REE and U present in an AMD system and to assess the stability of the precipitates formed by pH neutralization. The objectives of the current study were (i) study the influence of the initial Fe concentration on the co-precipitation of REE and U in a laboratory AMD solution through pH neutralization, (ii) study the influence of the initial Fe concentration on the co-precipitation of REE and U in a natural AMD effluent through pH neutralization, (iii) evaluate the stability of the precipitates formed at pH 8 by sequential extraction and (iv) investigate the influence of the presence of REE on the structure of the precipitates through ^{57}Fe Mössbauer spectroscopy analysis. The importance of the results to the understanding of the geochemistry of REE in AMD systems and the application of the findings to environmental sciences research along with the possibility of the recovery of REE are discussed in this chapter. Emphasis was placed on the role played by Fe in the co-precipitation of REE in AMD treatment through pH neutralization.

2. MATERIALS AND METHODS

2.1. Samples and Solutions

Natural AMD water samples were collected in two different impoundments in a closed uranium mine - under decommissioning - located in the municipality of Caldas, Minas Gerais, Brazil. The sampling was carried out in February/2018 and was described in detail in Chapter 1 (MORAES et al., 2020). The natural AMD water samples were coined W1, W2 and W3 in the current work. The W3 water sample was provided by the mining company and it consisted in a pre-treated W1 water sample, whose Mn and Ce were removed by ozonation and the removal of U and Th was carried out by ionic exchange.

Two water samples were used to study the role of iron on the co-precipitation of REE in AMD: W3 and a laboratory AMD-simulating solution. The latter was prepared using Milli-Q® deionized water and Sigma-Aldrich® high purity reagents (>99.9%). This sample was coined W-Lab. The salts used in the preparation of the W-Lab sample were $AlCl_3$, $MnSO_4$, $La_2(SO_4)_3$, $Nd_2(SO_4)_3$, $Sm_2(SO_4)_3$ and $Gd_2(SO_4)_3$. The REE lanthanum (La), neodymium (Nd), samarium (Sm) and gadolinium (Gd) were selected to this study considering that these elements are the most abundant in the AMD system studied. The sulphate content of the W-Lab sample was adjusted to 1 g L^{-1} using sulfuric acid, aiming to reproduce the natural effluent. A total of 60 L of the W-Lab sample was prepared and stored at room temperature in an acid-cleaned polyethene container.

The Fe/Al/REE molar ratios of the water samples were equal to 0.4/8/1 for the sample W1, 0/9/1 for the sample W2 and 0.05/12/1 for the sample W3. Relying on this information, the W-Lab sample was prepared in order to reach a Fe/Al/REE molar ratio equal to 0/6/1. This molar ratio was selected in order to simplify the interpretation of the data, whereas it contains half the amount of aluminium of the sample W3. Furthermore, basing on the works by Bau (1999), Verplanck et al. (2004) and Moraes et al. (2020), it was expected that the reduction of the Al:REE ratio of the W-Lab sample could facilitate the visualization of the influence of the amount of Fe added to the AMD due to the reduction of the adsorbent/co-precipitating agent.

2.2. Experimental section

2.2.1. Co-precipitation of REE and U

The co-precipitation batch experiments were carried out in glass beakers at room temperature and the solutions were constantly stirred by a glass helix. Each experimental

unit consisted of a 1 L aliquot of water sample. The co-precipitation process was carried out through forced hydrolysis with the addition of a 2 mol L^{-1} KOH solution. At the end of the precipitation, an amount of 0.4 µg of a gelatinized starch (inert flocculant) was added to promote flocculation of the precipitates formed. The suspensions were left to decant in glass separation funnels for 1 h, drained and centrifugated at 6000 g. The solids obtained were dried at 50°C, powdered, sieved through a 149 µm pore size sieve and stored at room temperature in polyethene acid-cleaned bottles until analysis.

The REE scavenging in the W1 and W2 samples were investigated at pH 4, 5, 6 and 7, without Fe addition, aiming on assessing the behaviour of the REE during the treatment through pH neutralization carried out by the mining company.

In order to evaluate the effect of the initial Fe^{3+} concentration, proper amounts of a 0.5 mol L^{-1} $FeCl_3$ solution was added to the W-Lab and W3 samples prior to the co-precipitation experiments to achieve pre-determined Fe/Al/REE molar ratios. The W3 sample was selected for these experiments among the natural AMD samples collected considering its lower U content. The W-Lab sample was also selected for this experiment considering that it was prepared with predetermined composition - half of the amount of Al of the W3 sample and selected REE – aiming on comparing the results of the experiments carried out with the W3 sample.

The concentrations of iron used in the experiments carried out with the W-Lab sample were 0, 3, 6, 9 and 12 times the total concentration of REE. For the W3 sample, the concentrations of iron used in the experiments were 0, 6, 12, 18 and 24 times the total concentration of REE. These values were chosen considering the total Al content of the samples, aiming at achieving a maximum Fe/Al molar ratio of 2/1. In the current study, the final pH of the W-Lab sample was adjusted to values equal to 5, 6, 7 and 8 and for the W3 sample it was adjusted to 6, 7 and 8 for all initial Fe concentrations.

2.2.2. Sequential extraction

A modified BCR sequential extraction, initially proposed by Rauret et al. (1999), was used to evaluate the stability of the precipitates obtained at pH 8 and different Fe/Al/REE molar ratios . The first step was performed by using acetic acid (0.11 mol L^{-1} CH_3COOH), which extracts the exchangeable fraction of REE and the fraction soluble in weak acid. In the second step, the extraction of the REE was carried out by using hydroxylammonium chloride (0.5 mol L^{-1} $HONH_2 \cdot HCl$), which dissolves the reducible fraction. The third step,

which extracts the oxidizable fraction, was not carried out in the present study, considering that there were no oxidizable components in the sample. The residual phase resulted from the difference between the total content (obtained by aqua regia digestion) and the sum of steps one and two. All extraction experiments were performed in duplicate.

2.2.3. Chemical analysis

The chemical composition of the aqueous solutions was determined mainly by inductively coupled plasma optic emission spectrometry (ICP-OES) via a SPECTRO ARCOS® apparatus. All samples were vacuum filtered through 0.45 μm pore size nitrocellulose membranes prior to analysis. The sulphate content was determined by turbidimetry and the fluorine content by a selective electrode. The chemical composition of the precipitates was determined by ICP-OES after digestion with aqua regia. The digestion was carried out in centrifuge tubes at 25°C for 2 h in a horizontal shaker at 1 Hz, followed by filtering and dilution before the analysis.

2.2.4. Mineralogical characterization

The precipitates obtained in the co-precipitation experiments were characterized by powder X-ray diffraction (XRD) with the use of a RIGAKU® X-ray diffractometer under Cu Kα radiation (λ = 0.15418 nm). The equipment was operated at a tube voltage of 40 kV and a tube current of 30 mA with a scanning rate of 4° min^{-1}, from 4 to 80°2θ and a step size of 0.02°.

2.2.5. Mössbauer spectroscopy studies

Mössbauer spectroscopy is a technique that can be used to provide information about the chemical, structural, magnetic and time-dependent properties of a given material. In order to evaluate the influence of the presence of REE on the structure of ferrihydrite-like precipitates due to the co-precipitation process, ^{57}Fe Mössbauer spectroscopy analysis was employed in the current study.

This analysis was carried out using two ferrihydrite samples that were prepared in the laboratory, with Fe/REE molar ratios of 500/0 and 500/1. These samples were coined Fh and Fh-REE, respectively. The molar ratios chosen for the preparation of the samples of this study were determined to assess the effect of the presence of a small amount of REE on the structure of the precipitates. In addition, as ^{57}Fe Mössbauer spectroscopy has some

limitations when analysing materials with low Fe content, even at low temperatures (YOSHIDA; GUIDO, 2013), the authors chose to prepare these samples for Mössbauer studies instead of analysing the precipitates obtained in the co-precipitation batch experiments.

Ferrihydrite ($Fe_2O_3{\cdot}0.5(H_2O)$) was synthesized by Fe^{3+} forced hydrolysis and consequent precipitation as proposed by Schwertmann & Cornell (2000), using $FeCl_3$ as the iron source and 2 mol L^{-1} KOH as the alkalinity source. The pH of the solution was raised to a value equal to 8. The sample Fh-REE was prepared using a light-REE-carbonate concentrate (99%) that was obtained from the processing of monazite ((REE, Th)PO_4) (ABREU; MORAIS, 2014). The $REE_2(CO_3)_3$ solution used for this preparation contained 930, 61, 17, 520, 19, 1 and 73 mg L^{-1} of La, Ce, Pr, Nd, Sm, Eu and Gd, respectively. The precipitates were prepared and stored using the same methodology of the co-precipitation experiments.

The ^{57}Fe Mössbauer spectra were collected at 25 K in a conventional transmission assembly with a ~ 30 mCi ^{57}Co/Rh source. The sample mass used for the measurement was estimated to contain ~ 10 mg Fe cm^{-2}. Isomeric shifts were corrected for αFe, a standard also used for Doppler velocity scale calibration. Data were numerically adjusted with Lorentzian functions by the least-squares method, using the computer program IGOR Pro 6.1.2.1 © WaveMetrics, Oregon, USA.

3. RESULTS AND DISCUSSION

3.1. Chemical characterization of the water samples

The chemical composition of the W1, W2, W3 (MORAES et al., 2020) and the W-Lab water samples are compiled in Table 1. The results show that the natural AMD samples present high concentrations of Ca, Al and Zn, as well as expressive concentrations of REE, mainly the light ones. The concentrations of Mn are also expressive and represent an aggravating for the AMD treatment, as the total dissolved Mn concentration required by Brazilian regulations for the effluent discharge into the environment is <1 mg L^{-1} and the required pH must be between 5 and 9 (CONAMA, 2011; FONSECA, 2009). The concentration of Fe in the AMD present in samples W1 and W2 is considered low for AMD, especially considering that the main source of acidity in this system is the oxidation of pyrite (FeS_2) (WABER; SCHORSCHER; PETERS, 1992). The W3 sample has a low

Mn, Fe and Ce content due to the ozonation treatment carried out by the mining company for Mn removal (MORAES et al., 2020).

The U content of the W1 and W2 samples is considered very high for AMD and are in consonance with the findings of Fernandes et al. (1998), Freitas et al. (2013) and Ladeira and Gonçalves (2007) who studied the same site. Fernandes et al. (1998) showed that the concentrations of U in the AMD of the studied site vary along the wet and dry seasons from 1 to 13 mg L^{-1}. The low U content of the W3 sample - < 1 mg L^{-1} - can be attributed to the effectiveness of the treatment of the AMD with ionic resins for U recovery carried out by the mining company.

Table 1 - Chemical composition of the water samples (mg L^{-1}).

	W1*	W2*	W3*	W-Lab	DL[(a)]
pH	3.4	3.6	2.5	2.7	-
Eh (mV)	664	774	791	781	-
F	88	110	116	< DL	0.3
Cl	5.29	4.21	14.1	447	0.009
SO_4^{2-}	1000	900	618	1000	0.1
Na	3.18	1.62	4.25	0.63	0.001
K	12.9	9.7	15.6	< DL	0.001
Mg	8.1	7.6	12.8	0.148	0.005
Ca	120	103	180	< DL	0.005
P	0.174	0.157	0.338	0.146	0.009
Al	127	118	172	131	0.004
Si	17.3	13.0	19.1	< DL	0.003
Mn	91.9	85.0	8.2	135	0.001
Fe	12.5	0.396	1.75	< DL	0.002
Zn	14.9	13.4	21.3	< DL	0.001
U	5.28	5.28	0.935	< DL	0.016
Y	3.49	3.05	4.69	< DL	0.002
La	33.1	28.9	48.6	65	0.001
Ce	27.9	22.7	<DL	< DL	0.003
Pr	3.53	2.84	4.92	< DL	0.003
Nd	10.1	7.7	14.3	20	0.002
Sm	1.26	0.872	1.55	12.2	0.002
Eu	0.474	0.347	0.683	< DL	0.002
Gd	0.889	0.597	1.08	13.3	0.001
Tb	0.033	< DL	0.109	< DL	0.002
Dy	0.616	0.476	0.818	< DL	0.001
Er	0.015	< DL	0.198	< DL	0.003
Yb	0.111	0.090	0.067	< DL	0.001
Total REE	81.5	67.5	77.0	110.5	

* Adapted from Moraes et al. (2020). (a) Detection Limit

3.2. REE co-precipitation process

The results of the co-precipitation batch experiments are compiled in Figs. 1 and 2, revealing the REE and U scavenging process that occurs when the pH of the AMD samples was set to pre-determined values.

The scavenging of the REE by the precipitates occurred in the W1 and W2 samples (Fig. 1) when the pH was raised to values equal to 4, 5, 6 and 7. When the pH was raised up to 7, REE removal efficiencies of about 100% were reached for the W1 and W2 samples, despite the relative absence of Fe in these samples (Table 1). The same pattern was observed for the W-Lab and the W3 samples (Fig. 2).

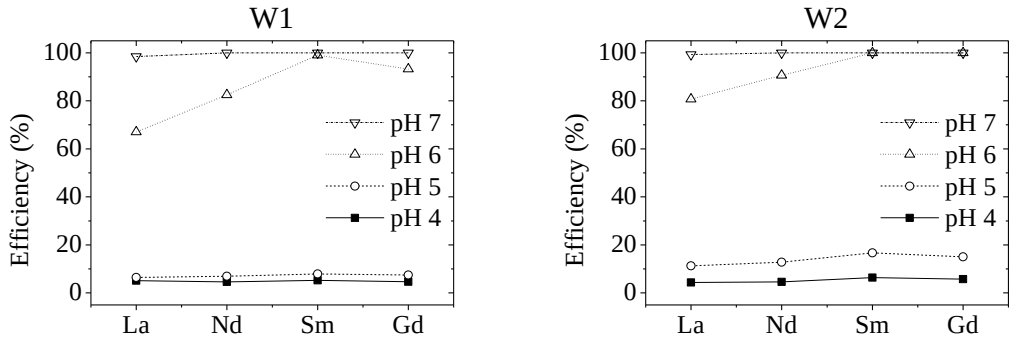

Fig. 1 – REE removal efficiency for the W1 and W2 samples at different pH values.

The amounts of Fe added in the experiments carried out with the W-lab and W3 samples were defined basing on the total content of Al and REE of each sample, as aforementioned in the materials and methods section. The results depicted in Fig. 2 show that at a pH < 6, the higher the initial Fe concentration in the AMD, the higher the REE removal efficiency. The same behaviour was observed for the W-Lab and W3 samples, although it was substantial in the W-Lab sample, probably due to its lower Al/REE molar ratio – less precipitates formed, i.e. less adsorbent in the suspension- and also probably due to its simpler composition, which leads to more adsorption sites available along with less competing ions, i.e., fewer interactions between the soluble elements and the precipitates formed by an increase in the pH.

The W-Lab sample at pH 5 presented an increase in the removal efficiencies from 0.6 to 17% for La, from 0.7 to 33% for Nd, from 4 to 41% for Sm and from 5 to 36% for Gd when the Fe/Al/REE molar ratios of the initial solution were equal to 0/6/1 and 12/6/1,

respectively. At pH 6 the removal efficiencies increased from 15 to 67% for La, from 51 to 92% for Nd, from 71 to 97% for Sm and from 72 to 97% for Gd when the Fe/Al/REE molar ratios of the initial solution were equal to 0/6/1 and 12/6/1, respectively.

Concurrently, the W3 sample at pH 6 presented an increase in the removal efficiencies from 78 to 88% for La, from 89 to 98% for Nd, from 96 to 100% for Sm and from 98 to 100% for Gd when the Fe/Al/REE molar ratios of the initial solution were equal to 0/12/1 and 24/12/1, respectively.

The addition of iron to the W3 sample was not relevant to the scavenging of the REE when the pH was adjusted to 7 and 8 (Fig. 2). As the Al/REE molar ratio of the W3 sample is the double of the W-Lab sample, at the former pH values, aluminium precipitates were formed and were responsible for the high removal of the REE present in the solution – up to 99% at pH 7 and 100% at pH 8, in consonance with the findings of Moraes et al. (2020). In conclusion, the addition of Fe to the AMD is not required to achieve high recovery of REE when the pH of AMD is set to 7 - 8, considering the amount of soluble aluminium present in the effluent – 172 mg L^{-1} – that precipitates and consequently co-precipitates the soluble REE present in the AMD.

The mechanism of REE removal and the importance of Al_{13}-polymers in this reaction in AMD treatment through pH neutralization were further discussed by Moraes et al. (2020). Moreover, when connecting the findings of the these authors to the work by Weatherill et al. (2016) about the role of Fe_{13}-Keggin clusters on the formation of ferrihydrite, it is possible to understand the co-precipitation phenomenon. The densification of the aggregates occurs in conjunction with precipitation of low molecular weight Al and Fe^{3+} species (e.g., monomers, dimers) to form mass fractal aggregates of nanoparticles when the pH of the solution is raised. The large surface area of the precipitates alongside with the reactive hydroxyl sites at the surface of the nanoparticles reacts with the soluble REE complexes, resulting in the co-precipitation of these REE. It seems that in the present case, a mixture of Al_{13} and Fe_{13} clusters compose the precipitate, and the large amount of REE – adsorbed and/or entrapped - contribute to a disorder in the structure of the precipitates, as evidenced by XRD (see topic 3.5) and ^{57}Fe Mössbauer spectroscopy (see topic 3.6).

The results depicted in Fig. 2 also show that the heavy REE – herein represented by Gd– are scavenged in a larger proportion than the light REE at lower pH values and at

any initial Fe concentration. This finding corroborates the works of Bau (1999) and Liu et al. (2017) who evidenced the greater affinity of heavy-REE over light-REE to be scavenged from waters by iron oxyhydroxides. Furthermore, the scavenging of Sm by the precipitates at pH 5 increases in higher proportion than La, Nd and Gd when Fe is added to the W-Lab sample.

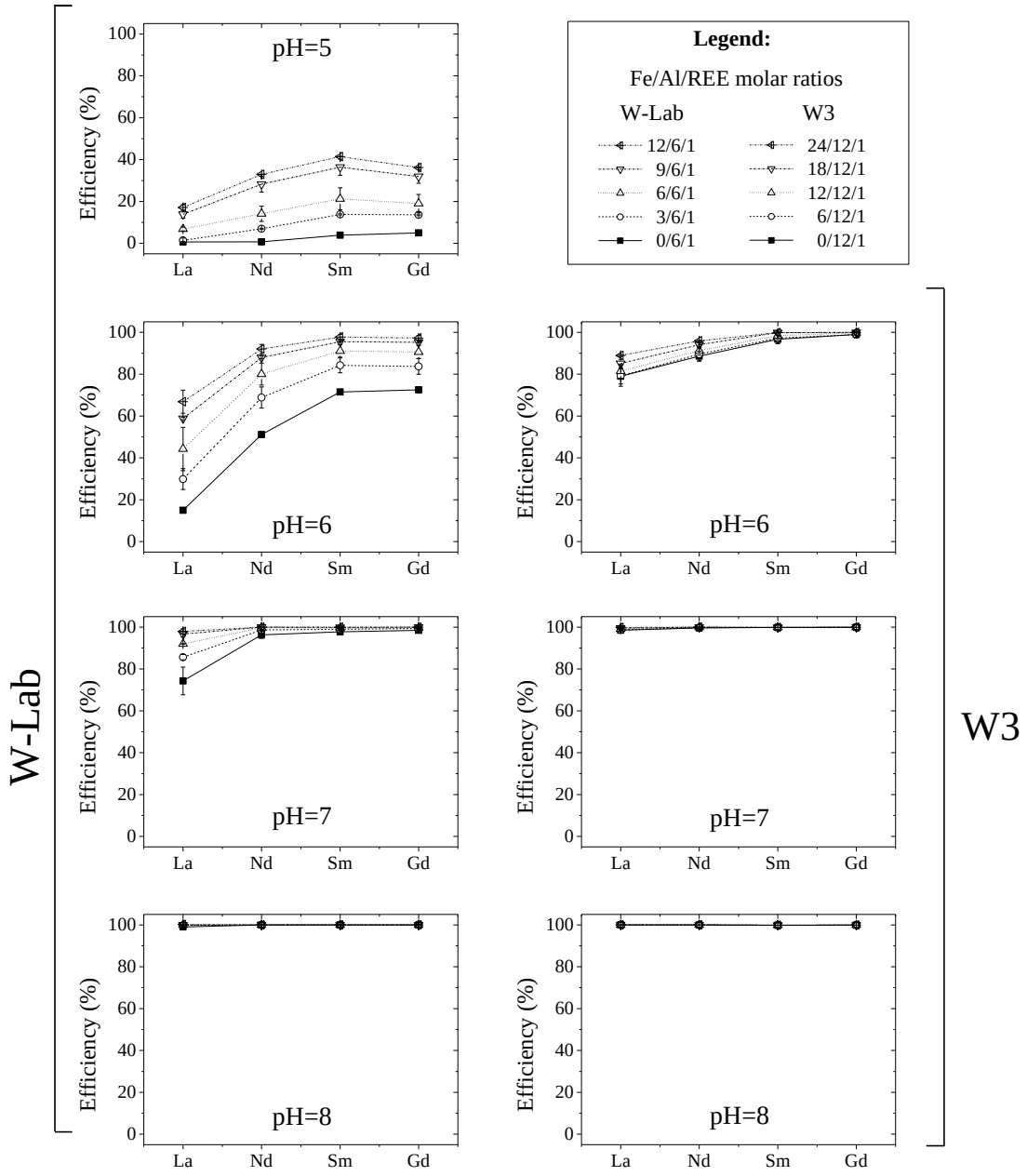

Fig. 2 – Effect of increasing initial Fe concentration on the REE removal efficiency at different pH values for the W-Lab and W3 samples.

Considering the results, the environmental implications to be hypothesized are related to the mobility of the REE due to the scavenging by the precipitates. AMD systems that have a high iron content should be "cleaned" by the scavenging effect carried out by the precipitates at lower pH values, i.e. < 6, what seems to be applicable in AMD passive treatment systems and even in natural systems, where the water parameters (pH, Eh, composition, etc.) can change due to the mixture of superficial and/or subsurface waters among other possible interactions and natural reactions. Moreover, when considering the possibility of recovering REE from AMD by co-precipitation, the concentration of the REE in a solid phase (REE-rich precipitates) should occur with high efficiency at lower pH (6 -7) due to the higher Fe content, meaning that less alkali agent (slaked lime, caustic soda, etc.) should be used to achieve the desired REE recovery.

3.3. Uranium co-precipitation process

The removal of uranium from the W1 and W2 samples at pH 4, 5, 6 and 7 are depicted in Fig. 3-a and revealed that the scavenging of U from the AMD increased from about 30 % at pH 5 to 100% at pH 6. Uranium was scavenged from the W3 sample by the precipitates with efficiencies higher than 96% at pH 6 and 100% at pH 7 and 8, independently of the initial Fe concentration (Fig. 3-b).

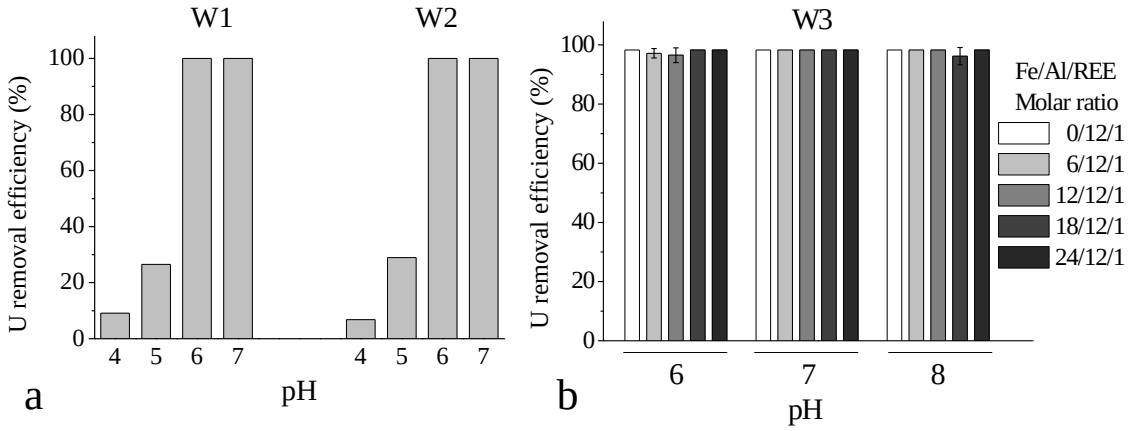

Fig. 3 – a) Uranium removal efficiency for the W1 and W2 samples at different pH values. b) Uranium removal efficiencies for the W3 sample at different pH values and different initial Fe concentration.

Waite et al. (1994) reported that uranium has great affinity to adsorb onto ferrihydrite surface at pH > 5 and that the major U^{6+} species at the ferrihydrite surface in the acidic pH range is an inner-sphere bidentate complex, involving two surface hydroxyls of an Fe

octahedron edge and the uranyl cation. Duff et al. (2002) reported the co-precipitation of U with hematite (α-Fe_2O_3) and showed the entrapment of U onto the structure of the precipitate through advanced spectroscopy techniques, reaffirming the strict relation between U and iron oxyhydroxides in aqueous systems.

In addition, the results obtained in the current study suggest that U can also be scavenged at high removal efficiencies from AMD solutions probably by Al_{13}-polymers, similar to the REE present in solution. It is possible that the structural similarity between the Al_{13}-Keggin ion (FURRER; LUDWIG; SCHINDLER, 1992; MORAES et al., 2020) and ferrihydrite (MICHEL et al., 2007) and, consequently, the surface chemistry related to the protonation, deprotonation and adsorption phenomena may be the key for understanding the U scavenging mechanism.

3.4. Stability of the precipitates

3.4.1. REE sequential extraction

A sequential extraction procedure was employed to evaluate the stability of the precipitates, assessing the relative affinities of the REE with the labile (acetic acid), reducible (hydroxylammonium chloride) and residual (total-labile-reducible) fractions of the precipitates.

The results depicted in Fig. 4 show the fractionation of La, Nd, Sm and Gd in the precipitates formed by an increase of the pH of the W-Lab and W3 samples until a value equal to 8, with different initial Fe/Al/REE molar ratios, obtained by sequential extraction.

All the four REE studied showed a similar pattern for the W-Lab precipitates: the higher the initial Fe concentration in the AMD, the lower the amount of REE in the labile fraction of the precipitates. This fraction reduced from 88 to 68% for La, from 78 to 56% for Nd, from 71 to 51% for Sm and from 74 to 58% for Gd when the initial Fe/Al/REE molar ratios were 0/6/1 and 12/6/1, respectively.

The W-Lab precipitates also presented a relative high amount of REE soluble in hydroxylammonium chloride, which corresponds to the fraction bound to the reducible fraction of the precipitates. Inversely, this fraction increased from 11 to 30% for La, from 22 to 40% for Nd, from 28 to 42% for Sm and from 25 to 39% for Gd when the initial

Fe/Al/REE molar ratios were 0/6/1 and 12/6/1, respectively. As iron is the only reducible major element that compose the precipitate, it is expected that the Fe content of the precipitate is directly related to the stronger retention of the REE in the structure of the material. This phenomenon is further discussed in topic 3.6, where the results of the ^{57}Fe Mössbauer spectroscopy are discussed.

It was also observed in the W-Lab precipitates that even when the initial Fe concentration was equal to the double of the Al concentration (i.e. Fe/Al/REE molar ratio of 12/6/1), the presence of REE in the residual fraction was very low, about 5%. In other words, this means that the W-Lab precipitates are not considered highly stable when analysing the behaviour of the REE because more than 50% of all REE present in the samples were found to be in the labile fraction for any amount of added Fe.

However, the fractionation of the REE in the precipitates obtained from the treatment of the W3 sample at pH 8 was revealed to be a little bit different. The influence of the addition of Fe over the stability of the precipitates produced with the W3 sample was higher, as it showed to be more stable than those produced with the W-Lab sample. However, a behaviour similar to the W-Lab was observed – decreasing labile fraction and increasing reducible and residual fractions when the Fe content was increased. The labile fraction of the W3 precipitates reduced from 46 to 35% for La, from 95 to 35% for Nd, from 84 to 22% for Sm and from 96 to 27% for Gd when the initial Fe/Al/REE molar ratios were 0/12/1 and 24/12/1, respectively. The reducible fraction increased from 2 to 41% for La, from 1 to 48% for Nd, from 0 to 31% for Sm and from 0 to 47% for Gd when the initial Fe/Al/REE molar ratios were 0/12/1 and 24/12/1, respectively.

At the maximum amount of Fe added (i.e. Fe/Al/REE molar ratio of 24/12/1), less REE were detected in the labile fraction and a greater amount of the studied elements were detected in the reducible and residual fractions. This means that the precipitates produced with the W3 sample tend to be more stable than those produced with the W-Lab sample when the overall Fe/Al molar ratio is 2/1. As the W3 contains the double amount of these elements than the W-Lab at the maximum molar ratio studied, the higher proportion of co-precipitant in relation to the REE leads to a higher stability of the material.

The environmental implications to be considered basing on these results are also related to the mobility of the REE. The more Fe in the AMD, the more stable will be the

precipitates formed due to an increase in the pH of the solution. This means that Fe-REE-rich precipitates should be more stable than Al-REE-rich precipitates under natural conditions. Another possibility to be considered is that Fe-rich precipitates containing REE should be more stable in sediments that are deposited under oxidic conditions, being able to immobilize the REE for long periods. The findings of the current work corroborate the works of Barcelos et al. (2018) and Pietralonga et al. (2017), who have studied the immobilization of REE by Fe oxyhydroxides in laboratory AMD solutions and concluded that REE-bearing precipitates that have higher Fe/Al molar ratios tend to be more stable under acetic acid leaching.

On the other hand, when the aim is the recovery of REE from AMD, the lower the Fe content of the AMD system, the easier will be the recovery of REE through acid leaching, considering that high amounts of REE are labile - soluble in acetic acid - when no Fe is added to the solution before pH neutralisation (Fig. 4). Neodymium should be highlighted among the REE studied considering that the precipitate produced with the W3 sample that had no Fe added - i.e. molar ratio of 0/12/1, its natural condition -presented an Nd extraction of more than 90% by acetic acid. It is a noteworthy result considering the criticality of the global demand for Nd (BAUER et al., 2010; EUROPEAN UNION, 2017). According to Moraes et al. (2020), about 100 kg of Nd could be recovered from the AMD daily in the studied site considering the W3 sample – Nd = 14.3 mg L^{-1} - and the current flow rate of the AMD treatment installed in that site – about 300 m^3 h^{-1}.

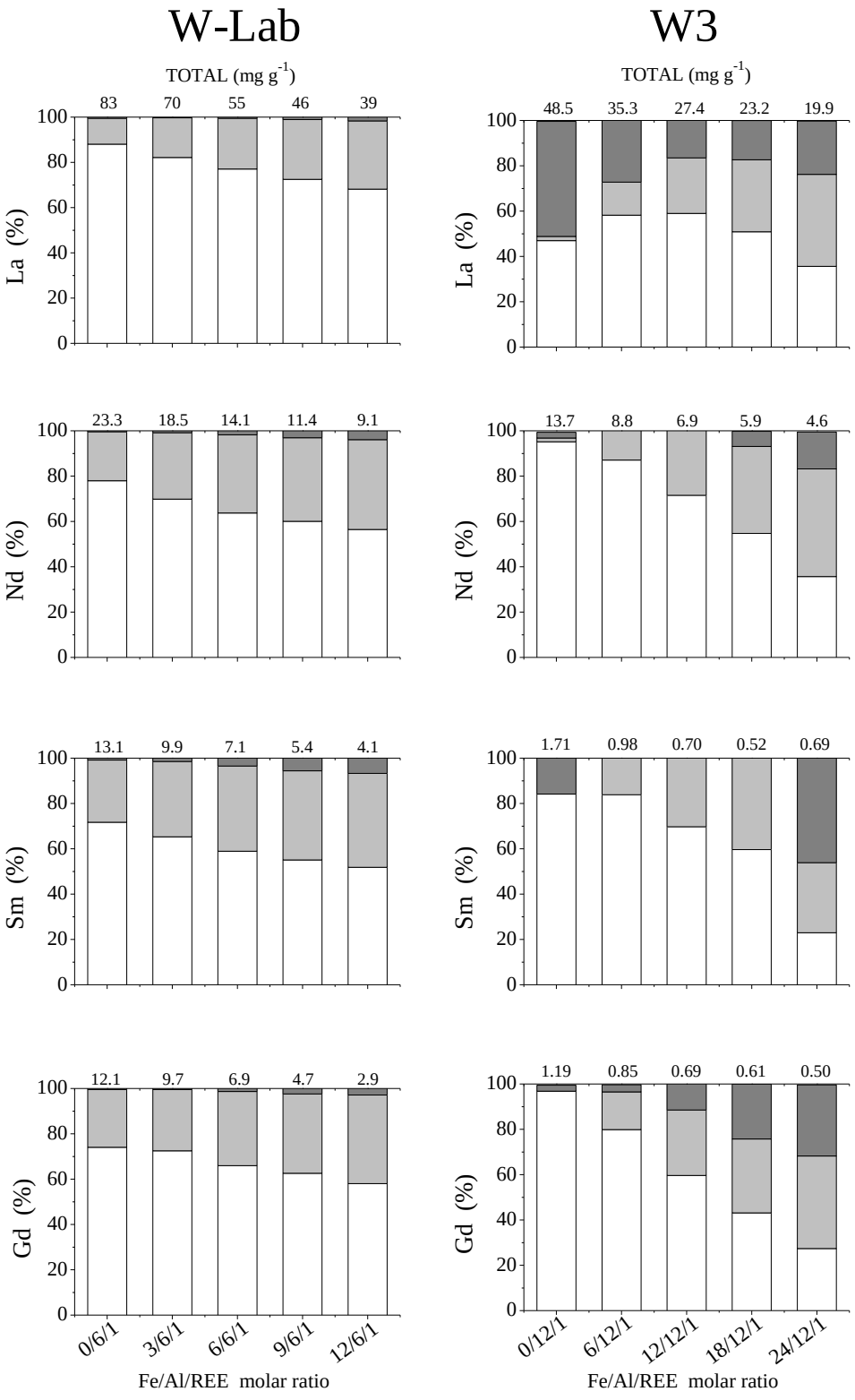

Fig. 4 – Fractionation of La, Nd, Sm and Gd in the precipitates obtained from the treatment of the W-Lab and W3 samples at pH 8 and different Fe/Al/REE molar ratios.

(Legend: [white]: labile; [grey]: reducible; [dark grey]: residual)

3.4.2. U, Al, Mn and Fe sequential extraction

The results depicted in Fig. 5 compile the results of the fractionation of U in the precipitates obtained through the treatment of the W3 sample with increasing initial iron content. Differently from the REE, uranium showed to be less labile (23%) and to remain in the residual fraction (77%) when iron was not added – i.e. molar ratio of 0/12/1. When the Fe/Al/REE molar ratio raised from 0/12/1 to 6/12/1, there was an increase in the labile fraction from 23 to 45%. Therefore, there was a reduction of this fraction when more Fe was added, reaching 32, 21 and 10% for the Fe/Al/REE molar ratios of 12/12/1, 18/12/1 and 24/12/1, respectively.

Uranium in the reducible fraction was only detected when the initial solution had equal amounts of Al and Fe (molar ratio of 12/12/1). It increased from less than 1% when the Fe/Al/REE molar ratio was 6/12/1 up to 8, 12 and 17% when the molar ratios were 12/12/1, 18/12/1 and 24/12/1, respectively. The amount of U in the residual fraction had also an expressive increase when iron was added to the initial solution, reaching a maximum of 73% at the highest Fe/Al/REE molar ratio investigated.

The same aforementioned considerations concerning the environmental implications due to an increase of the Fe content in AMD can be attributed to the possible behaviour of U when scavenged by precipitates – the greater the Fe content, the higher the stability of the precipitate, i.e. U is less labile. However, when considering the recovery of REE from AMD by co-precipitation and subsequent acid leaching, the fact that the U present in the precipitates can be extracted in less proportion by acetic acid is something to be considered positive, because the leachate containing REE will present a higher purity, i.e. a lower U content. Moreover, issues related to the radioactivity involved in the operations can be partially mitigated. Thus, the waste (leaching residue) to be generated will demand special concerning about radioactive materials disposal. New research projects can be purposed aiming the recovery of U from wastes, seeking the production of a uranium concentrate and the mitigation of future environmental issues.

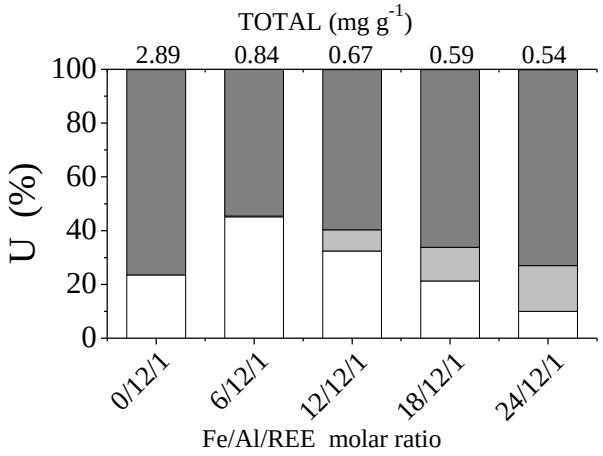

Fig. 5 – Fractionation of U in the precipitate obtained from the treatment of the W3 sample at pH 8 and different Fe/Al/REE molar ratios. (Legend: [white]: labile; [grey]: reducible; [dark grey]: residual)

The results depicted in Fig. 6 show the fractionation of Al, Mn and Fe in the precipitates obtained through the treatment of the W-Lab and W3 samples at pH 8 with increasing initial iron content.

The Al content of the W-Lab precipitates was found to be mostly in the residual fraction (≥ 80%) for all molar ratios studied. Concurrently, the amount of Al in the labile fraction was < 8% and the reducible fraction was about 10% for all molar ratios. As aluminium is not reducible, the amount of this element detected in the hydroxylammonium chloride extract of the precipitate produced at a Fe/Al/REE ratio of 0/6/1 can be attributed to the dissolution of the precipitate due to the acidity of the extractant solution, which is prepared with hydroxylammonium chloride and HNO_3 and have a pH=1.5 (RAURET et al., 1999).

In a similar way, about 80% of the Fe content of the W-Lab precipitates was also found to be in the residual fraction and the reducible fraction was < 20% for all the Fe/Al/REE ratios studied. No labile Fe was detected in any sample. The Mn fractionation was slightly affected by the addition of Fe in the initial solution, resulting in an increase in the residual fraction and a decrease in the labile fraction – it tends to be more stable with an increase in the iron content.

Differently, the precipitates obtained through the neutralization of the W3 sample presented a relative increase in their stability when looking only to the Fe and Mn fractionation. When the Fe content is increased, this element tends to be less extracted by

acetic acid and hydroxylammonium chloride and tend to remain in the residual fraction. Simultaneously, Mn increased in the reducible fraction and decreased in the labile fraction when there was an increase in the Fe content - it tends to be more stable with an increase in the iron content.

Regarding the behaviour of the element Fe, the works by Colombo (1996), Hansel et al. (2011) and Schwertmann & Murad (1990) suggest that Al substitution increases the stability of Fe oxyhydroxides.

Regarding the behaviour of the element Mn, Lan et al. (2017) showed that Fe oxyhydroxide surfaces promote Mn^{2+} oxidation via both conventional interfacial catalysis and electrochemical catalysis - i.e., electron transfer -because Fe^{3+} in ferrihydrite is an active electron acceptor. It may be able to transport electrons from Mn^{2+} to O_2 when Mn^{2+}-Fe^{3+}-O_2 complexes form at the surface of the Fe oxyhydroxides. On the other hand, although the surface functional groups on amorphous Al oxyhydroxide surfaces are similar to those of ferrihydrite surfaces, the catalytic activity of amorphous Al oxyhydroxide surfaces for Mn^{2+} oxidation is very weak. These authors suggest that this may be attributed to the fact that Al does not have variable valence, and amorphous $Al(OH)_3$ is an insulator material (BARRÓN; TORRENT, 2013), which is unfavourable to electron transfer and transport, whereas ferrihydrite is a type of semiconductor mineral, facilitating electronic transfer and inducing redox reactions.

Attention should be paid to the fact that no residual Mn was detected, in contrast to the fractionation of the element Fe, what means that Mn is more susceptible to reducible environments than Fe. It may cause serious issues concerning the disposal of AMD precipitates as Mn is extremely toxic to the environment and human health, especially in dams and impoundments, where anoxic conditions can occur.

Antithetically, the behaviour of the Al present in the precipitates obtained through the neutralization of the W3 sample showed to be different of the behaviour of Fe and Mn. Initially, when the Fe/Al/REE ratio was 0/12/1 – no Fe added, but there were 1.75 mg of iron per litter of AMD (Table 1) – the labile fraction corresponds to 22%, the reducible fraction to 4% and the residual fraction to 74%. An increase in the Fe content led to a small increase in the labile fraction of Al, an increase in the reducible fraction and a reduction of the residual fraction, when the Fe/Al/REE ratios were increased from 6/12/1

to 18/12/1. Then, when the ratio was 24/12/1, the residual fraction increased along with a small reduction of both labile and reducible fractions.

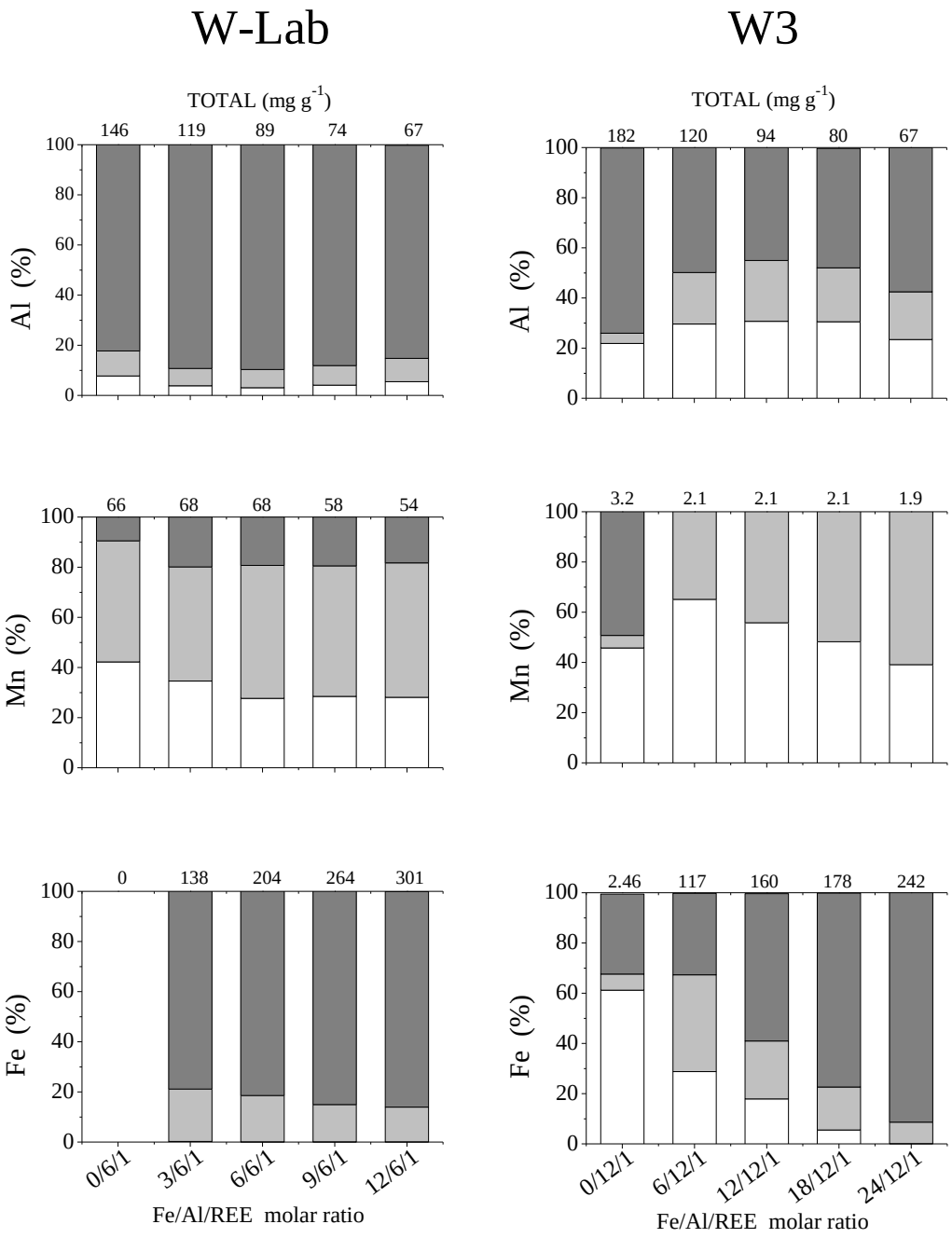

Fig. 6 –Al, Mn and Fe BCR sequential extraction results of the W-Lab and W3 samples at pH 8 and different Fe/Al/REE molar ratios. (Legend: [white]: labile; [grey]: reducible; [dark grey]: residual)

In other words, considering the sequential extraction results of the W3 precipitates for the REE, U, Fe and Mn as a whole, the higher the Fe initial concentration of the AMD before pH neutralization, the higher will be the stability of the precipitates produced.

3.5. Powder X-ray diffraction patterns

The results of the powder XRD analysis of the W-Lab and W3 precipitates and the samples prepared for the ^{57}Fe Mössbauer spectroscopy studies (Fh and Fh-REE) are compiled in Fig. 7.

The samples Fh and Fh-REE presented a typical 2-line ferrihydrite pattern, in consonance with those reported for natural and synthetic ferrihydrite reported by Cornell & Schwertmann (2003), Eusterhues et al. (2008); Jambor & Dutrizac (1998) and Schwertmann & Cornell (2000). The powder XRD patterns of all samples presented high background and no peaks were detected at all.

All the precipitates produced by the neutralization of the W-Lab and W3 samples at pH 8 were diagnosed by powder XRD as being amorphous, independently of the Fe content of the sample. It was expected that in the samples containing the highest Fe content this element should precipitate as ferrihydrite, according to Cismasu et al. (2012) who studied the effects of Al content and precipitation rate on the structure of 2-line ferrihydrite or even as other Fe oxyhydroxides such like lepidocrocite (γ-FeO(OH)), goethite (α-FeO(OH)) or magnetite (Fe_3O_4), as reported by Barcelos et al. (2018) and Pietralonga et al. (2017). The presence of REE in the solution may also contribute to a relative disorder in the structure of the precipitates, impeding the formation of well-crystallised minerals or mineral phases with some degree of crystallinity, such as ferrihydrite (HUA et al., 2019; MORAES et al., 2020).

Moraes et al. (2020) reported a detailed mineralogical study about Al-REE-rich precipitates formed in the same conditions of the current study. By using nuclear magnetic resonance and transmission electron microscopy techniques, these authors showed the importance of Al_{13}-polymers in the removal of REE from the AMD. The amorphous structure of the material did not present any peaks when analysed through powder X-ray diffraction nor when analysed through electron diffraction.

Apparently, the samples Fh and Fh-REE look equal under powder XRD analysis as typical two-line ferrihydrites, however, the ^{57}Fe Mössbauer spectroscopy analysis revealed structural changes that can possibly be attributed to the presence of REE in the precipitates, as discussed further.

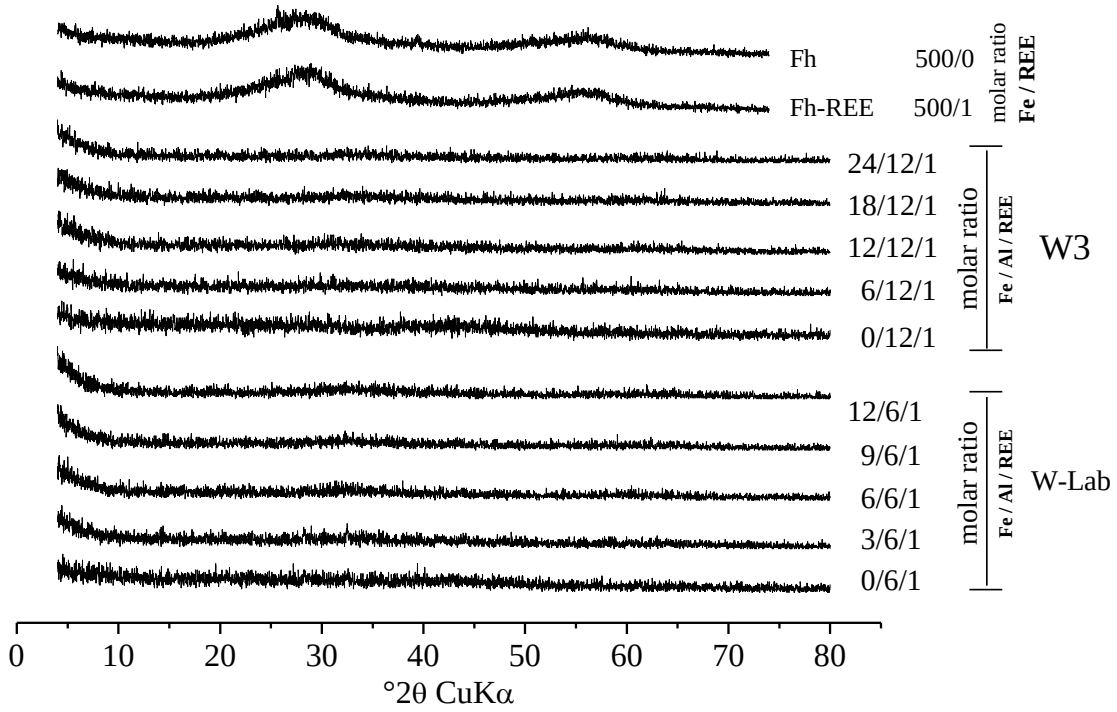

Fig. 7 – Powder X-ray diffraction patterns of the studied samples. The numbers after each pattern for the W3 and W-Lab samples represent the molar ratios studied at pH 8.

3.6. ^{57}Fe Mössbauer spectroscopy studies

The results of the ^{57}Fe Mössbauer spectroscopy studies and the calculated Mössbauer parameters are compiled in Fig. 8 and Table 2, respectively. The peaks of the spectra obtained for both Fh and Fh-REE samples are considerably wide and the samples presented a low absorbance of the γ-rays. This occurs due to the low crystallinity of the sample, normally observed in ferrihydrite (MURAD, 1988; WANG et al., 2016). However, the sample Fh-REE presented wider peaks and a lower absorbance than the Fh sample.

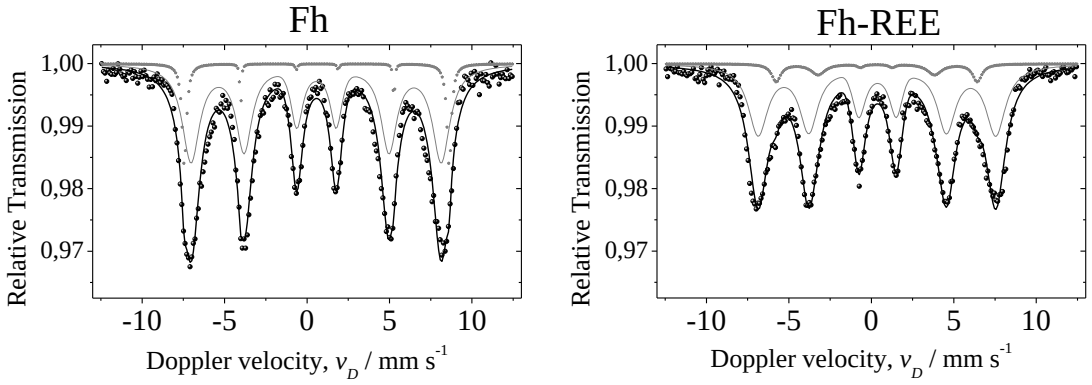

Fig. 8 – ^{57}Fe Mössbauer spectra at 25 K of the Fh and Fh-REE samples.

Table 2 – Calculated Mössbauer parameters of the Fh and Fh-REE samples. (δ/αFe = isomeric shift; Δ = quadrupole splitting; Bhf = magnetic hyperfine field).

Sample	Sub-spectrum	Area	Width	δ/αFe	Δ	B_{hf}
Fh	A	0.262	0.889	0.57	-0.025	47.052
	B	0.007	0.166	0.59	-0.029	49.806
Fh-REE	A	0.227	1.015	0.36	-0.039	44.683
	B	0.011	0.484	0.30	0.028	37.802

Another fact to be observed in the ^{57}Fe Mössbauer spectra obtained at 25 K is the presence of two sub-spectra in each sample (Fig. 8). These results reveal the presence of two distinct sites in the ferrihydrite structure: one tetrahedral - Fe(4) - and another octahedral - Fe(6) – (HIEMSTRA, 2013; MICHEL et al., 2007; WANG et al., 2016), as depicted in Fig. 9.

Mössbauer spectra collected at 25 K have a higher likelihood of resonance than those collected at room temperature, as the samples present a greater amount of iron atoms at the zero-phonon fraction at lower temperatures. At such condition, the magnetic hyperfine interaction can then be accessed (YOSHIDA; GUIDO, 2013). An hyperfine magnetic field (Bhf) of 47.052 was found for the sub-spectrum A and a value of 49.806 for the sub-spectrum B of the Fh sample (pure ferrihydrite), corroborating the expected results for the ferrihydrite, which normally present a Bhf of about 46 to 50 (STEVENS et al., 2005).

However, the sample Fh-REE presented a Bhf = 44.683 for its sub-spectrum A and 37.802 for its sub-spectrum B. This reduction in the hyperfine magnetic field may be attributed to the possible presence of the REE inside the structure, according to Murad

and Schwertmann (1983). The REE have a coordination number of 6 when in solution, resulting in an octahedron, although the REE have ionic radius bigger than Fe (HUANG, 2010). Thus, during the co-precipitation process, REE hydroxides can occupy the octahedral sites of the mineral structure that is forming. The electronic configuration of the REE present in the Fh-REE sample (adsorbed and/or trapped) modifies the hyperfine field of the probe atoms – Fe atoms population at the zero-phonon fraction – considering that the electron pairing with the same spin is different from those of iron atoms. In other words, the distance between the Fe atoms of the sample is increasing due to the presence of the REE and consequently reducing the hyperfine magnetic interactions between the atoms of iron. However, further investigation with the use of synchrotron-based techniques are required for a precise understanding of this mechanism.

By connecting these findings obtained through the ^{57}Fe Mössbauer spectroscopy with the results of the sequential extraction (topics 3.4.1 and 3.4.2), a better understanding of the reason why the precipitates become more stable when the Fe content increases can be achieved. As the REE can possibly enter in the structure of the material, occupying Fe sites, the higher the Fe/Al/REE ratio, the lower the lability of the REE.

In Fig. 9, the understanding of the results was synthesized, showing the structure of ferrihydrite and its tetrahedral – Fe(4) – and octahedral – Fe(6) – sites and the possible occupation of some sites by the REE. The data concerning the ferrihydrite structure used for drawing Fig. 9 was those available in the work by Michel et al. (2007).

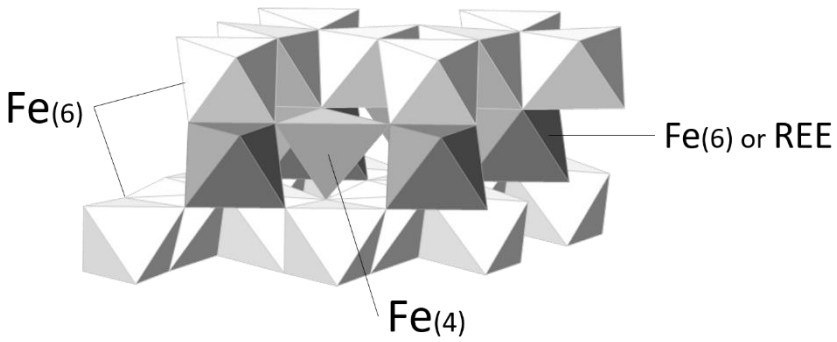

Fig 9 –Structure of ferrihydrite and the possible occupation of octahedral sites by REE.

4. CONCLUSIONS

The results of the current study revealed the important role played by Fe^{3+} in the precipitates that are responsible for the scavenging of REE and U in AMD systems. The initial amount of soluble Fe^{3+} at the acid environment defines the stability of the amorphous REE-rich precipitates formed when there is an increase in the pH of the system. The higher the amount of Fe in the system, the higher will be the REE removal efficiency due to the scavenging – co-precipitation/adsorption - carried out by the precipitates formed and also, the higher will be the stability of the precipitates, as revealed through the sequential extraction results. When concerning Fe precipitates composed of ferrihydrite, the possible entrance of the REE in its structure can occur, as revealed by ^{57}Fe Mössbauer spectroscopy, corroborating the aforementioned sequential extraction results.

Extrapolating the results of the current study to other AMD systems, the environmental implications to be considered concern about the mobility of the REE and U in the environment, superficial and groundwaters, dams and impoundments, passive treatment systems, sedimentology, between many other fields of science. However, when the aim is recovering REE from AMD by co-precipitation and subsequent acid leaching, the higher stability of the precipitates formed in systems that may have higher amounts of soluble Fe will lead to an inevitable stronger leaching using more concentrated acids to solubilize all the potentially recoverable REE.

5. REFERENCES

ABREU, R. D.; MORAIS, C. A. Study on separation of heavy rare earth elements by solvent extraction with organophosphorus acids and amine reagents. **Minerals Engineering**, v. 61, p. 82–87, jun. 2014.

AYORA, C. et al. Recovery of Rare Earth Elements and Yttrium from Passive-Remediation Systems of Acid Mine Drainage. **Environmental Science and Technology**, v. 50, n. 15, p. 8255–8262, 2016.

BARCELOS, G. S. et al. Immobilization of Eu and Ho from synthetic acid mine drainage by precipitation with Fe and Al (hydr)oxides. **Environmental Science and Pollution Research**, v. 25, n. 19, p. 18813–18822, 2018.

BARRÓN, V.; TORRENT, J. Iron, manganese and aluminium oxides and oxyhydroxides. In: **Minerals at the Nanoscale**. London: Mineralogical Society of Great Britain and Ireland, 2013. v. 14-Chaptp. 297–336.

BAU, M. Scavenging of dissolved yttrium and rare earths by precipitating iron oxyhydroxide: Experimental evidence for Ce oxidation, Y-Ho fractionation, and lanthanide tetrad effect. **Geochimica et Cosmochimica Acta**, v. 63, n. 1, p. 67–77, 1999.

BAU, M.; KOSCHINSKY, A. Oxidative scavenging of cerium on hydrous Fe oxide: Evidence from the distribution of rare earth elements and yttrium between Fe oxides and Mn oxides in hydrogenetic ferromanganese crusts. **Geochemical Journal**, v. 43, n. 1, p. 37–47, 2009.

BAUER, D. et al. US Department of Energy: Critical Materiasl Strategy, December 2010. **Agenda**, n. December, p. 1–166, 2010.

BINNEMANS, K. et al. Recycling of rare earths: A critical review. **Journal of Cleaner Production**, v. 51, p. 1–22, 2013.

CISMASU, A. C. et al. Properties of impurity-bearing ferrihydrite I. Effects of Al content and precipitation rate on the structure of 2-line ferrihydrite. **Geochimica et Cosmochimica Acta**, v. 92, p. 275–291, 2012.

COLOMBO, C. Effect of Time and Temperature on the Chemical Composition and Crystallization of Mixed Iron and Aluminum Species. **Clays and Clay Minerals**, v. 44, n. 1, p. 113–120, 1996.

CONAMA. **Resolution N°430, 13/05/2011 - provides conditions and standards for effluent discharge. Conselho Nacional do Meio Ambiente**Brazilian National Envirnonmet Concil, , 2011.

CORNELL, R. M.; SCHWERTMANN, U. **The Iron Oxides - Structure, Properties, Reactions, Occurences and Uses**. 2nd. ed. Weinheim: WILEY-VCH, 2003.

DUFF, M. C.; COUGHLIN, J. U.; HUNTER, D. B. Uranium co-precipitation with iron oxide minerals. **Geochimica et Cosmochimica Acta**, v. 66, n. 20, p. 3533–3547, 2002.

EUROPEAN UNION, E. U. **Study on the review of the list of critical raw materialsEuropean Comissmion**. Brussels: [s.n.]. Disponível em: <https://publications.europa.eu/en/publication-detail/-/publication/08fdab5f-9766-11e7-b92d-01aa75ed71a1/language-en>.

EUSTERHUES, K. et al. Characterization of Ferrihydrite-Soil Organic Matter Coprecipitates by X-ray Diffraction and Mössbauer Spectroscopy. **Environmental Science & Technology**, v. 42, n. 21, p. 7891–7897, nov. 2008.

FERNANDES, H. M.; FRANKLIN, M. R.; VEIGA, L. H. Acid rock drainage and radiological environmental impacts. A study case of the Uranium mining and milling facilities at Pocos de Caldas. **Waste Management**, v. 18, n. 3, p. 169–181, 1998.

FONSECA, V. Mais energia, menos impacto para o ambiente. **Publicação trimestral da Fundação de Amparo à Pesquisa do Estado de Minas Gerais - FAPEMIG, N°39 - Set-Nov**, p. 62, 2009.

FREITAS, R. M. et al. Oxidative Precipitation of Manganese from Acid Mine Drainage by Potassium Permanganate. **Journal of Chemistry**, v. 2013, n. JANUARY 2013, p. 1–8, 2013.

FURRER, G.; LUDWIG, C.; SCHINDLER, P. W. On the chemistry of the Keggin Al13 polymer I. Acid-base properties. **Journal of Colloid and Interface Science**, v. 149, n. 1, p. 56–67, mar. 1992.

HANSEL, C. M. et al. Effect of adsorbed and substituted Al on Fe(II)-induced mineralization pathways of ferrihydrite. **Geochimica et Cosmochimica Acta**, v. 75, n. 16, p. 4653–4666, ago. 2011.

HIEMSTRA, T. Surface and mineral structure of ferrihydrite. **Geochimica et Cosmochimica Acta**, v. 105, p. 316–325, 2013.

HUA, J. et al. Effects of Rare Earth Elements' Physicochemical Properties on Their Stabilization during the Fe(II) aq -induced Phase Transformation of Ferrihydrite. **ACS Earth and Space Chemistry**, v. 3, n. 6, p. 895–904, 20 jun. 2019.

HUANG, C. (ED.). **Rare Earth Coordination Chemistry: fundamentals and applications**. Singapore: John Wiley & Sons (Asia) Pte Ltd, 2010.

JAMBOR, J. L.; DUTRIZAC, J. E. Occurrence and Constitution of Natural and Synthetic Ferrihydrite, a Widespread Iron Oxyhydroxide. **Chemical Reviews**, v. 98, n. 7, p. 2549–2586, 1998.

LADEIRA, A. C. Q.; GONÇALVES, C. R. Influence of anionic species on uranium separation from acid mine water using strong base resins. **Journal of Hazardous Materials**, v. 148, n. 3, p. 499–504, 2007.

LAN, S. et al. Mechanisms of Mn(II) catalytic oxidation on ferrihydrite surfaces and the formation of manganese (oxyhydr)oxides. **Geochimica et Cosmochimica Acta**, v. 211, p. 79–96, ago. 2017.

LIU, H. et al. Rare earth elements sorption to iron oxyhydroxide: Model development and application to groundwater. **Applied Geochemistry**, v. 87, n. December, p. 158–166, dez. 2017.

MICHEL, F. M. et al. The Structure of Ferrihydrite, a Nanocrystalline Material. **Science**, v. 316, n. 5832, p. 1726–1729, 22 jun. 2007.

MORAES, M. L. B. et al. The role of Al13-polymers in the recovery of rare earth elements from acid mine drainage through pH neutralization. **Applied Geochemistry**, v. 113, p. 104466, fev. 2020.

MURAD, E. The Mössbauer spectrum of "well"-crystallized ferrihydrite. **Journal of Magnetism and Magnetic Materials**, v. 74, n. 2, p. 153–157, set. 1988.

MURAD, E.; SCHWERTMANN, U. The influence of aluminium substitution and crystallinity on the Mössbauer spectra of goethite. **Clay Minerals**, v. 18, n. 3, p. 301–312, 9 set. 1983.

PIETRALONGA, A. G. et al. Lanthanum immobilization by iron and aluminum colloids. **Environmental Earth Sciences**, v. 76, n. 7, p. 1–7, 2017.

QUINN, K. A.; BYRNE, R. H.; SCHIJF, J. Comparative scavenging of yttrium and the rare earth elements in seawater: Competitive influences of solution and surface chemistry. **Aquatic Geochemistry**, v. 10, n. 1–2, p. 59–80, 2004.

RAURET, G. et al. Improvement of the BCR three step sequential extraction procedure prior to the certification of new sediment and soil reference materials. **Journal of Environmental Monitoring**, v. 1, n. 1, p. 57–61, 1999.

SCHWERTMANN, U.; CORNELL, R. M. **Iron Oxides in the Laboratory: Preparation and characterization**. 2nd. ed. Weinheim, Germany: Wiley-VCH Verlag GmbH, 2000.

SCHWERTMANN, U.; MURAD, E. The Influence of Aluminum on Iron Oxides: XIV. Al-Substituted Magnetite Synthesized at Ambient Temperatures. **Clays and Clay Minerals**, v. 38, n. 2, p. 196–202, 1990.

STEVENS, J. G. et al. **Mössbauer Mineral Handbook**. Asheville, North Carolina, USA.: Mössbauer Effect Data Center, The University of North Carolina, 2005.

U.S. GEOLOGICAL SURVEY. **Mineral Commodity SummariesMineral Commodity Summaries**. Reston, Virginia, USA: [s.n.].

U.S. GEOLOGICAL SURVEY. **Mineral Commodity Summaries**. [s.l: s.n.]. Disponível em: <https://doi.org/10.3133/70202434>.

VASS, C. R.; NOBLE, A.; ZIEMKIEWICZ, P. F. The Occurrence and Concentration of Rare Earth Elements in Acid Mine Drainage and Treatment Byproducts. Part 2: Regional Survey of Northern and Central Appalachian Coal Basins. **Mining, Metallurgy & Exploration**, v. 36, n. 5, p. 917–929, 1 out. 2019a.

VASS, C. R.; NOBLE, A.; ZIEMKIEWICZ, P. F. The Occurrence and Concentration of Rare Earth Elements in Acid Mine Drainage and Treatment By-products: Part 1—Initial Survey of the Northern Appalachian Coal Basin. **Mining, Metallurgy & Exploration**, v. 36, n. 5, p. 903–916, 25 out. 2019b.

VERPLANCK, P. L. et al. Rare earth element partitioning between hydrous ferric oxides and acid mine water during iron oxidation. **Applied Geochemistry**, v. 19, n. 8, p. 1339–1354, 2004.

VERPLANCK, P. L. Partitioning of Rare Earth Elements between Dissolved and Colloidal Phases. **Procedia Earth and Planetary Science**, v. 7, p. 867–870, 2013.

WABER, N.; SCHORSCHER, H. D.; PETERS, T. Hydrothermal and supergene uranium mineralization at the Osamu Utsumi mine, Poços de Caldas, Minas Gerais, Brazil. **Journal of Geochemical Exploration**, v. 45, n. 1–3, p. 53–112, nov. 1992.

WAITE, T. D. et al. Uranium(VI) adsorption to ferrihydrite: Application of a surface complexation model. **Geochimica et Cosmochimica Acta**, v. 58, n. 24, p. 5465–5478, dez. 1994.

WANG, X. et al. Effects of crystallite size on the structure and magnetism of ferrihydrite. **Environ. Sci.: Nano**, v. 3, n. 1, p. 190–202, 2016.

WEATHERILL, J. S. et al. Ferrihydrite formation: The role of Fe13 Keggin clusters. **Environmental Science and Technology**, v. 50, n. 17, p. 9333–9342, 2016.

YOSHIDA, Y.; GUIDO, L. **Mössbauer Spectroscopy**. Berlin, Heidelberg: Springer Berlin Heidelberg, 2013.

ZIEMKIEWICZ, P. (WEST V. U.; NOBLE, A. (VIRGINIA T. **Annual repport: Recovery of Rare Earth Elements (REEs) from Coal Mine Drainage - Apr/2019**. Pittsburgh PA: [s.n.]. Disponível em: <https://www.netl.doe.gov/sites/default/files/2019-05/2019_Annual_Reports/Tuesday/ree/4 - 20190409_1130A_FE0026927_NETL.pdf>.

Chapter 3

Influence of soluble Ca^{2+} and Zn^{2+} on the co-precipitation of rare earth elements with Al_{13}-polymers through pH neutralization

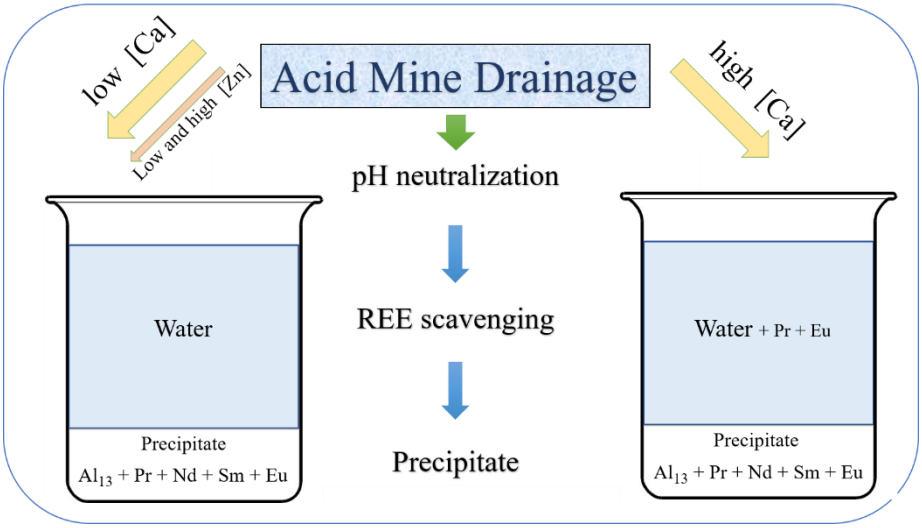

ABSTRACT: As rare earth elements (REE) are crucial for the development of new technologies, techniques to recover these elements from secondary sources, such as acid mine drainage (AMD), are being developed in many sites worldwide. Previous studies showed that the elements praseodymium (Pr) and europium (Eu) have a behaviour of co-precipitation with aluminium precipitates different from other REE when neutralizing AMD, possibly due to competition with soluble cations. The current work seeks to evaluate the influence of soluble calcium (Ca^{2+}) and zinc (Zn^{2+}) over the co-precipitation of Pr^{3+}, neodymium (Nd^{3+}), samarium (Sm^{3+}) and Eu^{3+} with amorphous aluminium precipitates. A series of co-precipitation and adsorption experiments were carried out in this investigation using AMD-simulating solutions. The results showed that Ca exerts a negative influence over the co-precipitation and over the adsorption of Pr^{3+} and Eu^{3+} onto amorphous aluminium precipitates, contrasting to the elements Nd and Sm whose co-precipitation and adsorption is independent of the presence of Ca in the solution. The element Zn did not influence the co-precipitation of the REE. The implications of the findings on environmental sciences and on the recovery of REE from AMD are discussed, highlighting the impact of the use of calcium hydroxide to that by pH neutralization.

KEYWORDS: rare earth elements, amorphous aluminium precipitates, metal recovery, calcium, zinc, co-precipitation, adsorption.

1. INTRODUCTION

The recovery of rare earth elements (REE) from secondary sources, such as coal ashes and acid mine drainage (AMD) is a tendency among researchers worldwide. This process has been investigated over the past few years, especially in Spain (AYORA et al., 2016) and in the United States of America (KING et al., 2018; STEWART et al., 2017; VASS; NOBLE; ZIEMKIEWICZ, 2019a, 2019b; ZHANG; HONAKER, 2018), where the recovery of REE from AMD is already a reality (NATIONAL ENERGY TECHNOLOGY LABORATORY; U.S. DEPARTMENT OF ENERGY, 2019).

The main phenomenon responsible for the success of many endeavours to recover REE from aqueous solutions is the adsorption of these elements on the surface of determined materials. The adsorption of REE on many adsorbents was reviewed on the work by Anastopoulos et al. (2016) and the recent advances in the hydrometallurgical recovery of rare earth metals were reviewed in the work by Jha et al. (2016) where the importance of adsorption is also highlighted.

Moraes et al. (2020) studied the role of Al_{13}-polymers in the recovery of rare earth elements from AMD through pH neutralization considering an AMD system located in Brazil. The concentration of REE in that site is extremely high and the treatment of the AMD is carried out through pH neutralization. The aforementioned authors showed that, at pH 8, Al_{13}-polymers are responsible for the removal of the soluble REE at efficiencies of about 100%, however, the elements praseodymium (Pr^{3+}) and europium (Eu^{3+}) were not completely removed from the AMD, possibly due to the competition with other soluble cations for adsorption sites on the surface of the aluminium precipitates. These authors suggested that calcium (Ca^{2+}) and zinc (Zn^{2+}) could be the most probable competitors due to their high concentration in the effluent.

In this scenario the current work aimed at studying the influence of soluble Ca and Zn over the co-precipitation of Pr^{3+}, neodymium (Nd^{3+}), samarium (Sm^{3+}) and Eu^{3+} by the Al_{13}-polymers formed due to pH neutralization. The research employed a batch co-precipitation and an adsorption experiment. The influence of Ca^{2+} and Zn^{2+} over the co-precipitation and adsorption of Pr and Eu, the possible mechanism of competition and the implications to be considered, are discussed in this work.

2. MATERIALS AND METHODS

2.1. Reactants and solutions

To study the influence of Ca and Zn on the co-precipitation of REE in AMD by precipitates composed of Al_{13}-polymers (Al gel), a laboratory AMD-simulating solution was prepared using Sigma-Aldrich® high purity reagents (>99.9%). This solution was coined WCP sample. The reactants used in the preparation of the WCP sample were $AlCl_3$, Pr_2O_3, $Nd_2(SO_4)_3$, $Sm_2(SO_4)_3$ and Eu_2O_3. The Pr and Eu REE oxides were previously solubilized in hot sulfuric acid before dilution. The REE content of the WCP sample was adjusted to contain about 20 mg L^{-1} of each studied element to establish a controlled and comparable condition.

The elements Pr, Nd, Sm and Eu were selected to this study considering that they are among the most abundant REE in the AMD system studied. Furthermore, as the influence of competing soluble elements on the co-precipitation of REE in the AMD from Brazil was reported as affecting the recovery only of Pr and Eu (MORAES et al., 2020), Nd and Sm - their neighbours in the periodic table - were selected aiming on comparing the results for each element, foreseeing a possible novel separation technique.

The WCP sample was prepared to be similar to the AMD system described in the work by Moraes et al. (2020) with a concentration of Al of about 140 mg $L^{-1}$and a sulphate content of 1 g L^{-1}. All the solutions were prepared using Milli-Q® deionized water. A total of 12 L of the WCP sample were prepared at 25±2°C and stored in acid-cleaned polyethene bottles.

2.2. Co-precipitation experiment

Aiming to evaluate the effect of Ca^{2+} and Zn^{2+} on the co-precipitation of REE by aluminium precipitates, an experiment using a 2x3 factorial design was carried out. The factorial design was chosen to identify the influence of each variable as well as their possible interactions over the co-precipitation of the REE. The experiment was carried out with Ca and Zn at concentrations of 0, 180 and 360 mg L^{-1} and 0, 20 and 40 mg L^{-1}, respectively. The concentrations of Ca and Zn were defined to be equal to zero, one and two times the concentrations reported for the AMD described in the work by Moraes et al. (2020).

The co-precipitation batch experiments were carried out in glass beakers at 25±2°C and the solutions were constantly stirred by a glass helix at an 8 Hz frequency. Each

experimental unit consisted of 0.5 L of the WCP sample. Proper amounts of anhydrous $CaCl_2$ salt (solid) and proper volumes of a 20 g L^{-1} $ZnSO_4$ solution were added to the WCP sample to achieve the desired concentrations of Ca and Zn for each experimental unit. The co-precipitation process was carried out with the addition of a 2 mol L^{-1} KOH solution until the pH reached a value equal to 8.0±0.5. At the end of the precipitation, an amount of 0.4 µg of a gelatinized starch (inert flocculant) was added to promote flocculation of the precipitate formed. The suspension was then left to decant in glass separation funnels for 1 h, drained and centrifugated at 6000 g for 10 min. An aliquot of the supernatant was collected and stored at 4°C in polyethene acid-cleaned bottles until analysis. Each experiment was replicated once.

A two-way analysis of variance (ANOVA) with a level of confidence of 95% for repeated measures ($\alpha = 0.05$) was employed to determine the individual effects of the presence of Ca and Zn and their interaction over the co-precipitation of Pr and Eu with the precipitates. The software Minitab® was used for the analysis and plotting the results.

2.3. Adsorption experiments

Aiming to evaluate the influence of Ca on the adsorption of REE on amorphous aluminium gel, a series of experiments evaluating each REE separately were carried out. It was prepared an Al gel suspension using an $AlCl_3$ solution containing 150 mg L^{-1} of Al, whose pH was raised to 8 using 2 mol L^{-1} KOH, aiming to reproduce the Al content of the AMD system described by Moraes et al. (2020). This synthesis method was adapted to the required conditions relying on several references (BRADLEY; KYDD; HOWE, 1993; KINNIBURGH; JACKSON; SYERS, 1976; KINNIBURGH; SYERS; JACKSON, 1975; LEETMAA et al., 2014), considering that Al_{13}-polymers are the solid phase formed, i.e. the adsorbent to be studied.

Different solutions containing 2 g L^{-1} of each REE were prepared using Pr_2O_3, $Nd_2(SO_4)_3$, $Sm_2(SO_4)_3$ and Eu_2O_3 and Mili-Q® deionized water, with a final pH of 5±0.2 that was adjusted using 2 mol L^{-1} KOH. The REE oxides (Pr and Eu) were previously solubilized in hot sulfuric acid before dilution and pH control. A proper volume of each REE solution was then added to an aliquot of the Al gel to achieve a REE concentration of 20 mg L^{-1} of each element in each suspension. The pH of the suspensions was not adjusted.

Afterwards, proper volumes of a 100 g L^{-1} $CaCl_2$ solution was added to the suspension containing the REE in order to achieve a concentration of Ca of 1000 mg L^{-1}. A neutral treatment – deionized water without Al gel nor Ca– was carried out in parallel for determining the initial concentration of REE to be used to calculate the removal efficiency. Each experiment had a final volume of 25 ml. The reactions were carried out in acid-cleaned polyethene centrifuge tubes. After mixing all the desired reactants the tubes were stirred in a horizontal shaker at 25±2°C for 60 min. The suspensions were then centrifugated at 6000 g for 10 min. An aliquot of the supernatant was collected and stored at 4°C in polyethene acid-cleaned bottles until analysis. The experiments were carried out for each REE individually and replicated once.

A one-way analysis of variance (ANOVA) with a level of confidence of 95% for repeated measures ($\alpha = 0.05$) was employed to determine the effects of Ca and Zn over the co-precipitation of Pr and Eu with the precipitates. The software Origin Pro8® was used for the calculations.

2.4. Chemical analysis

The chemical composition of the aqueous solutions was determined mainly by inductively coupled plasma optic emission spectrometry (ICP-OES) via a SPECTRO ARCOS® apparatus. All samples were vacuum filtered through 0.45 µm pore size nitrocellulose membranes prior to analysis. The sulphate content was determined by turbidimetry.

3. RESULTS

3.1. The influence of Ca and Zn on the co-precipitation of REE by Al precipitates

The results of the co-precipitation experiments are compiled in Table 1. Part of the results was also represented in Fig. 2 as a matrix plot, where the individual effect of Ca^{2+} and Zn^{2+} over the co-precipitation of Pr^{3+} and Eu^{3+} become evident.

The co-precipitation of the elements Nd^{3+} and Sm^{3+} by the Al precipitates was not affected by Ca nor Zn at any of the conditions studied. The concentrations of both Nd and Sm in the supernatants of all treatments were lower than the detection limits. However, the co-precipitation of Pr^{3+} and Eu^{3+} was affected only by the presence of Ca. This negative effect on the removal efficiency was increased when the concentration of Ca was also increased. The presence of Zn at any of the concentrations studied did not affect the co-precipitation of any of the REE studied.

The average removal efficiency of Pr was 99.48±0.09%, 93.63±0.11% and 90.46±0.11% when the Ca concentrations were equal to 0, 180 and 360 mg L^{-1}, respectively. A less expressive negative effect of the presence of Ca was detected for Eu. The average removal efficiencies of Eu were equal to 99.84±0.15% and 99.84±0.07% when the Ca concentrations were equal to 0 and 180 mg L^{-1}, respectively. It decreased to 99.34±0.04% only when the Ca concentration was equal to 360 mg L^{-1}.

The two-way analysis of variance results evidenced that an increase in the concentration of Ca in the solution before the rise in the pH causes a significant decrease in the co-precipitation of Pr^{3+} and Eu^{3+} by Al precipitates (Fig. 1) at a 95% level of confidence. The effect of the presence of Zn in any of concentrations studied was not significant for the co-precipitation of Pr and Eu. The interaction between Ca and Zn was also not significant.

Table 1 - Concentrations of the REE in the solutions and in the supernatants of the co-precipitation experiments and removal efficiencies (R.Eff) of each experiment, expressed in mg L^{-1} and as a percentage, respectively.

			Pr mg L^{-1}	R.Eff %	**Nd** mg L^{-1}	R.Eff %	**Sm** mg L^{-1}	R.Eff %	**Eu** mg L^{-1}	R.Eff %
Initial			**18.4**	*	**20.4**	*	**23.3**	*	**18.8**	*
[Ca] [Zn] mg L^{-1}	R.Eff.(%) **Ca**	R.Eff.(%) **Zn**								
[0] [0]	*	*	0.096	99.48	< DL[a]	100	< DL	100	0.025	99.87
	*	*	0.099	99.46	< DL	100	< DL	100	0.015	99.92
[0] [20]	*	100	0.082	99.55	< DL	100	< DL	100	0.007	99.96
	*	100	0.076	99.59	< DL	100	< DL	100	0.023	99.88
[0] [40]	*	100	0.118	99.36	< DL	100	< DL	100	0.023	99.88
	*	100	0.109	99.41	< DL	100	< DL	100	0.087	99.54
[180] [0]	0.18	*	1.17	93.63	< DL	100	< DL	100	0.030	99.84
	0.22	*	1.18	93.59	< DL	100	< DL	100	0.028	99.85
[180] [20]	0.14	100	1.20	93.48	< DL	100	< DL	100	0.031	99.84
	0.33	100	1.17	93.66	< DL	100	< DL	100	0.020	99.89
[180] [40]	2.02	100	1.18	93.58	< DL	100	< DL	100	0.054	99.71
	2.34	100	1.14	93.81	< DL	100	< DL	100	0.015	99.92
[360] [0]	3.38	*	1.77	90.37	< DL	100	< DL	100	0.135	99.28
	3.55	*	1.74	90.56	< DL	100	< DL	100	0.136	99.28
[360] [20]	2.86	100	1.77	90.40	< DL	100	< DL	100	0.121	99.36
	4.81	100	1.75	90.48	< DL	100	< DL	100	0.120	99.36
[360] [40]	3.08	100	1.73	90.63	< DL	100	< DL	100	0.124	99.34
	2.87	100	1.78	90.34	< DL	100	< DL	100	0.116	99.38

[a] DL = Detection Limit, (Pr, Nd, Sm, Eu) = 0.003 mg L^{-1}

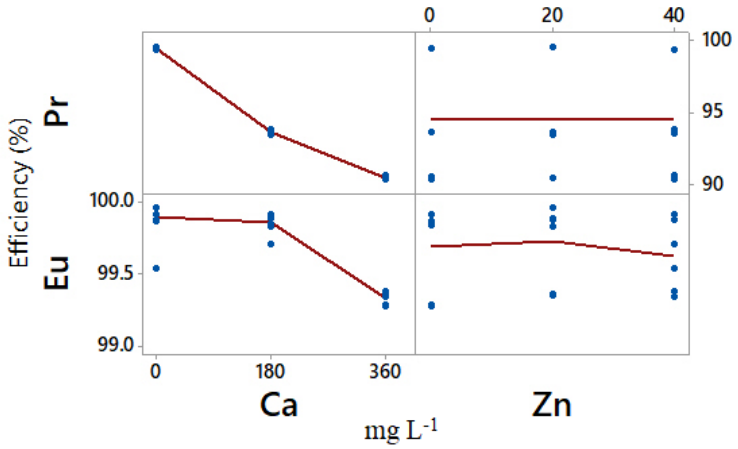

Figure 1 – Matrix plot showing the influence of Ca and Zn over the removal efficiency of Pr and Eu at pH 8.

3.2. The influence of Ca on the adsorption of REE onto Al precipitates

The results of the adsorption experiment are compiled in Table 2. Among the four REE studied, the adsorption of only Pr and Eu showed to be influenced by the presence of Ca. The analysis of variance evidenced that an increase in the Ca concentration at an initial pH equal to 8 causes a significant decrease in the adsorption of Pr and Eu by Al precipitates and that the presence of 1000 mg L^{-1} of Ca did not affect the adsorption of Nd and Sm, at a 95% level of confidence.

The adsorption of Pr and Eu on the Al gel reduced from 99.05±0.13% to 72.18±0.23% and from 100±0% to 96.25±0.04%, respectively, when the concentrations of Ca in the suspension were equal to 0 and 1000 mg L^{-1} (Table 2). Simultaneously, the adsorption of Ca was equal to 30.33±0.18%, 30.42±0.16%, 30.44±0.79% and 30.29±0.40% when 1000 mg L^{-1} of Ca were added to the experiments carried out with Pr, Nd, Sm and Eu, respectively.

The final pH of the supernatants of the experiments carried out with Pr and Sm tended to fall when Ca was added. However, in the experiments carried out with Nd the final pH tended to rise and also presented the lowest value when there was no Ca in the system (Table 2). The experiments carried out with Eu did not show a significant pH variation.

Table 2: Concentrations of REE on the solutions and supernatants of the adsorption experiments (mg L^{-1}), average percentage adsorbed (Ads) followed by standard deviation and final pH of each experiment.

	Replica	**Pr** mg L^{-1}	Ads (%)	final pH	**Nd** mg L^{-1}	Ads (%)	final pH	**Sm** mg L^{-1}	Ads (%)	final pH	**Eu** mg L^{-1}	Ads (%)	final pH
Initial	*	**14.9**	*	*	**20.1**	*	*	**23.1**	*	*	**19.5**	*	*
[Ca] = 0 mg L^{-1}	A	0.126	99.05	7.56	<DL[a]	100	5.74	<DL	100	7.02	<DL	100	6.83
	B	0.155	±0.13	7.54	<DL	±0.00	5.99	<DL	±0.00	6.66	<DL	±0.00	6.53
[Ca] = 1000 mg L^{-1}	A	4.13	72.18	7.05	0.015	99.96	6.75	0.049	99.89	6.45	0.728	96.25	6.51
	B	4.18	±0.23	7.10	<DL	±0.05	7.05	0.073	±0.15	6.51	0.738	±0.04	6.84
Ca adsorbed at [Ca] = 1000 mg L^{-1}			30.33 ±0.18			30.42 ±0.16			30.44 ±0.79			30.29 ±0.40	

[a] DL: Detection Limit = 0.003 mg L^{-1}

4. DISCUSSION

The works by Ohta et al. (2009a, 2009b) studied the coordination states of REE adsorbed onto amorphous Fe oxyhydroxides by extended X-ray absorption fine structure spectroscopy (EXAFS) and showed that La-, Pr-, Nd-, and Sm-adsorbed present a mixture of eightfold- and ninefold-coordination spheres. On the other hand, the aforementioned authors also showed that La, Pr, and Nd adsorbed onto δ-MnO_2 have a distorted tenfold-coordination sphere. Furthermore, the work by Nakada et al. (2013) also used EXAFS to study the stable isotopic fractionation of Nd and Sm during adsorption on ferrihydrite and δ-MnO_2 and concluded that the bond length of the first coordination sphere (REE–O bond) of Nd and Sm adsorbed on manganese oxide is shorter than that of their aqua-ions, although this was not clear in the ferrihydrite systems. The shorter bond length relative to the aqua ion is indicative of stronger bonds.

Considering the statements of the aforementioned authors and the similarity of the structure of amorphous Al and Fe precipitates - both are composed of Kegging ions (FURRER et al., 2002; WEATHERILL et al., 2016) - it is possible to hypothesize that Pr, Nd, Sm and Eu may have different adsorption affinities with the surface of the aluminium precipitates that are formed at a neutral pH. The precipitates formed are composed of Al_{13}-polymers and are responsible for the co-precipitation due to the adsorption and the entrapment of REE (MORAES et al., 2020). In addition, Al_{13}-polymers are polyprotic acids (FURRER; LUDWIG; SCHINDLER, 1992) in which the deprotonation of the terminal water ligands generates hydroxyl groups that interact with the REE in the solution, therefore, the possible differences in the coordination numbers of Pr, Nd, Sm and Eu when adsorbed may cause differences in the pH, as the ones found in the adsorption experiments of the current study (Table 2).

For example, it is possible that the greater affinity of Nd to adsorb onto the surface of Al_{13}-polymers - as shown by the results of the current study - perhaps because it can form stronger bonds with the hydroxyl groups present in the surface of the adsorbent – i.e. larger coordination numbers. Therefore, more protons should be released to the solution, then reducing the pH, as observed in Table 2 when no Ca was added. Further studies on the adsorption of light REE onto Al_{13}-polymers using synchrotron-based techniques should be carried out to prove this hypothesis.

The results of the co-precipitation and adsorption experiments clearly show the influence that soluble Ca exerts over the removal of Pr and Eu by Al precipitates in AMD.

One possible explanation for the mechanism is that soluble Ca species - such as Ca^{2+} and $CaSO_{4(aq)}$ - compete with Pr and Eu complexes – such as Ln^{3+}, $LnSO_4^+$ and LnF^{2-} (MORAES et al., 2020) - for specific adsorption sites in the surface of the precipitates. The higher the amount of Ca in the AMD, the lower should be the co-precipitation/adsorption of Pr and Eu on the Al precipitates, although the effect over Pr should be much more intense than over Eu.

The work by Kinniburgh et al. (1975) reports the specific adsorption of trace amounts of Ca and strontium (Sr) by hydrous oxyhydroxides of Fe and Al. These authors have studied the adsorption of Ca on an Al gel suspension with about 0.08 mg L^{-1} of Ca. The maximum adsorption rate of Ca occurred at pH 10 and 50% of the Ca in the solution was adsorbed on the Al gel at pH 8 - i.e. $pH_{50} = 8$.

In addition, the work by Kinniburgh et al. (1976) reports the adsorption of alkaline earth, transition, and heavy metal cations by hydrous oxide gels of iron and aluminium. These authors have also studied the adsorption of Ca on fresh Al gel, with a Ca concentration of about 10 mg L^{-1} in the suspension. In this case, the maximum adsorption rate of Ca occurred at pH 11 and the adsorption of Ca was only triggered at pH 8, and the pH_{50} was equal to 9.5. According to Kinniburgh et al. (1976), this may merely reflect the fact that for a given cation, the pH_{50} generally decreases as the cation concentrations fall.

Furthermore, the work by Lozano et al. (2019) reports the role of sulphate and pH on the adsorption of rare earth elements onto basaluminite ($Al_4(SO_4)(OH)_{10}\cdot 5(H_2O)$), highlighting the importance of sulphate complexes for the adsorption and consequent removal of REE from AMD in passive treatment systems. Simultaneously, the work by Moraes et al. (2020) reports the chemical speciation of the REE present in the AMD system that was the basis for the current study and showed that the element Pr does not present sulphate complexes and tend to be in solution as Pr^{3+}, while Eu tend to be in solution as an $EuSO_4^+$ complex, as most of the REE present in the AMD system.

By connecting the findings of the aforementioned authors with the results of the current study, the possible explanation hypothesized above about the influence of Ca over the co-precipitation of Pr and Eu by Al precipitates gets structured. Considering that in the current study the concentrations of Ca are much higher than those considered by

Kinniburgh et al. (1976) – about 100 times - the excess of soluble Ca can become an obstacle for the adsorption of Pr and Eu at pH 8. Probably these elements compete for specific adsorption sites on the surface of the freshly formed Al precipitates. Moreover, the fact that Pr does not present sulphate complexes in solution – according to the geochemical modelling reported by Moraes et al. (2020) – and that sulphate complexes play an important role on the adsorption of REE on Al-based minerals – according to the findings of Lozano et al. (2019) – may be a key for the understanding of the distinct behaviour of Pr when recovering REE from AMD through the co-precipitation process.

The implications to be considered taking into account the findings of the current study are directly connected to the AMD treatment carried out by the company at the site studied, done through pH neutralization using lime ($Ca(OH)_2$). As the flow rate of the AMD treatment plant is 150 to 300 $m^3\ h^{-1}$, it consumes about 12 tons of slaked lime per day (FONSECA, 2009). When considering that the AMD treatment plant has been ceaselessly operating for about 28 years, using slaked lime to raise the pH of the effluent before discharge, the findings of the current work suggest that it is possible that part of the Pr and Eu that were present in the AMD were not removed when the AMD was treated, flowing downstream. Possibly, after the contact of the treated water with soil and sediment particles, the scavenging of Pr and Eu may occur in situ. This reasoning leads to an inevitable supposition: there might be occurring an accumulation of Pr and Eu on the downstream path of the treated water for three decades, perhaps in a proportion that can lead to future exploration. Further investigation is demanded to confirm this hypothesis.

5. CONCLUSIONS

Increasing concentrations of Ca in AMD solutions before pH neutralization leads to a reduction of the removal of Pr and Eu when co-precipitating REE with amorphous aluminium gels at pH 8. This effect occurs in a much higher proportion for the element Pr. The effect of Ca over the adsorption of Pr and Eu onto amorphous aluminium gel was also revealed and it occurs in a similar way. The element Zn did not influence the co-precipitation of the REE.

The interaction between Ca, Pr and Eu interfere with the removal efficiencies of these REE especially when the AMD is neutralized with the use of $Ca(OH)_2$ at industrial scale. As the neutralized AMD can contain soluble Pr and Eu, there is a possibility of a Pr-Eu-enrichment of the sediments located downstream of the treatment plant over time due to the scavenging of these REE by suspended soil clay and sediment particles.

6. REFERENCES

ANASTOPOULOS, I.; BHATNAGAR, A.; LIMA, E. C. Adsorption of rare earth metals: A review of recent literature. **Journal of Molecular Liquids**, v. 221, n. June, p. 954–962, set. 2016.

AYORA, C. et al. Recovery of Rare Earth Elements and Yttrium from Passive-Remediation Systems of Acid Mine Drainage. **Environmental Science and Technology**, v. 50, n. 15, p. 8255–8262, 2016.

BRADLEY, S. M.; KYDD, R. A.; HOWE, R. F. The Structure of Al Gels Formed through the Base Hydrolysis of Al3+ Aqueous Solutions. **Journal of Colloid and Interface Science**, v. 159, n. 2, p. 405–412, set. 1993.

FONSECA, V. Mais energia, menos impacto para o ambiente. **Publicação trimestral da Fundação de Amparo à Pesquisa do Estado de Minas Gerais - FAPEMIG, N°39 - Set-Nov**, p. 62, 2009.

FURRER, G. et al. The origin of aluminum flocs in polluted streams. **Science**, v. 297, n. 5590, p. 2245–2247, 2002.

FURRER, G.; LUDWIG, C.; SCHINDLER, P. W. On the chemistry of the Keggin Al13 polymer I. Acid-base properties. **Journal of Colloid and Interface Science**, v. 149, n. 1, p. 56–67, mar. 1992.

JHA, M. K. et al. Review on hydrometallurgical recovery of rare earth metals. **Hydrometallurgy**, v. 161, p. 77–101, 2016.

KING, J. F. et al. Aqueous acid and alkaline extraction of rare earth elements from coal combustion ash. **International Journal of Coal Geology**, v. 195, n. March, p. 75–83, 2018.

KINNIBURGH, D. G.; JACKSON, M. L.; SYERS, J. K. Adsorption of Alkaline Earth, Transition, and Heavy Metal Cations by Hydrous Oxide Gels of Iron and Aluminum. **Soil Science Society of America Journal**, v. 40, n. 5, p. 796–799, set. 1976.

KINNIBURGH, D. G.; SYERS, J. K.; JACKSON, M. L. Specific Adsorption of Trace Amounts of Calcium and Strontium by Hydrous Oxides of Iron and Aluminum. **Soil Science Society of America Journal**, v. 39, n. 3, p. 464–470, maio 1975.

LEETMAA, K. et al. Comparative molecular characterization of aluminum hydroxy-gels derived from chloride and sulphate salts. **Journal of Chemical Technology and Biotechnology**, v. 89, n. 2, p. 206–213, 2014.

LOZANO, A.; AYORA, C.; FERNÁNDEZ-MARTÍNEZ, A. Sorption of rare earth elements onto basaluminite: The role of sulfate and pH. **Geochimica et Cosmochimica Acta**, v. 258, p. 50–62, ago. 2019.

MORAES, M. L. B. et al. The role of Al13-polymers in the recovery of rare earth elements from acid mine drainage through pH neutralization. **Applied Geochemistry**, v. 113, p. 104466, fev. 2020.

NAKADA, R.; TANIMIZU, M.; TAKAHASHI, Y. Difference in the stable isotopic fractionations of Ce, Nd, and Sm during adsorption on iron and manganese oxides and its interpretation based on their local structures. **Geochimica et Cosmochimica Acta**, v. 121, p. 105–119, nov. 2013.

NATIONAL ENERGY TECHNOLOGY LABORATORY; U.S. DEPARTMENT OF ENERGY. **FY19-RARE EARTH ELEMENTS PEER REVIEW OVERVIEW REPORT**. [s.l: s.n.]. Disponível em: <https://netl.doe.gov/sites/default/files/2019-12/FY19-REE-Peer-Review-Overview-Report.pdf>.

OHTA, A. et al. Coordination study of rare earth elements on Fe oxyhydroxide and Mn dioxides: Part I. Influence of a multi-electron excitation on EXAFS analyses of La, Pr, Nd, and Sm. **American Mineralogist**, v. 94, n. 4, p. 467–475, 1 abr. 2009a.

OHTA, A. et al. Coordination study of rare earth elements on Fe oxyhydroxide and Mn dioxides: Part II. Correspondence of structural change to irregular variations of partitioning coefficients and tetrad effect variations appearing in interatomic distances. **American Mineralogist**, v. 94, n. 4, p. 476–486, 1 abr. 2009b.

STEWART, B. W. et al. Rare earth element resources in coal mine drainage and treatment precipitates in the Appalachian Basin, USA. **International Journal of Coal Geology**, v. 169, p. 28–39, 2017.

VASS, C. R.; NOBLE, A.; ZIEMKIEWICZ, P. F. The Occurrence and Concentration of Rare Earth Elements in Acid Mine Drainage and Treatment Byproducts. Part 2: Regional Survey of Northern and Central Appalachian Coal Basins. **Mining, Metallurgy & Exploration**, v. 36, n. 5, p. 917–929, 1 out. 2019a.

VASS, C. R.; NOBLE, A.; ZIEMKIEWICZ, P. F. The Occurrence and Concentration of Rare Earth Elements in Acid Mine Drainage and Treatment By-products: Part 1—Initial Survey of the Northern Appalachian Coal Basin. **Mining, Metallurgy & Exploration**, v. 36, n. 5, p. 903–916, 25 out. 2019b.

WEATHERILL, J. S. et al. Ferrihydrite formation: The role of Fe13 Keggin clusters. **Environmental Science and Technology**, v. 50, n. 17, p. 9333–9342, 2016.

ZHANG, W.; HONAKER, R. Q. Rare earth elements recovery using staged precipitation from a leachate generated from coarse coal refuse. **International Journal of Coal Geology**, v. 195, p. 189–199, 2018.

Chapter 4

Recovery of rare earth elements by co-precipitation with Al_{13}-polymers from acid mine drainage using $Ca(OH)_2$ for pH control: a feasible low-cost route.

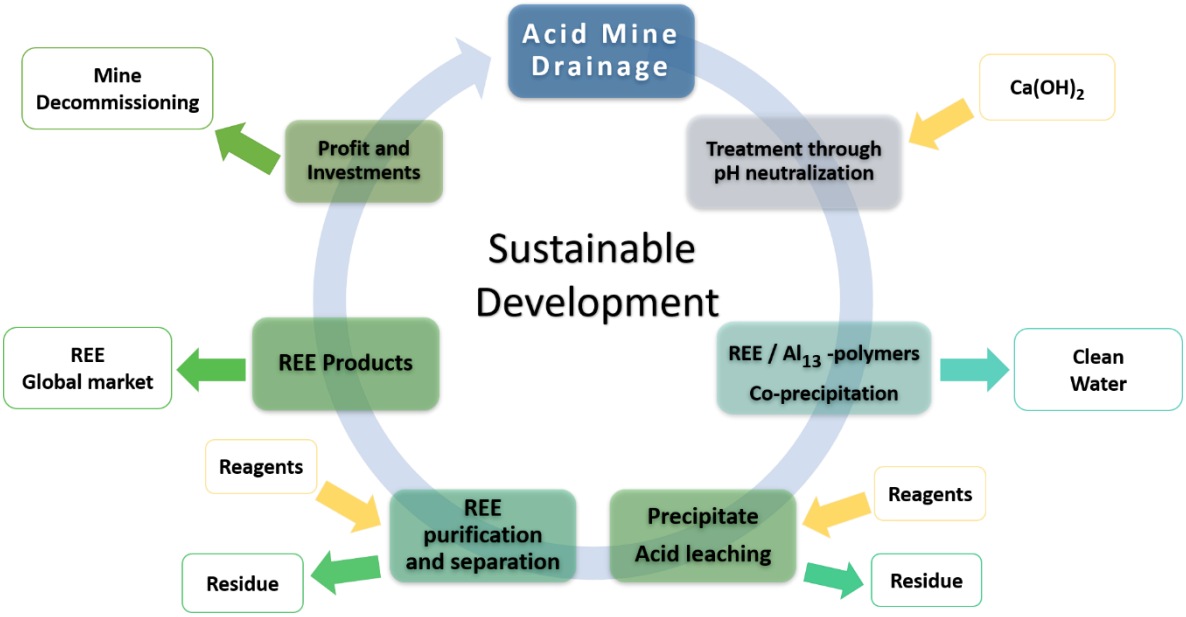

ABSTRACT: As the importance of rare earth elements (REE) in the current global market increase, the search for new sources of these strategic raw materials increases as well. It is promoted mainly because China dominates the global REE market. The dynamic economic relationship between developed and developing countries in the current globalized world also push the development of a new chain of production and recycling of REE. The use of co-precipitation techniques for the recovery of REE from acid mine drainage (AMD) is a current issue among researchers and appears to be a feasible route. Furthermore, the use of calcium hydroxide for pH control and consequent co-precipitation is already being used in the USA for recovering REE from AMD. The current work seeks to evaluate the use of a commercial-grade calcium hydroxide for the recovery of REE from an AMD sample by co-precipitation with amorphous Al precipitates through pH neutralization. The characterization of the precipitates and an acid-leaching experiment using acetic acid, hydrochloric acid and sulphuric acid are also presented and discussed. The results show that about 90% of the REE present in the AMD sample could be recovered by co-precipitation with amorphous Al-precipitates composed of Al_{13}-polymers. The results of the acid-leaching experiment show

that about 60% to 85% of the REE can be extracted from the precipitates, depending on the leaching agent used. The economic potential of the REE-recovery activity considering an AMD sample from a closed uranium mine in Brazil was also estimated and discussed, revealing the great potential of REE production in compliance with the United Nations Sustainable Development Goals.

KEYWORDS: rare earth elements, acid mine drainage, metal recovery, co-precipitation, calcium hydroxide.

1. INTRODUCTION

The multiple applications of rare earth elements (REE) make these strategic metals crucial to produce renewable energy, energy-efficient lighting and electric mobility on the path to a green and low-carbon world economy. The increasing demand for REE over the last decades is expected to expand continuously (SCHMID, 2019). This demand may accelerate as the relevance of REE was once more acknowledged by resolutions reached at the UN Climate Change Conference in Paris in 2015, which will consequently lead to a necessary shift from CO_2 emitting technologies to carbon-neutral alternatives.

In the next decade, the most disruptive technology for the consumption of REE is forecast to be the growth in hybrid electric vehicles (HEVs) and full electric vehicles (EVs), which are expected to cause changes in the volumes and types of raw materials consumed by the automotive industry. NdFeB (neodymium-iron-boron) magnets are not unfamiliar to the automotive industry, with most internal combustion engine vehicles, HEVs and EVs containing between 40 and 100 small electric motors in components such as windscreen wiper motors and air conditioning systems. However, the ongoing automotive electrification has increased the intensity of use in all vehicle types. NdFeB magnets are used in the powertrain in HEVs and EVs as well as in numerous other smaller applications, with up to 2.5 kg of NdFeB magnets being used in the powertrain of current models (GOODENOUGH; WALL; MERRIMAN, 2018). The ‘law of demand’ leads to the high prices of praseodymium (Pr) and neodymium (Nd) in the current global market of REE.

The extraction of REE as by-products from existing mines is potentially an attractive way to bring new supplies rapidly on stream, reacting quickly to changes in demand (GOODENOUGH; WALL; MERRIMAN, 2018). In response to the increasing global demand and the dominance of the REE mining played by China, alternative sources of REE have become a necessity for other countries. Recycling in-use stocks can be an alternative source, especially for the "big four," i.e., La, Ce, Nd, and Pr. However, the availability of less-abundant REE – i.e. heavy rare earths - continues to be a challenge (AYORA et al., 2016). Given the disparity between current REE supply and future REE demand, many stakeholders including researchers, national governments, and private companies have attempted to identify alternative and unconventional REE resources, such as Acid Mine Drainage (AMD).

Lapido-Loureiro & Santos (2013) affirmed that the concept of responsible investment in mining excludes predatory mining - those that do not meet the complete poly-mineral exploitation of a deposit, including by-products, tailings, slag and waste, mainly because production costs can be reduced by the utilization of all the available materials. In other words, an eco-friendly activity should be the goal of the novel mining industry.

The recovery of REE from AMD is a current issue among researchers. There are some recent works available in the literature reporting the efforts that are being made specially in Spain, the USA and Brazil, using adsorption, co-precipitation, nanofiltration and ion exchange techniques (AYORA et al., 2016; FELIPE; BATISTA; LADEIRA, 2020; LÓPEZ et al., 2018; MORAES et al., 2018, 2020; VASS; NOBLE; ZIEMKIEWICZ, 2019a, 2019b; ZIEMKIEWICZ; NOBLE, 2019). The use of calcium hydroxide for pH control and co-precipitation of REE is something to be considered for the REE-recovery from the AMD on the studied site - a closed uranium mine in Minas Gerais - Brazil. This technology is already being applied in West Virginia-USA for the recovery of critical rare earths from coal mine drainage (ZIEMKIEWICZ; NOBLE, 2019).

The current work addresses the investigation about the use of calcium hydroxide for pH control of an AMD water sample, aiming at recovering soluble REE by co-precipitation. The study focused on evaluating the REE removal efficiency and the consumption of $Ca(OH)_2$ as well as on the characterization of the precipitate by powder X-ray diffraction (XRD),

transmission electron microscopy (TEM), X-ray photoelectron spectroscopy (XPS) and ^{27}Al magic angle spinning nuclear magnetic resonance (^{27}Al MAS-NMR). REE-leaching experiments were also carried out seeking to evaluate the use of acetic, hydrochloric and sulphuric acids for the dissolution of the precipitates formed at pH 8. A preliminary economic assessment of the recovery of REE from the studied AMD water sample was also estimated and discussed.

2. MATERIALS AND METHODS

2.1. Water sample and precipitation

The characterization of the water sample and its respective chemical modelling were previously presented and discussed in Chapter 1 (MORAES et al., 2020). The water sample previously coined W3 was selected for the current study.

For the obtention of the REE-rich precipitates, 2 L aliquots of the W3 sample were mixed with a suspension of 2 mol L^{-1} $Ca(OH)_2$ to raise the pH to 8. The calcium hydroxide reagent used in the current study was the commercial-grade product CALFIX (produced by the company Ical® at Matozinhos, Minas Gerais, Brazil) aiming to reproduce the conditions of an AMD treatment system at an industrial scale. The reaction was carried out in glass beakers at 25±2°C for 15 min. The suspensions were constantly stirred with the use of a glass helix at an 8 Hz frequency.

The precipitate obtained was left to decant with the addition of 0.2 μg L^{-1} of gelatinized starch (inert flocculant agent) in glass separation funnels for 1 h, centrifuged at 7000 g for 10 min, dried at 50°C, powdered, sieved through a 150 μm pore size stainless steel sieve and stored in polyethene bottles at ambient temperature until analysis. This precipitate was coined W3P.

2.2. Samples characterization

The chemical composition of the water sample was determined mainly by inductively coupled plasma optic emission spectrometry (ICP-OES) via a SPECTRO ARCOS® apparatus. The chemical composition of both W3P precipitate and calcium hydroxide used

for the precipitation was determined by ICP-OES after digestion with aqua regia. The digestion was carried out in centrifuge tubes at 25°C for 2 h in a horizontal shaker at 1 Hz, followed by filtering and dilution before the analysis.

The precipitate was characterized by powder X-ray diffraction (XRD) with the use of a RIGAKU® X-ray diffractometer under Cu Kα radiation (λ = 0.15418 nm). The equipment was operated at a tube voltage of 40 kV and a tube current of 30 mA with a scanning rate of 4° min^{-1}, from 4 to 80°2θ and a step size of 0.02°. For this analysis, the dried samples were sieved through a 150 μm pore size stainless steel sieve.

Transmission electron microscopy (TEM) and associated techniques (SAED – selected area electron diffraction, HAADF-STEM - high-angle annular dark-field scanning transmission electron microscopy and EDS - energy dispersive spectroscopy mapping), as well as ^{27}Al magic angle spin nuclear magnetic resonance (^{27}Al MAS-NMR) analysis, were carried out to determine the structure of the W3P precipitate. TEM imaging and related analysis were carried out by a JEM 3000F microscope operating at 300 kV at the *Centro Nacional de Microscopía Electrónica – CNME,* in Madrid-Spain.

The ^{27}Al MAS-NMR spectrum was collected at 104.26 MHz by a BRUKER AVANCE 400MHz WIDE BORE and the sample was spun at 12 kHz. The ^{27}Al chemical shifts (δ) are reported in parts per million (ppm), i.e. Hz/MHz, relative to 1 mol L^{-1} $AlCl_3$ solution. The ^{27}Al MAS-NMR analysis was performed at the Faculty of Chemistry of the *Universidad Complutense de Madrid*.

The chemical composition of the surface of the W3P precipitate was investigated using X-ray photoelectron spectroscopy (XPS). The survey spectra were obtained using monochromatic Al Kα radiation (1486.6 eV) and an electron energy analyser (Specs, Phoibos-150) that enables high energy resolution and excellent signal-to-noise ratio. The signal of adventitious carbon (C 1s at 284.6 eV) was employed as a reference in the calibration of the binding energies (BE) of the elements detected. CasaXPS software was used to analyse the data. The XPS analysis was performed at the CDTN Laboratory of Applied Physics, in Belo Horizonte, Brazil.

2.3. Leaching experiments

Leaching experiments were carried out to evaluate some possible extractants to be used for the recovery of the REE present in the W3P precipitate. It consisted in the addition of proper amounts of a determined acid to 0.5 g of the precipitate to achieve around 10% of solids in the suspension and a pH ≤ 4, at 25±2°C. This pH was determined considering the results presented in Chapter 1, especially the PHREEQ-C chemical model, aiming at dissolving the Al_{13}-polymers and solubilizing the REE. For this study were selected 2 mol L^{-1} acetic acid (CH_3COOH), 2 mol L^{-1} hydrochloric acid (HCl) and 1.7 mol L^{-1} sulfuric acid (H_2SO_4), considering previous results of exploratory experiments and several references concerning REE leaching from different ores and secondary sources (ABREU; MORAIS, 2010; HABASHI, 2013; JHA et al., 2016; MOLDOVEANU; PAPANGELAKIS, 2013; NASCIMENTO et al., 2019; PEELMAN et al., 2014; VOSSENKAUL et al., 2015; WANG et al., 2017; WU et al., 2018; ZIEMKIEWICZ et al., 2018).

The reaction was carried out in centrifuge tubes and the suspensions were stirred by a magnetic stirrer. After 15 min of the addition of the leaching solutions, the suspensions were centrifuged at 7000 g for 10 min and the leachate was collected in acid-cleaned polyethene bottles and stored at 4°C until analysis. The chemical composition of the leachates was determined by ICP-OES, as aforementioned. The mass of the residue was determined after drying at 50°C until constant mass. All leaching experiments were replicated.

3. RESULTS AND DISCUSSION

3.1. Co-precipitation of the REE

As previously shown in Chapter 1 (p.12, Table 1), the W3 water sample contains about 77 mg L^{-1} of REE (total), 172 mg L^{-1} of Al, 180 mg L^{-1} of Ca, 1000 mg L^{-1} of SO_4^{2-}, 116 mg L^{-1} of F^-, among other constituents, and a pH 2.5.

The amount of $Ca(OH)_2$ demanded for increasing the pH of 1 litre of the W3 water sample to 8 was equal to 0.85 ±0.04 g and the amount of precipitate generated in this reaction was equal to 1.2 ±0.02 g. This represents about 52% less than the average amount of lime used in the AMD treatment of Minas Gerais-Brazil (FONSECA, 2009), which is about 350 Mg (megagrams or tonnes) per month. Considering a maximum flow of 300 m^3 of AMD treated per hour, the consumption is ~ 1.62 g of lime per litre of effluent. However, the current AMD treatment increases the pH to 11, to achieve a complete precipitation of the Mn present in the effluent. Then, to set the pH of the W3 sample at 8, it should be expected a monthly generation of about 260 Mg of precipitate and a consumption of about 182 Mg of lime per month.

The precipitation of the W3 water sample at pH 8 using a commercial-grade $Ca(OH)_2$ reached a 100% removal efficiencies for the majority of the REE, except for Pr and Eu, whose average removal efficiencies were equal to 50 and 38%, respectively (Fig 1). An overall REE recovery of 96.47±0.19% was achieved.

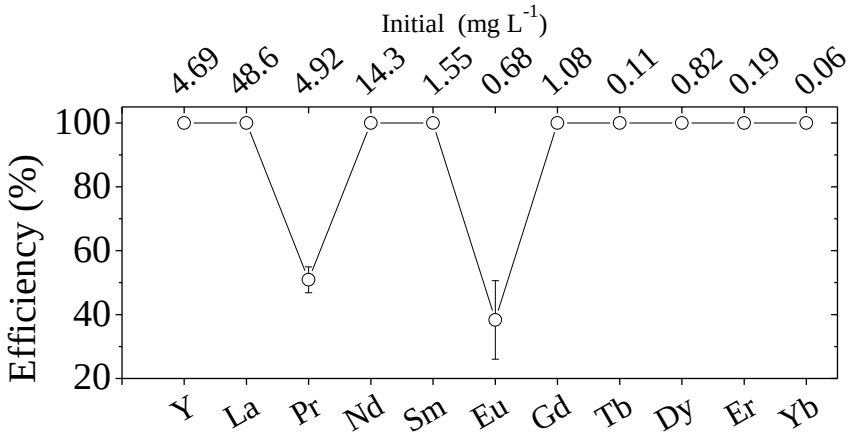

Fig.1 – REE removal efficiencies (%) for the W3 water sample. Addition of a commercial-grade $Ca(OH)_2$ 2 mol L^{-1} to adjust the pH to 8.

Considering the initial total REE concentration of the W3 sample (77 mg L^{-1}) and the total REE concentration of the W3P precipitate - 59 mg g^{-1} (Table 1), the REE were concentrated about 766 times.

A lower removal efficiency of Pr and Eu was expected, considering the results presented in Chapter 3, due to the high concentrations of Ca in the suspension caused by the dissolution of the lime. However, the use of a commercial-grade reagent is linked to the obtained results, as it contains trace amounts of Ce, Pr, Nd and Eu (Table 1) – about 3 mg g^{-1}.

The presence of Pr and Eu in the commercial-grade $Ca(OH)_2$ increased the amount of these elements in the system affecting the mass balance, as the initial concentrations used for the calculation of the removal efficiencies were those of the W3 sample. Furthermore, the effect of soluble Ca over the co-precipitation of these elements, shown in the previous chapter, resulted in the remain of Pr and Eu in the supernatant, and consequently, lower removal efficiencies were found.

Aiming at evaluating the dissolution of the REE present in the reagent, a series of tests were carried out, dissolving 0.85 g L^{-1} of the $Ca(OH)_2$, i.e., the amount demanded to increase the pH of the W3 sample to 8, in deionized water (pH ~11.7), in deionized water with the addition of sulfuric acid to reach the same content of sulphate of the W3 sample – about 1 g L^{-1} - and in deionized water with pH set to 8 with sulphuric acid. The results revealed that 100% of the REE were solubilized at any of the abovementioned conditions.

In conclusion, the recalculated removal efficiencies of Pr and Eu are equal to 67% and 44%, respectively. It considers the input of REE from the dissolution of the lime (0.85 g L^{-1}) to the initial REE concentration of the W3 sample – a sum of 1.49 mg L^{-1} of Pr and 0.15 mg L^{-1} of Eu. The recalculated overall REE removal efficiency is about 97%.

3.2. Characterization of the W3P precipitate and commercial-grade $Ca(OH)_2$

The chemical composition of the W3P precipitate and the commercial-grade calcium hydroxide used for the pH control are compiled in Table 1. The results show that the precipitate is composed mainly of Al and Ca. The moisture content (110°C), the molecular water content (450°C) and the CO_2 content (950°C) is equal to 0.5%, 30%, and 6.7%, respectively.

A total of about 7% of REE oxides was determined when the REE content of the W3P (59 mg g^{-1}) was converted to oxides (Table 1). The REE content is very high when compared to other Brazilian REE ores described in the work by Lapido-Loureiro & Santos (2013), such as the Morro do Ferro deposit in Poços de Caldas, Minas Gerais, which has about 5% of REE oxides.

Table 1 – Major chemical composition of the W3P precipitate and commercial-grade $Ca(OH)_2$ (Calfix-Ical®), determined by aqua-regia / ICP-OES.

	W3P	Calfix-Ical®
	mg g^{-1}	mg g^{-1}
Mg	1.34	1.64
Ca	203	490
Al	126	-
Si	1.77	3.45
Mn	1.46	0.053
Fe	3.38	2.09
Zn	11.75	-
U	1.19	0.30
Th	0.14	0.13
Y	5.04	-
La	36.9	-
Ce	0.403	0.396
Pr	3.63	1.76
Nd	10	0.800
Sm	1.31	-
Eu	0.293	0.184
Gd	0.862	-
Tb	0.119	-
Dy	0.140	-
Er	0.361	-
Yb	0.133	-
∑ REE	**59.2**	**3.14**
∑ REE oxides	**69.8**	**3.68**

The results of the powder XRD analysis revealed that the W3P precipitate presented the minerals calcite ($CaCO_3$) and fluorite (CaF_2) in its composition (Fig. 2). The presence of calcite can be attributed to the incomplete dissolution of the calcium hydroxide added to the W3 water sample. Moreover, the mineral fluorite was most probably formed during the precipitation due to the reaction between the Ca from the AMD and the calcium hydroxide with the soluble F^- present in the W3 sample - 100 mg L^{-1} (Chapter 1 - p. 12, Table 1). The

formation of fluorite was predicted by the geochemical modelling carried out with the use of PHREEQ-C computer program, where a saturation index of 2.1 was found for this mineral at pH 8.

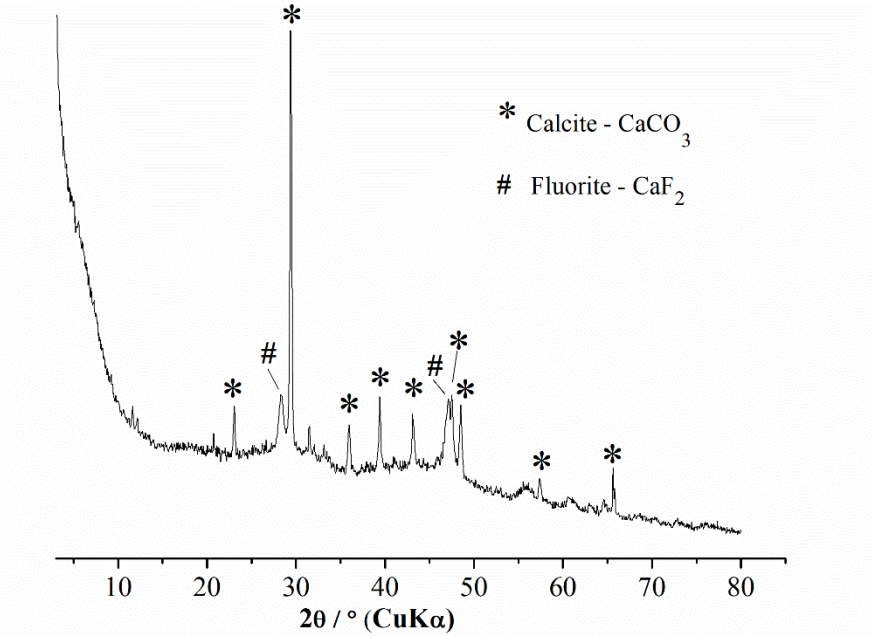

Fig. 2 – Powder XRD pattern of the W3P precipitate.

The TEM images of the W3P precipitate (Fig. 3-a-c) shows the sheet-like pseudo-hexagonal morphology of the nanomaterial, visible at a magnification of 300,000 times. The sheets have an average size of 20 nm, resembling a plate-like boehmite (γ-AlO(OH)), as reported by Souza Santos et al. (2009). Iijima et al. (2016) report atomic organization in pseudo-boehmite nanowires at high magnifications; however, this occurrence was not visualised even at a magnification of 500,000 times. The morphology of the nanomaterial is remarkably similar to the precipitates that were obtained with the use of KOH for pH control, reported in Chapter 1 (p. 16, Fig. 5).

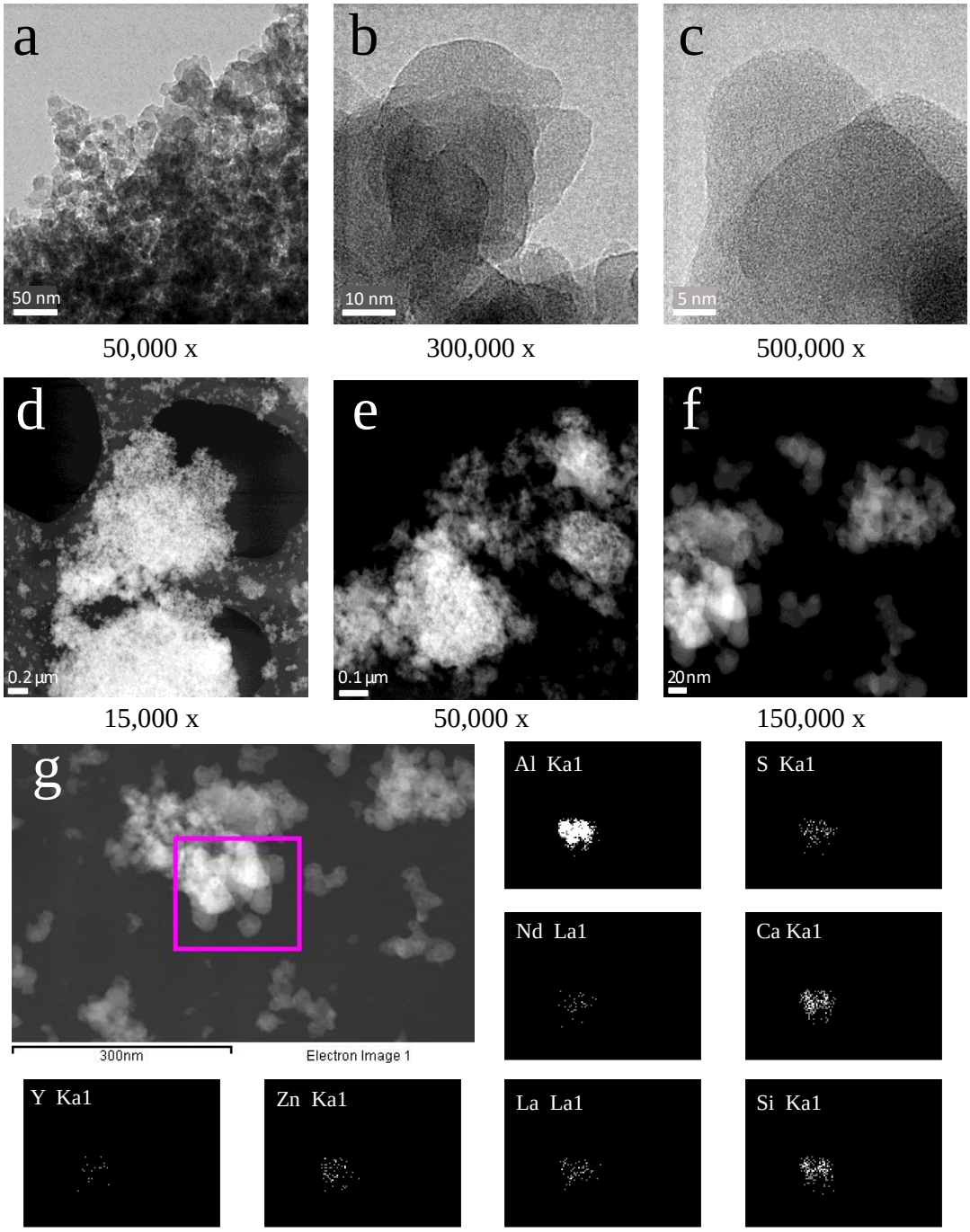

Fig. 3 – TEM images of the W3P precipitate. (a-c) Bright-field images; (d-f) HAADF-STEM images; (g) HAADF-STEM image used in the EDS mapping and element maps; elements are followed by its characteristic X-ray lines analysed.

The element mapping by EDS analysis (Fig 3-g) revealed that the nanomaterial is uniformly composed of Al (55.68%), Si (7.42%), S (3.27%), Ca (13.76%), Zn (0.91%), Y

(0.52%) La (14.89%) and Nd (3.50%) (dry-weight basis). The nanomaterial was diagnosed as being amorphous as it presented no electron diffraction pattern (data not shown). The electron diffraction pattern of the W3P precipitate was identical to the pattern observed in the P3 precipitate, reported in Chapter 1 (p. 16, Fig. 5-c).

Characteristic binding energies of Al, Ca, F, La, Nd and Zn were identified in the XPS spectra of the W3P precipitate (Fig. 4). As the XPS analysis brings information about the chemical composition of the most superficial atoms layer of the material (~5 nm), it is expected that these elements compose the surface of the precipitate. The detection limits and other limitations of the XPS analysis, such as the Auger electron superposition, i.e., KLL peaks - on some target elements, among other issues, did not allow the identification of other REE. These results also corroborate the findings reported in Chapter 1, reinforcing the similarity of the precipitates generated through the pH control of the W3 water sample with KOH and with a commercial-grade $Ca(OH)_2$.

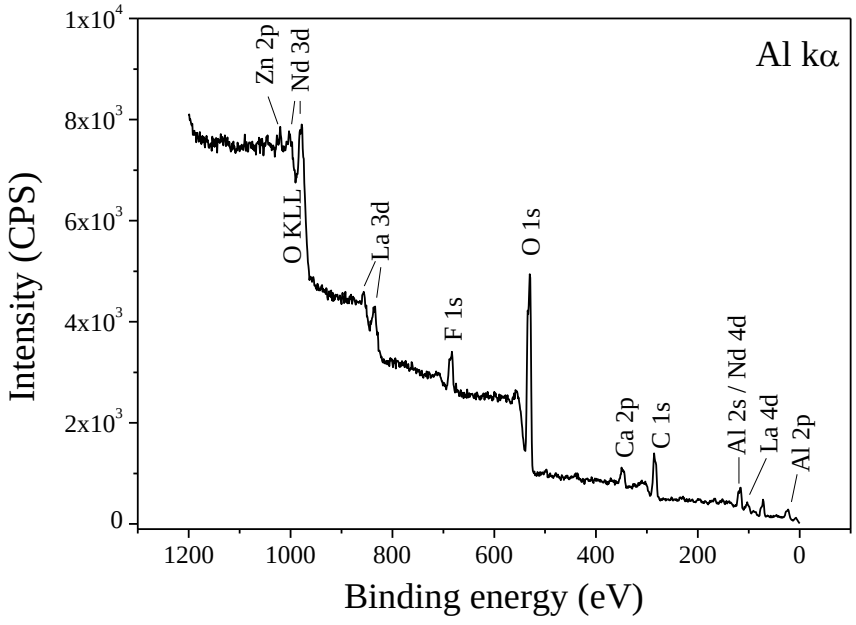

Fig. 4 - XPS spectrum of the W3P precipitate (the C 1s signal refers to the carbon tape used to hold the powder).

The ^{27}Al MAS-NMR results revealed the presence of both Al(6) and Al(4) (Fig. 5). The chemical shift peak at 5.90 ppm is indicative of the octahedrally coordinated aluminium, whereas the peak at 60 ppm is presented in the literature as corresponding to a tetrahedrally coordinated aluminium (FURRER et al., 2002; KIM, 2015). Therefore, in addition to the TEM results, the ^{27}Al MAS NMR spectrum of the W3P precipitate also suggests that the material is made up of an amorphous phase formed by the aggregation of Al_{13}-Keggin ions and Al_{13}-polymers - in accordance with the findings of Furrer et al. (2002), Leetmaa et al. (2014) and Moraes et al. (2020).

In conclusion, the W3P precipitate is remarkably similar to the P3 precipitate reported in Chapter 1 (MORAES et al., 2020), that was produced with the use of KOH for pH control.

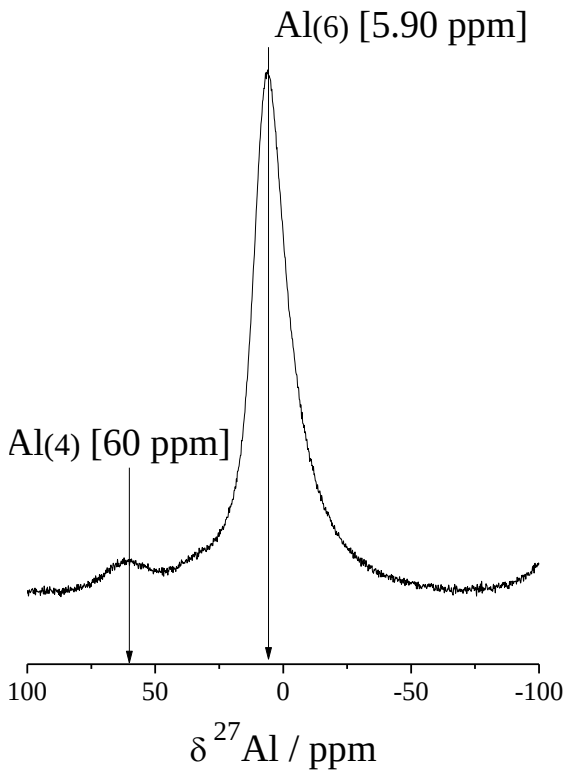

Fig. 5 - ^{27}Al MAS-NMR spectrum of the W3P precipitate.

3.3. Leaching experiments

The results of the leaching experiments are compiled in Table 3, reporting only the results for Al and the major REE of the sample – Y, La, Pr and Nd. The results showed that the leaching of the W3P precipitate with acetic acid (CH_3COOH), hydrochloric acid (HCl) and sulphuric acid (H_2SO_4) resulted in an overall REE-leaching of 85, 60 and 65%, respectively, under the conditions studied. The solubilization of the Al of the precipitate was about 80% for the three leaching agents tested.

Table 2 – Results of the Al and major REE leaching of the W3P precipitate with acetic acid (CH_3COOH), hydrochloric acid (HCl) and sulphuric acid (H_2SO_4).

	S:L [a] ratio	final pH	Residue [b] (%)	Leaching efficiency (%)				
				Al	Y	La	Pr	Nd
CH_3COOH	1:9	4.11 ±0.01	28 ±1	80 ±4.7	86 ±3.0	83 ±2.2	80 ±0.5	87 ±2.3
HCl	1:6	3.20 ±0.01	12 ±1	80 ±0.4	72 ±0.5	45 ±1.3	80 ±0.3	88 ±1.0
H_2SO_4	1:9	3.18 ±0.02	76 ±1	81 ±9.6	74 ±2.6	67 ±1.9	43 ±1.6	59 ±2.5
		W3P	Total (mg g^{-1})	126	5	36	3.6	10

(Parameters: [CH_3COOH] and [HCl] = 2 mol L^{-1}, [H_2SO_4] = 1.7 mol L^{-1}; Temperature: 25°C; Reaction time: 15 min). [a] S:L = solid/liquid ratio. [b] The amount of residue after the leaching is expressed as a percentage of the mass of the leached precipitate.

The amount of the leaching solutions that were added to the precipitate to reach the desired pH (< 4), resulted in a solid/liquid ratio of 1:9 for both acetic acid and sulfuric acid. The acetic acid leachate had a final pH of 4.1, whereas the sulfuric acid leachate had a final pH of 3.1. However, the hydrochloric acid leaching resulted a solid/liquid ratio of 1:6 and a final pH of 3.2.

Among the three leaching solutions tested, the one that generated the largest amount of residue per gram of precipitate was sulfuric acid (0.76 g), followed by acetic acid (0.28 g) and hydrochloric acid (0.12 g). The larger amount of residue generated with the use of H_2SO_4

can be attributed to the formation of gypsum ($CaSO_4 \cdot 2H_2O$) due to the reaction between the calcium present in the precipitate (adsorbed in the Al_{13}-polymers and also present in the calcite and fluorite minerals, identified by XRD) and the soluble sulphate ions produced by the dissociation of the acid.

Acetic acid seems to be the best option among the acids tested, considering the conditions studied (15 min of reaction at 25°C) because it presented the higher REE-leaching efficiency (85%) when compared to HCl (60%) and H_2SO_4 (65%) and a relatively small amount of residue generated after leaching - 28% of the initial mass. However, the annual costs of the leaching operation can become very expensive due to the high prices of acetic acid, considering the large amount to be demanded along the year, as it is expected a generation of about 260 Mg of precipitate to be leached per month (see topic 3.1).

Moreover, the REE must be concentrated and purified after the leaching to obtain commercial-grade high-purity REE-oxides products to be commercialized. If sulphuric acid leaching is chosen, the most indicated route to concentrate the REE from the leach liquor should be the precipitation of Na-REE double sulphates followed by calcination, resulting in an REE-oxides concentrate (KUL; TOPKAYA; KARAKAYA, 2008). This concentrate can be solubilized in acid and then sent to solvent extraction for separating and purifying the individual REE (JHA et al., 2016). However, if acetic acid or hydrochloric acid is chosen, the concentration by selective precipitation of the REE from the leaching liquor before solvent extraction can be carried out using oxalic acid, as reported by Chi & Xu (1999).

Seeking to reduce the costs of the recovery of the REE from the precipitates, the cheapest option to be further investigated in batch experiments and pilot-scale processing should most probably be the leaching with H_2SO_4, due to it lower costs and the possibility of the production of this reagent ‘in situ’. However, the amount of residue, i.e., gypsum, to be generated may become a new issue to be solved. Depending on the concentrations of hazardous contaminants determined in local regulations, such as U, Th and Mn, the residual gypsum can be converted into a commercial product to be used in agriculture for soil pH control, among other possible uses in the industry of civil construction.

3.4. The economic potential of the recovery of REE from the AMD of Minas Gerais-Brazil.

A preliminary assessment of the economic potential of the recovery of REE from the W3 effluent was carried out to arouse the interest of legislators and investors in recovering REE from AMD at the studied site. The results are compiled in Table 3.

The calculations were made considering the W3 water sample as the source of REE. A flow of 300 m^3 h^{-1} at the AMD treatment station was considered for the estimative, taking into account the work by Fonseca (2009). A theoretical REE recovery of 100% was also considered. The estimated value to be raised over one year is based on the prices of rare earth oxides adopted in the global market, for the month of February/2020, as well as on the average exchange rate between the Brazilian Real and the US dollar for that period - 4.35 R$/USD. The REE oxides content per litre of water was calculated and used to estimate the monetary values.

The results revealed that the recovery of REE from the AMD of the studied site may generate around $3.9 million (about €4.2 million or R$21 million) per year. Considering the results presented in section 3.1 – i.e. consumption of 182 Mg per month - and an average price for slaked lime equal to R$0.60 per kg, a consumption of about 2,180 Mg of $Ca(OH)_2$ with a cost of about R$1,310,000 is expected. These results evidence that the recovery of the REE from the W3 water sample by co-precipitation using slaked lime with subsequent leaching and purification can become a profitable business for the company, as the balance between costs and potential profits appears to be positive, even if the AMD treatment flow rate or the BRL/USD exchange rate decrease in the future.

Although many variables will influence the size of the final profits, such as the alkali agent to be used in the co-precipitation process, the leaching process, the route to be chosen for concentrating the REE after leaching (for example, Na-REE double sulphates or oxalic acid selective precipitation), the costs of reagents, personnel, infrastructure, investments, etc., concerning the obtention of high-purity REE oxides, it still seems to be an inviting business.

Furthermore, as it is not possible to predict when the AMD generation will stop, this REE source can be exploited for an incalculable period, differently from conventional mining projects that consider a limited amount of ore to be mined during a pre-determined period.

Table 3 – Economic potential of the recovery of REE from the AMD of Minas Gerais-Brazil, considering the W3 water sample as the source of REE.

	W3 water sample		Production potential [b]			Prices (Apr/2020) [c]		Economic potential [d]	
	mg L^{-1}	REEO[a]	g h^{-1}	kg day^{-1}	Mg $year^{-1}$	\$ kg^{-1}	R\$ kg^{-1}	\$ $year^{-1}$	R\$ $year^{-1}$
Y	4.69	5.96	1,787	43	16	2.95	15.66	46,174.56	245,186.90
La	48.6	57.00	17,099	410	150	3.40	18.05	509,277.48	2,704,263.41
Pr	4.92	5.76	1,727	41	15	42.50	225.68	643,106.77	3,414,896.96
Nd	14.3	16.68	5,004	120	44	40.00	212.40	1,753,326.23	9,310,162.30
Sm	1.55	1.80	539	13	5	1.83	9.72	8,643.79	45,898.55
Eu	0.683	0.75	226	5	2	30.50	161.96	60,509.16	321,303.66
Gd	1.08	1.24	373	9	3	24.65	130.88	80,633.19	428,162.22
Tb	0.109	0.13	38	1	0.33	557.00	2.957.67	183,647.81	975,169.84
Dy	0.818	0.94	282	7	2.5	255.00	1.354.05	629,132.56	3,340,693.87
Ho	0.016	0,02	5	0.2	0.05	48.59	258.01	2,340.41	12,427.56
Er	0.198	0.23	68	2	0.6	21.80	115.76	12,971.11	68,876.62
Yb	0.067	0.08	23	0.5	0.2	14.79	78.53	2,965.34	15,745.95
TOTAL	**77**	**91**	**27**	**652**	**238**	**-**	**-**	**\$ 3,932,728.41**	**R\$ 20,882,787.85**

[a] REEO: Calculated rare earth oxides content; expressed in milligrams of oxides per litre;

[b] The production potential was calculated considering the REEO content of the W3 sample (MORAES et al., 2020), a flow of 300 m^3 h^{-1} in the treatment station (FONSECA, 2009) and a theoretical recovery of 100%;

[c] Prices (Apr/2020): The current global market Rare Earth Oxides prices of April/2020 were those available in the website of the Dutch Institute of Rare Earths and Strategic Metals (https://institute-rare-earth-elements.com, accessed in 27/Apr/2020), coted in United States Dollars (USD). The exchange rate adopted was the average for the month of April/2020 (in 27/Apr/2020), equal to 5.31 BRL/USD, provided by the Central Bank of Brazil (https://www.bcb.gov.br/).

[d] Economic potential: The economic potential was calculated by multiplying the annual production potential (Mg $year^{-1}$ or tonnes $year^{-1}$) by the adopted prices.

An example of a feasible REE-recovery from AMD project is currently being developed in West Virginia-USA, where rare earths are being recovered from coal-mining wastes (VASS; NOBLE; ZIEMKIEWICZ, 2019a, 2019b; ZIEMKIEWICZ; NOBLE, 2019). The average concentration of REE in the AMD is reported to be ±400 µg L^{-1} and the average concentration of the AMD precipitates is reported to be ±0.7 mg g^{-1}. Note that these concentrations are much lower than those found in the AMD system described in the current study.

The researchers of the National Energy Technology Laboratory (NETL), developers of the aforementioned REE-recovery project in the USA, report the presence of higher concentrations of Fe in the precipitates (~59%) when compared to the W3P sample (~0.3% - this study, Table 1), the use of slacked lime for pH control, the use of geotube cells for dewatering and a subsequent sulphuric acid-leaching procedure, with the generation of gypsum. The leach-liquor, which have a pH<1, is sent directly to solvent extraction, where the REE are separated, purified and precipitated into a saleable product. The NETL research team also reports that they expect to recover about 2.2 tonnes of REE from AMD per year. Their successful experience should be noted by Brazilian researchers, legislators and REE-industry as an incentive to keep investing in the recovery of these precious metals from AMD.

More than a profitable business, the recovery of REE from the AMD from the closed uranium mine of Minas Gerais-Brazil, can become an industrial activity in compliance with some of the Sustainable Development Goals that were established by the United Nations General Assembly in 2015, and generate direct and indirect development. Some of these goals are directly linked with the current topic and deserve a quote here, such as the goal n° 6 – clean water and sanitation; goal n° 7 – affordable and clean energy; goal n° 8 – decent work and economic growth; goal n° 9 – industry, innovation and infrastructure and goal n° 12 – responsible consumption and production.

4. CONCLUSIONS

The use of a commercial-grade $Ca(OH)_2$ for the pH control of the W3 water sample resulted in high REE-removal efficiencies and produced an REE-rich precipitate with about 7% of REE oxides at a pH = 8. Amorphous Al_{13}-polymers are responsible for the removal of the REE from the solution by co-precipitation and entrapment processes.

The use of commercial-grade calcium hydroxide leads to the presence of non-dissolved calcite and the formation of fluorite in the REE-rich precipitates. These minerals can influence the leaching due to the consumption of acid. The acid leaching of the precipitates with acetic, hydrochloric and sulphuric acids showed that there are feasible ways to recover the REE from the precipitate, although further studies are demanded for optimizing the process. However, the use of calcium hydroxide (slaked lime) seems to be the cheapest technique for the pH control in large scales, like in the case of a flow of 300 $m^3 h^{-1}$.

The economic potential of the recovery of the REE from the AMD from a closed uranium mine at Minas Gerais-Brazil is considerable and could generate financial resources for the treatment of the effluent and the decommissioning of that mine, besides producing a considerable amount of REE. If an REE-recovery, separation and purification system was implemented in that mine, Brazil's REE production could increase considerably, concurrently developing a sustainable industrial production in compliance with the UN Sustainable Development Goals.

5. REFERENCES

ABREU, R. D.; MORAIS, C. A. Purification of rare earth elements from monazite sulphuric acid leach liquor and the production of high-purity ceric oxide. **Minerals Engineering**, v. 23, n. 6, p. 536–540, 2010.

AYORA, C. et al. Recovery of Rare Earth Elements and Yttrium from Passive-Remediation Systems of Acid Mine Drainage. **Environmental Science and Technology**, v. 50, n. 15, p. 8255–8262, 2016.

CHI, R.; XU, Z. A solution chemistry approach to the study of rare earth element precipitation by oxalic acid. **Metallurgical and Materials Transactions B**, v. 30, n. 2, p. 189–195, abr. 1999.

FELIPE, E. C. B.; BATISTA, K. A.; LADEIRA, A. C. Q. Recovery of rare earth elements from acid mine drainage by ion exchange. **Environmental Technology**, v. 0, n. 0, p. 1–12, 20 jan. 2020.

FONSECA, V. Mais energia, menos impacto para o ambiente. **Publicação trimestral da Fundação de Amparo à Pesquisa do Estado de Minas Gerais - FAPEMIG, N°39 - Set-Nov**, p. 62, 2009.

FURRER, G. et al. The origin of aluminum flocs in polluted streams. **Science**, v. 297, n. 5590, p. 2245–2247, 2002.

GOODENOUGH, K. M.; WALL, F.; MERRIMAN, D. The Rare Earth Elements: Demand, Global Resources, and Challenges for Resourcing Future Generations. **Natural Resources Research**, v. 27, n. 2, p. 201–216, 20 abr. 2018.

HABASHI, F. Extractive metallurgy of rare earths. **Canadian Metallurgical Quarterly**, v. 52, n. 3, p. 224–233, 2013.

IIJIMA, S.; YUMURA, T.; LIU, Z. One-dimensional nanowires of pseudoboehmite (aluminum oxyhydroxide γ-AlOOH). **Proceedings of the National Academy of Sciences**, v. 113, n. 42, p. 11759–11764, 2016.

JHA, M. K. et al. Review on hydrometallurgical recovery of rare earth metals. **Hydrometallurgy**, v. 165, p. 2–26, 2016.

KIM, Y. Mineral phases and mobility of trace metals in white aluminum precipitates found in acid mine drainage. **Chemosphere**, v. 119, p. 803–811, 2015.

KUL, M.; TOPKAYA, Y.; KARAKAYA, I. Rare earth double sulfates from pre-concentrated bastnasite. **Hydrometallurgy**, v. 93, n. 3–4, p. 129–135, 2008.

LAPIDO-LOUREIRO, F. E.; SANTOS, R. L. C. **O Brasil e a reglobalização da indústria das terras raras.** [s.l: s.n.]. v. 1

LEETMAA, K. et al. Comparative molecular characterization of aluminum hydroxy-gels derived from chloride and sulphate salts. **Journal of Chemical Technology and Biotechnology**, v. 89, n. 2, p. 206–213, 2014.

LÓPEZ, J. et al. Application of nanofiltration for acidic waters containing rare earth elements: Influence of transition elements, acidity and membrane stability. **Desalination**, v. 430, n. October 2017, p. 33–44, 2018.

MOLDOVEANU, G. A.; PAPANGELAKIS, V. G. Leaching of lanthanides from various weathered elution deposited ores. **Canadian Metallurgical Quarterly**, v. 52, n. 3, p. 257–264, 2013.

MORAES, M. L. B. et al. **Seeing Environmental Issues as a Source of Rare Earths**. Proceedings of the 4th World Congress on Mechanical, Chemical, and Material Engineering (MCM'18) Madrid, Spain – August 16 – 18, 201. **Anais**...2018Disponível em: <https://avestia.com/MCM2018_Proceedings/files/paper/MMME/MMME_119.pdf>

MORAES, M. L. B. et al. The role of Al13-polymers in the recovery of rare earth elements from acid mine drainage through pH neutralization. **Applied Geochemistry**, v. 113, p. 104466, fev. 2020.

NASCIMENTO, M. et al. Modeling of REE and Fe Extraction from a Concentrate from Araxá (Brazil). **Minerals**, v. 9, n. 7, p. 451, 2019.

PEELMAN, S. et al. Leaching of Rare Earth Elements : Past and Present. **ERES2014: 1st European Rare Earth Resources Conference**, p. 446–456, 2014.

SCHMID, M. Mitigating supply risks through involvement in rare earth projects: Japan's strategies and what the US can learn. **Resources Policy**, v. 63, n. August, p. 101457, out. 2019.

SOUZA SANTOS, P. et al. Hydrothermal synthesis of well-crystallised boehmite crystals of various shapes. **Materials Research**, v. 12, n. 4, p. 437–445, 2009.

VASS, C. R.; NOBLE, A.; ZIEMKIEWICZ, P. F. The Occurrence and Concentration of Rare Earth Elements in Acid Mine Drainage and Treatment Byproducts. Part 2: Regional Survey of Northern and Central Appalachian Coal Basins. **Mining, Metallurgy & Exploration**, v. 36, n. 5, p. 917–929, 1 out. 2019a.

VASS, C. R.; NOBLE, A.; ZIEMKIEWICZ, P. F. The Occurrence and Concentration of Rare Earth Elements in Acid Mine Drainage and Treatment By-products: Part 1—Initial Survey of the Northern Appalachian Coal Basin. **Mining, Metallurgy & Exploration**, v. 36, n. 5, p. 903–916, 25 out. 2019b.

VOSSENKAUL, D. D. et al. Extraction of Rare Earth Elements from non- Chinese Ion Adsorption Clays. p. 1–11, 2015.

WANG, J. et al. Recovery of rare earths and aluminum from FCC waste slag by acid leaching and selective precipitation. **Journal of Rare Earths**, v. 35, n. 11, p. 1141–1148, 2017.

WU, S. et al. Recovery of rare earth elements from phosphate rock by hydrometallurgical processes – A critical review. **Chemical Engineering Journal**, v. 335, n. August 2017, p. 774–800, 2018.

ZIEMKIEWICZ, P. et al. **Design and evaluation of an acid leaching-solvent extraction process to extract rare earth elements from acid mine drainage precipitates. 2018 Annual Review, USDOE/NETL Rare Earth Elements Program**Pittsburgh PA, 2018.

ZIEMKIEWICZ, P. (WEST V. U.; NOBLE, A. (VIRGINIA T. **Annual repport: Recovery of Rare Earth Elements (REEs) from Coal Mine Drainage - Apr/2019**. Pittsburgh PA: [s.n.]. Disponível em: <https://www.netl.doe.gov/sites/default/files/2019-05/2019_Annual_Reports/Tuesday/ree/4 - 20190409_1130A_FE0026927_NETL.pdf>.

GENERAL CONCLUSIONS

It was concluded that the dominant REE species in the AMD system at pH 3.5 are Ln^{3+}, $LnSO_4^+$ and LnF^{2+}. The neutralization of the AMD with KOH promoted a high REE recovery and produced an amorphous precipitate containing 14% of REE oxides. The precipitate contains Al_{13}-polymers and accounts for the REE removal when the pH is raised to 8, thus promoting adsorption and entrapment simultaneously. Sequential extraction revealed that the REE could be efficiently leached with the use of acetic acid.

The presence and the amount of Fe in the initial solution can positively influence the REE removal efficiency, especially at a slightly acid pH. The influence caused by the addition of Fe was irrelevant when the pH of the AMD was raised up to values equal to 7-8. The scavenging of U was not influenced by the addition of Fe to the AMD before pH neutralization. The sequential extraction results showed that in precipitates containing higher amounts of Fe, the REE tended to be less labile. The ^{57}Fe Mössbauer spectroscopy studies revealed that the REE can occupy iron sites in the structure of the amorphous precipitates.

The element Ca exerted a negative influence over the co-precipitation and over the adsorption of Pr and Eu onto amorphous aluminium precipitates, contrasting to the elements Nd and Sm whose co-precipitation and adsorption did not suffer any influence of the presence of Ca in the solution. The implications of the findings on environmental sciences and on the recovery of REE from AMD highlights the impacts of the use of calcium hydroxide for pH control.

Concerning the study of the recovery of REE by co-precipitation with Al_{13}-polymers from AMD using $Ca(OH)_2$ for pH control, the results show that about 90% of the REE present in the AMD sample could be recovered by co-precipitation with amorphous Al-precipitates. The precipitate contains about 7% of REE oxides. The results of the acid-leaching experiment show that about 60%, 65% and 85% of the REE can be extracted from the precipitates using 2 mol L^{-1} HCl, 1.7 mol L^{-1} H_2SO_4 and 2 mol L^{-1} CH_3COOH, respectively. The economic potential of the REE-recovery activity considering an AMD sample from the studied site was also estimated, revealing the great potential of AMD treatment combined with REE production, in compliance with the United Nations Sustainable Development Goals.

CONCLUSIONES GENERALES

Se concluyó que las especies de TR dominantes en el sistema de DAM estudiado a pH 3.5 son Ln^{3+}, $LnSO_4^+$ y LnF^{2+}. La neutralización del DAM con KOH promovió una alta recuperación de TR y produjo un precipitado amorfo que contenía el 14% de óxidos de TR. El precipitado está formado por polímeros de Al_{13}, que son los responsables de la eliminación de TR cuando el pH se eleva a 8, promoviendo así la adsorción y el atrapamiento de estas simultáneamente. La extracción secuencial reveló que las TR pueden ser lixiviadas eficientemente utilizando ácido acético.

La presencia y la cantidad de Fe en la solución inicial pueden influir positivamente en la eficiencia de la eliminación de las TR, especialmente a pH ligeramente ácido. La influencia de la adición de Fe fue irrelevante cuando el pH del DAM se elevó a valores iguales a 7-8. La eliminación de uranio no se vio influenciada por la adición de Fe al DAM antes de la neutralización del pH. Los resultados de extracción secuencial mostraron que en los precipitados que contienen mayores cantidades de Fe las TR tienden a ser menos lábiles. Los estudios de espectroscopía Mössbauer del ^{57}Fe revelaron que las TR pueden ocupar posiciones del Fe en la estructura de los precipitados amorfos.

El elemento Ca ejerció una influencia negativa en la coprecipitación y en la adsorción de Pr y Eu en los precipitados de aluminio amorfo, en contraste con los elementos Nd y Sm, cuya coprecipitación y adsorción no se vieron influenciadas por la presencia de Ca en la solución. Las implicaciones de los resultados en las ciencias ambientales y en la recuperación de las TR a partir del DAM destacan los impactos del uso de hidróxido de calcio para el control del pH.

Con respecto al estudio de la recuperación de TR del DAM por coprecipitación con polímeros de Al_{13} usando $Ca(OH)_2$ para el control del pH, los resultados muestran que aproximadamente el 90% de las TR presentes en la muestra de DAM pueden ser recuperadas por coprecipitación con precipitados de aluminio amorfos. El precipitado tiene aproximadamente el 7% de óxidos de TR. Los resultados del experimento de lixiviación ácida muestran que alrededor del 60%, 65% y 85% de las TR se pueden extraer de los precipitados empleándose HCl 2 mol L^{-1}, H_2SO_4 1,7 mol L^{-1} y CH_3COOH 2 mol L^{-1}, respectivamente. También se estimó el potencial económico de la actividad de recuperación de TR, considerando una muestra de DAM del sitio estudiado, revelando el gran potencial del tratamiento del DAM combinado con la producción de TR, en consonancia con los Objetivos de Desarrollo Sostenible de las Naciones Unidas.

CONCLUSÕES GERAIS

Concluiu-se que as espécies dominantes de ETR no sistema de DAM estudado a pH 3,5 são Ln^{3+}, $LnSO_4^+$ e LnF^{2+}. A neutralização da DAM com KOH promoveu uma alta recuperação de ETR e produziu um precipitado amorfo contendo 14% de óxidos de ETR. O precipitado contém polímeros de Al_{13} e é responsável pela remoção dos ETR quando o pH é elevado para 8, promovendo assim a adsorção e o aprisionamento dos ETR simultaneamente. A extração sequencial revelou que os ETR podem ser lixiviados com eficiência usando-se ácido acético.

A presença e a quantidade de Fe na solução inicial podem influenciar positivamente a eficiência de remoção dos ETR, especialmente em um pH ligeiramente ácido. A influência causada pela adição de Fe foi irrelevante quando o pH da DAM foi elevado para valores iguais a 7-8. A remoção de urânio não foi influenciada pela adição de Fe à DAM antes da neutralização do pH. Os resultados de extração sequencial mostraram que nos precipitados contendo maiores quantidades de Fe, os ETR tendem a ser menos lábeis. Os estudos de espectroscopia Mössbauer do ^{57}Fe revelaram que os ETR podem ocupar sítios de ferro na estrutura de precipitados amorfos.

O elemento Ca exerceu influência negativa na co-precipitação e na adsorção de Pr e Eu nos precipitados de alumínio amorfo, em contraste com os elementos Nd e Sm, cuja co-precipitação e adsorção não sofreram influência da presença de Ca na solução. As implicações dos resultados em ciências ambientais e na recuperação de ETR de DAM destacam os impactos do uso do hidróxido de cálcio no controle do pH.

Em relação ao estudo da recuperação de ETR de DAM por co-precipitação com polímeros de Al_{13} usando $Ca(OH)_2$ para o controle de pH, os resultados mostram que aproximadamente 90% dos ETR presentes na amostra de DAM podem ser recuperados por co-precipitação com precipitados de alumínio amorfos. O precipitado possui aproximadamente 7% de óxidos de ETR. Os resultados do experimento de lixiviação ácida mostram que cerca de 60%, 65% e 85% dos ETR podem ser extraídos dos precipitados utilizando 2 mol L^{-1} HCl, 1,7 mol L^{-1} H_2SO_4 e 2 mol L^{-1} CH_3COOH, respectivamente. O potencial econômico da atividade de recuperação de ETR também foi estimado e discutido no capítulo 4, considerando-se uma amostra de DAM do local estudado, revelando o grande potencial do tratamento de DAM combinado com a produção de ETR, em consonância com os Objetivos de Desenvolvimento Sustentável das Nações Unidas.